
The Egyptian Journal of Genetics and Cytology is published twice a year (January and July in one volume of approximately pp. 400 by the Egyptian Society of Genetics, Egypt).

Subscription of the journal to individuals is $ 40.00 a year plus $ 12.00 for postage. Subscription price to institution is $ 100.00 per year plus $ 12.00 for postage.

The journal is open to all papers of original work in Genetics, Cytology and related subjects. Manuscripts and all editorial correspondences should be mailed (by registered AIR MAIL) to the Editor, Department of Genetics. Faculty of Agriculture, Ain Shams University Cairo, Egypt.

Cost of publication is $20.00/page for internationals or 120 L.E./page for Egyptians to the 10th pages and 120 L.E./page for each extra page and each page of figure or table. The cost for colored figures is 300 L.E./page. All checks should be addressed to “The Egyptian Society of Genetics”.

Subscriptions are to be ordered through the office of the secretary, Department of Genetics, Faculty of Agriculture, Ain Shams University Cairo, Egypt. Notice of changes address should be sent to the secretary.

Back Numbers and supplements are available on request.

REVIEWERS

First name	Last name	E-mail address	Country	Specialty 1	Specific 2
Abdel-Fattah	Badr	abdelfattahbadr@yahoo.com	Egypt	Plant Genomics	Evolutionary Genetics
Abdel-Salam	Draz	abdelsalamdr70@gmail.com	Egypt	Rice Breeding	Pathological Genetics
Ahmed	Abodoma	aabodoma99@hotmail.com	Egypt	Molecular Genetics	Crop Breeding
Aiman	Atta	pa_aiman@yahoo.com	Egypt	Molecular Genetics	Genetics
Anfu	Hou	houa@agr.gc.ca	Canada	Breeding	Genetics
Arthur	Weissinger	arthur@ncsu.edu	USA	Crop Science	Genetics
Ayman	Diab	aymanalidiab@gmail.com	Egypt	Genomics	Biotechnology
Benjamin F	Matthews	bmatthew@asrr.arsusda.gov	USA	Genetics	Molecular Biology
Christopher	Vulpe	vulpe@berkeley.edu	USA	Toxicogenomics	Molecular Biology
Danica	Baines	danica.baines@agr.gc.ca	Canada	Host-Microbe Interaction	Genetics
Daniel C.	Bowman	dbowman@unity.ncsu.edu	USA	Crop Science	Genetics
Dina	El-Khishin	dina_elkhishin@yahoo.com	Egypt	Genomics	Genetics
Dirk	Prufer	pruefer@ime.fraunhofer.de	Germany	Applied Genomics	Proteomics
Haley	Catton	haley.catton@canada.ca	Canada	Cereal Crop Entomology	Genetics
Hassan	Moawad	inogeb@oiccom.asrt.sci.eg	Egypt	Biotechnology	Microbial Genetics
Herbert W	Ohm	hohm@purdue.edu	USA	Genetics	Crop Science
Hossein	Borhan	hossein.borhan@agr.gc.ca	Canada	Molecular Plant Pathology	Genetics
Joe M	Anderson	janderson@purdue.edu	USA	Genetics	Crop Science
Johann	Schernthaner	johann.schernthaner@agr.gc.ca	Canada	Genomics	Molecular Biology
Lucia Helena Oliveria	de Souza	luciadesouza@uol.com.br	Brazil	Biosafety And Biohazards	Genetics
Mahmoud	Abdelhafiez	mahmoudabdelhafiez2015@gmail.com	Egypt	Animal Genetics	Biotechnology
Maie	Ali	maiefali@gmail.com	Egypt	Physiological Genetics	Poultry
Naglaa	Abdallah	naglaa.abdallah@agr.cu.edu.eg	Egypt	Genomics	Biotechnology
Nourtan	Abdeltawab	nourtan.abdeltawab@pharma.cu.edu.eg	Egypt	Bioinformatics	Immunogenetics
Parthiba	Balasubramanian	parthiba.balasubramanian@agr.gc.ca	Canada	Dry Bean Breeding	Genetics
Patrick	Gulick	pgulick@alcor.concordia.ca	Canada	Molecular Biology	Genetics
Perry B.	Cregan	pcregan@asrr.arsusda.gov	USA	Genetics	Molecular Biology
Rajinder	Dhindsa	raj.dhindsa@mcgill.ca	Canada	Molecular Biology	Genetics
Steven	Spiker	steven_spiker@ncsu.edu	USA	Plant Chomosomology	Molecular Cytogenetics
Tuan-hua David	Ho	ho@wustlb	USA	Biomedical Sciences	Genetics
Wagida A.	Anwar	wanwar2@hotmail.com	Egypt	Molecular Epidemiology	Medical Genetics

Egyptian Journal Of

GENETICS AND CYTOLOGY

INTERNATIONAL JOURNAL DEVOTED TO GENETICAL AND CYTOLOGICAL SCIENCES

Published by

THE EGYPTIAN SOCIETY OF GENETICS

Volume 51 **January 2022** **No. 1**

MOLECULAR CLONING AND CHARACTERIZATION OF TERPENE SYNTHASE 4 (*SgTPS4*) GENE FROM *Salvia guaranitica* PLANT

ESRAA A. ELSHERBENY[†], MOHAMMED ALI [†*], F. A. EL-RAMAH[†] AND MANAL K. AHMED[†]

[†]*Genetic Resources Department, Desert Research Center (DRC), 1, Mathaf El-Matariya Street, El-Matariya B.O.P 11753 El-matariya, Cairo, Egypt.*

* To whom correspondence should be addressed:Mohammed Ali, Ph.D.

Department of Genetic Resources Desert Research Center (DRC) 1 Mathaf El-Mataria St, 11753 Matariya, Cairo, Egypt.Phone: +2 01553727631 . Fax: (+202) 26357858

Email: mohammedalidrc@gmail.com

Profile URL: https://www.researchgate.net/profile/Mohammed_Ali268

Google Scholar: https://scholar.google.com/citations?hl=en&user=uWcwSCgAAAAJ

ORCID: https://orcid.org/0000-0001-9232-1781

[†] ESRAA A. ELSHERBENY and MOHAMMED ALI contributed equally to this work.

Abbreviations: OE: Overexpression, EOs: Essential oils. TPS: Terpene synthase. SgTPS4: *S. guaranitica* Terpene synthase 4. Semi-RT-PCR: Semiquantitative RT-PCR

Terpenoid is considered the largest group of natural products and a class of secondary metabolites, which have been identified from different plant species and many other organisms with more than 40,000 different structures (Bohlmann *et al.*, 1998). Terpenoid derives its shape from odd backbone

molecule called isopentenyl diphosphate (IPP), which have five carbon atoms (C5) (Wang *et al*., 2019 and Volke *et al*., 2019). The origin name of these different structures comes from the terebinth tree (*Pistacia terebinthus*), so we give these different structures names of terpene (Degenhardt *et al*., 2009). The structure of these units was illustrated by Wallach then modified by Ruzicka (Wallach, 1887; Ruzicka, 1953; 1959; 1973 and Pott *et al*., 2019). The plant produces multiple terpenoid compounds with highly diverse structures. Some terpenes are related to the primary plant metabolism such as the carotenoid pigments, phytol side chain of chlorophyll, gibberellin plant hormones, and phytosterols of cellular membranes (Trapp and Croteau, 2001; Gershenzon, 1999; Gutensohn *et al*., 2013 and Luck *et al*., 2020) and are important for plant growth and development. However, large majority of terpenes that have been identified are categories as secondary metabolites and play essential roles in the interactions of plants with the environment (Christianson *et al*., 2006). Both non-volatile and volatile terpenes have roles in such processes as the predators of herbivores and protection against photo-oxidative stress, attraction of both pollinators and the direct defense against insects and microbes (Tholl *et al*., 2006; K ollner *et al*., 2008 and Korankye *et al*., 2017). Numerous studies are found for understand in-depth the mechanisms of terpene and terpenoid functions.

The genus *Salvia* (*Lamiaceae*) includes over than 1,000 species of woody aromatic shrubs, among which e.g., *S. epidermindis, S. japonica, S. fruticosa, S. tuxtlensis, S. miltiorrhiza, S. aureus, S. przewalskii, S. santolinifolia, S. hydrangea, S. tomentosa, S. isensis, S. lavandulifolia, S. chloroleuca, S. glabrescens, S. nipponica, S. allagospadonopsis, S. macrochlamys* and *S. recognita* are economically important and cultivated worldwide for its vast medicinal properties and the production of their essential oils (EOs). Most of wild and cultivated salvia species are distributed in Central America, South America, East Asia and West Asia, while the remaining species are spread around the world (Alziar, 1988-1993; Ali *et al*., 2017 and Ali *et al*., 2018). Recently, *Salvia* species EOs have become a valuable source for aromatic and pharmaceutical research for discovering and identifying biologically active compounds (Takano and Okada, 2011; Ali *et al*., 2017 and 2018). Essential oils of *Salvia* species exhibit significant bioactivities, antimicrobial activities, including antimicrobial, anticancer, choleretic, anti-inflammatory, antioxidant and antimutagenic,

The fragrant oil of the *Salvia* mainly contains monoterpenes, sesquiterpenes, diterpene and triterpene. The composition of the terpenes in the salvia genus depends on the species or cultivars and type of tissues (Ali *et al*., 2017; 2018 and Aminfar *et al*., 2019). This study aimed at clone and functionally characterizes Terpene synthase 4 (*SgTPS4*) cDNA from *Salvia*

guaranitica. Here, we report the expression and functional characterization of *SgTPS4* cDNA in *Nicotiana tabacum*. The recombinant *SgTPS4* catalyses (2E, 6E)-farnesyl diphosphate to product bicyclogermacrene as a sesquiterpene through the pathway of sesquiterpenoid and triterpenoid biosynthesis.

MATERIALS AND METHODS

Plant materials and tissue collection

Plantlets of *S. guaranitica* L. were sampled from the Wuhan Botanical Garden farm, China. For gene cloning, three biological replicates from leaves were sampled from four years- old *S. guaranitica* plants. The samples were immediately frozen in liquid nitrogen and then stored at −20ºC until RNA extraction.

In silico analysis of *SgTPS4* gene

The nucleotide sequence of *SgTPS4* gene was selected from our previous RNA-Seq (Ali *et al*., 2018). The physiochemical properties of the *SgTPS4* were determined using PROTPARAM software(http://web.expasy.org/protparam). The amino acid sequencing for *SgTPS4* protein was further analyzed for protein subcellular location prediction using bioinformatics tools, WoLF PSORT Prediction(https://www.genscript.com/wolf-psort.html). Comparative sequence analysis of *SgTPS4* was performed using NCBI blastx against the protein database (http://blast.ncbi.nlm.nih.gov/).Phylogenetic tree was built using PhyML server with the default parameters of the (http://www.phylogeny.fr/) (Dereeper *et al*. 2008). To assess the phylogeny of the *SgTPS4* protein sequence in relation to other orthologous plant *TPS* genes, the protein sequences of functionally characterized *TPS* genes were retrieved from the National Center for Biotechnology Information (NCBI) database.

RNA extraction and cDNA library preparation

Total RNAs from three biological leaf replicates were extracted for *SgTPS4* gene cloning. Moreover, total RNAs from three biological replicates of *N. tabacum* were extracted for semi-quantitative RT-PCR using the TransZol Reagent (Focus Bioscience, Australia) and treated with DNase I (Takara). RNA quality was examined on 1.2% agarose gels, and the purity was analyzed using a Nanodrop ND1000 (NanoDrop technologies, Wilmington, DE, USA). RNAs from three replications were mixed into one tube for prepare RNA pools that will used to syntheses cDNA libraries. Two micrograms of total RNA (900 ng approximately) per sample was used for the synthesis of total cDNA with TransScript® First-Strand cDNA Synthesis SuperMix (TransGen Biotech, Beijing, China). Afterwards, PCR was performed for cDNA synthesis at 42ºC for 15 min followed by 85ºC for 5 second

(Ali *et al*., 2017 and 2018).

Full-length terpene synthase cDNA clone and vector

Full-length cDNAs for *SgTPS4* was obtained by PCR amplification using short and long gene-specific primers based on RNA-Seq sequence information from our transcriptome sequencing of *S. guaranitica* leaves (Ali *et al*., 2017 and 2018). Leaf cDNA was used as a template for the initial PCR amplification and performed using short primers, such as *SgTPS4*

Forward:
5′-ATGAAACACCAACACTCTTCTCTCT-3′
Reverse:
5-TTCAGTGTTCATCTGTGATTACAACGATT-3

with the TaKaRa Ex Taq® DNA Polymerase (TaKaRa, China) under the following PCR conditions: 4 min at 96ºC followed by 12 s at 98ºC; 30 s at 58ºC (Annealing temperatures), 2.20 min at 72ºC, and then 10 min at 72ºC. This process was repeated for 30 cycles. The first PCR products was used as a template for the PCR cloning using long primers, such as *SgTPS4*

Forward:
5′-GGGGACAAGTTTGTACAAAAAAGCA GGCTTCATGAAACACCAACACT-3′
Reverse:
5′-GGGGACCACTTTGTACAAGAAAG CTGGGTTTCAGTGTTCATCTGT-3′

with the TaKaRa Ex Taq® DNA Polymerase for the Gateway pDONR221 vector. The amplified PCR bands were purified from agarose gel and binding to pDONR221 vector, then our target gene were transfer to pB2GW7 overexpression vector for *N. tabacum* plant transformation. The positive construct vectors that containing our target gene was confirmed by sequencing.

Semiquantitative RT-PCR analysis

Semiquantitative real-time PCR was performed on a Eppendorf PCR (Master cycler Nexus PCR Machine from Eppendorf, UK) system with a total reaction volume of 25 µl. A gene-specific primer for *NtEF-1α* forward: 5′-TGGTTGTGACTTTTGGTCCCA-3′ and reverse: 5′-ACAAACCCACGCTTGAGATCC-3′ was used as a reference gene with 155 bp, and *SgTPS4* forward: 5′-ATCTTCGTGCTTTGCTACTC -3′ and reverse: 5′-ATTATGCGACTCGTCTTCTTC-3′ with 155 bp length, gene involved in the biosynthesis of Terpene synthase 4 (*SgTPS4*), were designed using the primer designing tools of IDTdna (http://www.idtdna.com/scitools/Applications/RealTimePCR/). Semi-qRT-PCR was ran using the following program [95°C for 4 min, 95ºC for 30 s, 58ºC for 30 s, 72ºC for 1 min and 72ºC for 10 min] for 35 cycles. The PCR products were resolved on 1.6 % agarose gel, and the expression levels of *NtEF-1α* and *SgTPS4* genes were detected.

***Nicotiana* plant growth conditions and preparation of *Agrobacterium* cultures for infection**

Wild-type *N. tabacum* plant seeds were grown under standard greenhouse conditions for ten days at our lab. Our construct vector pB2GW7-*SoTPS4* was

inserted into *Agrobacterium* strain EHA105 using direct electroporation method. Recombinant *A. tumefaciens* was grown for two days at 28ºC in solid LB media supplemented with 50 µg/ml each of rifampicin and spectinomycin. An individual colony was inoculated into 1.0 ml of liquid medium and grown at 28ºC under 200 rpm agitation overnight with the same media composition. After one day, 1.0 ml from liquid medium sample was transferred to a 250-ml conical flask containing 50 ml of LB media supplemented with the same compositions; the sample was grown at 28°C in a shaker overnight until an optical density of 0.7-1.0 (OD 600) was reached. Overnight cell culture was harvested by centrifugation at 4,500 rpm for 12 min at 4ºC, and the pellet was re-suspended in the infection medium (50 ml of LB-free media + 50 µl of acetosyringone). *N. tabacum* plantlet leaves were sampled and sterilized using 70% ethanol for 30 s, then 0.1% HgCl for 6 min, after that washing three times for 3 min using sterilized cold water. Then, leaves without petiole and midrib were cut into small pieces and soaked into infection media for 10 min. The transformation procedure was performed as described previously (Sunjung, 2006 and Ali *et al*., 2017). More than 12 individual transgenic tobacco lines were generated and examined with PCR for positive transgenic lines. The positive transgenic tobacco plants were selected for isolation the terpenoid.

Phenotypic evaluation

Transformed plants were watered and fertilized regularly with Miracle Gro fertilizer (Scott's Company, USA) prepared according to manufacturer's instructions for phenotypic comparisons between *N. tabacum* plants transformed with *SgTPS4* and its counterpart wild-type plants. Plants were grown in growth chamber at a temperature of 22ºC day/20ºC night with humidity of 60-70%, and photoperiod at 16 hours day/8 hours night, with a light density of 100–150 µ moles m−2 s−1 using fluorescent bulbs for vegetative growth and for flowering, respectively. Plants were assessed about leaf morphology, growth and terpene metabolic.

Metabolite extraction from transgenic *N. tabacum* leaves

Terpenoid compounds from non-transgenic *N. tabacum* leaves (wild type) and transgenic *N. tabacum* leaves containing *SgTPS4* expression construct were extracted and isolated. For this, twelve leaves from each transgenic *N. tabacum* line (one leaf from each plant) and wild type were homogenized in liquid nitrogen with a mortar and pestle, then the powder was soaked in Amber storage bottles ((20 ml screw-top vials with silicone/PTFE septum lids) (http://www.sigmaaldrich.com)) containing n-hexane as a solvent. After that, Amber storage bottles were

incubated in shaking at 37ºC and 210 rpm for 70 h. Afterward, the supernatant solvent was collected by centrifuged at 5,000 rpm for 10 minutes at 4ºC, then pipette into glass vials and concentrated to 1.5 ml of concentrated oils under a stream of nitrogen gas with a nitrogen evaporator (Organomation; Toption-China-WD-12). The concentrated oils were transferred to a fresh 1.5 ml crimp vial amber glass, and placed on the auto-sampler of the gas chromatography mass spectrometer (GC-MS) system for GC-MS analysis as described previously by (Ali *et al*. (2017 and 2018).

GC-MS analysis of essential oil components

Shimadzu model GCMS-QP2010 Ultra (Tokyo, Japan) system was used for GC analysis. An approximately 1µl aliquot of each sample was injected (split ratios of 15:1) into a GC-MS equipped with an HP-5 fused silica capillary column (30 m x 0.25 mm ID, 0.25 µm film thicknesses), and Helium at 1.0 ml/min^{-1} as carrier gas.. The mass spectra were monitored between 50- 450 m/z. Temperature was initially under isothermal conditions at 60ºC for 10 minutes. Temperature was then increased at a rate of 4ºC/min^{-1} to 220ºC, held isothermal at 220ºC for 10 minutes, increased by 1ºC/ min^{-1} to 240ºC, held isothermal at 240°C for 2 min, and finally held isothermal for 10 minutes at 350ºC. The volatile constituents were identified based on the mass spectra stored in the NIST Library (2014 edition), Volatile Organic Compounds (VOC), Wiley GC/MS Library (10th Edition) (Wiley, New York, NY, USA), and the Analysis S/W software. The relative % amount of each component was calculated by comparing its average peak area to the total areas. The GC-mass experiments was repeated three times with the same conditions, with total GC running time was 80 minutes (Ali *et al*., 2017 and 2018).

RESULTS AND DISCUSSION

Isolation of full-length terpene synthase 4 (*SgTPS4*) genes and sequence characterization

The *SgTPS4* gene has an open reading frame of 2289 bp, which encodes a 763 amino acid protein with a calculated molecular mass of 82.54 kDa and a theoretical isoelectric point (pI) of 9.59. The WoLF PSORT Prediction tools used to analyzed the *SgTPS4* protein subcellular location prediction, suggests that *SgTPS4* is localized at different organelles (such as, Mitochondrial, Chloroplast, Peroxisomal, Nuclear, Golgi and Vacuolar) with different presence and identity level from 13.9723% to 11.1732% (https://www.genscript.com/tools/wolfpsort/detail?file=2021/10/02/htdocs/results/163320872328765.detailed1.html#163320872328765). Based on the blastx analysis (Table 1), the closest homologue to *SgTPS4* is the Bicyclogermacrene synthase-like from *Salvia splendens*, which it shares 97.07 % identity. Although the level of amino acid

sequence similarity between *SoAMYS* and the other homologues was relatively higher (≧84.89%). On the other hand, Phylogenetic analysis of the deduced amino acid sequence of *SgTPS4* showed that it belongs to the TPS-c subfamily of angiosperm sesquiterpene synthases which may be encodes sesquiterpene and diterpenes (Chen *et al*., 2011; Bohlmann *et al*., 1998; Külheim *et al*., 2015 and Danner *et al*., 2011) (Fig. 1). To date, seven TPS subfamilies have been detected and identified in various plant species genomes, including *Selaginella moellendorffii* (Li *et al*., 2012), *Camellia sinensis* (Zhou *et al*., 2020), *Eucalyptus globulus* (Külheim *et al*., 2015), *Daucus carota* (Keilwagen *et al*., 2014), *Arabidopsis thaliana* (Aubourg *et al*., 2002), *Solanum lycopersicum* (Falara *et al*., 2011), *Malus domestica* (Nieuwenhuizen *et al*., 2013), and *Vitis vinifera* (Martin *et al*., 2010).

Functional characterization of Terpene synthase 4 (*SgTPS4*) genes in transgenic *N. tabacum* leaves

The role and product specificity of *SgTPS4* was determined by generating transgenic *N. tabacum*. Overexpression of *SgTPS4* in *N. tabacum* was accomplished using *A. tumefaciens* strain EHA105 harboring the transformation vector pB2GW7-*SgTPS4*. Using the *Agrobacterium*-mediated transformation method, more than twelve transgenic *N. tabacum* plants were successfully generated. These plants have large green oval leaves (Fig. 2A). In contrast, the non-transformants plants showed small green oval leaves (Fig. 2A). The putative transformants were further verified using semiquantitative RT-PCR of the plant genomic cDNA. Fully mature leaves from twelve putative transgenic plants and three wild type plants were collected for RNA extraction and cDNA synthesis. All the putative transformants showed high expression of the *SgTPS4* gene by the amplification of a distinct band at 155 bp, which was absent in the wild type plants (Fig. 2B). This result confirmed the presence of the *SgTPS4* gene in the genomes of the transgenic plants. Two of the transgenic plants, designated as *OE- SgTPS4-1* and *OE- SgTPS4-2*, were selected for further analysis. Meanwhile, from the morphological analysis, wild type plants showed a little delayed in growth with a few number of leaf compared to the transgenic plants (Figs. 2A and B). In context, the obtained findings are in line with our previous works of Ali *et al*. (2017 and 2018) who reported that the overexpression of genes that involved in the terpenoid biosynthesis, such as *SoLINS, SoNEOD, SoTPS6, SoSABS, SoCINS, SgGPS, SgFPPS* and *SgLINS* from *S. officinalis* and *Salvia guaranitica* in *N. tabacum* and *A. thaliana*, also resulted in delayed growth and flowering formation in wild type plants compared to the transgenic plants.

Metabolite extraction from transgenic and non- transgenic *N. tabacum* leaves

Phytochemicals were extracted from transgenic and non- transgenic (wild type) *N. tabacum* leaves with hexane and

analyzed by GC-MS to identify the specific product produced by transformation with the *SgTPS4* gene. Various types and amounts of terpene compounds were observed, and the quantities of terpene were represented by the percentage of peak area (% peak area). Compounds were identified in transgenic *N. tabacum* and non- transgenic (wild type plants) as the control by comparing their mass spectra of the compounds with mass spectra libraries. The detected components were also confirmed by comparing them with the published references and extracts of wild-type *N. tabacum* which produce different types and amounts of terpenoids. Overexpression of *SgTPS4* genes in *N. tabacum* plants produced different amounts of sesqui-, di- and triterpenes. Moreover, from the results shown in Table (2) and Fig. (3), very clear differences were observed for the transgenic plants, as an additional peak was present at the retention time of 50.461. This peak was characterized as Bicyclogermacrene compound, based on the closest mass spectra with the data stored in the Wiley GC/MS Library (10th Edition) (Wiley, New York, NY, USA) https://www.chromservis.eu/p/wiley-10th-edition-library-in-nist-format, volatile organic compounds (VOC) http://www.physchem.uni-wuppertal.de/voc-database, analysis S/W software https://www.acronymfinder.com/Software-(S%2FW).html, and the NIST Library (2014 edition) https://webbook.nist.gov/cgi/cbook.cgi?Name=hopanoid&Units=SI.The production of Bicyclogermacrene by *SgTPS4* was in agreement with the findings from Ali *et al*., (2017 and 2018) and Su-Fang *et al*., (2014). These results also showed that the overexpression of terpene syntheses genes introduced by Ali *et al*., (2017 and 2018) and Su-Fang *et al*., (2014), does not affect the product specificity of *SgTPS4* in producing Bicyclogermacrene. Having obtained the similar terpene products in both *N. tabacum* and *A. thaliana*, we have showed that *SgTPS4* was responsible for the production of Bicyclogermacrene as a sesquiterpene through the pathway of sesquiterpenoid (Wang *et al*., 2016 and Ro *et al*., 2006).

In conclusions, the diversity of the sesquiterpenes found in *S. guaranitica* renders this plant a major resource for research related to sesquiterpene biosynthesis. In this study, we cloned and functionally characterized one of the scarcely expressed sesquiterpene synthase (*SgTPS4*), which is responsible for the production of Bicyclogermacrene in *S. guaranitica*. Also, transgenic technology was applied by overexpressing *SgTPS4* in *N. tabacum*. Positive growth acceleration was clearly observed in the transgenic lines *OE-SgTPS4-1* and *OE-SgTPS4-2*. These two plants showed a high expression of the *SgTPS4* gene, which resulted in the production of Bicyclogermacrene. The Bicyclogermacrene produced in these *N. tabacum* transgenic plants indicated the effectiveness of *N. tabacum* in synthesizing the same product as a sesquiterpene through the common pathway of sesquiterpenoid and

triterpenoid biosynthesis. *SgTPS4* protein exhibits a strong sequence similarity to other sesquiterpene synthases, and clustered under TPS-c group. This research strongly suggests the potential usage of the *N. tabacum* plant as a model system for studying the Bicyclogermacrene synthase gene from *S. guaranitica* for understanding of plant sesquiterpenoid biosynthesis and the potential for biotechnology application.

SUMMARY

Salvia guaranitica is a medicinal and aromatic plant with highly valued in traditional medicine for its abundance of terpenes, especially the monoterpenes (C10) and sesquiterpenes (C15). Various terpenes were believed to contribute to the many useful biological properties in plants. This study aimed at cloning and functionally characterizes a full length sesquiterpene synthase gene from *S. guaranitica*. Terpene synthase 4 (*SgTPS4*) has a complete open reading frame (ORF) of 2289 base pairs encoding a 763 amino acids protein. The phylogenetic tree demonstrates that *SgTPS4* protein was clustered into the subfamily TPS-c, which belongs to the angiosperm terpenoid synthase. To examine the function of *SgTPS4*, we expressed this gene in *N. tabacum*. Two transgenic lines, designated as *OE- SgTPS4 -1* and *OE-SgTPS4 -2* were further characterized, both molecularly and functionally. The wild type plants showed a little delayed growth compared to the transgenic plants. Gas chromatography-mass spectrometry analysis of the transgenic plants showed that *SgTPS4* was responsible for the production of Bicyclogermacrene. This is the first report of a gene involved in the Bicyclogermacrene as a sesquiterpene from *S. guaranitica* plant.

Ethics approval and consent to participate

No investigations were undertaken using humans/human samples in this study. No experimental animals were used to conduct any of the experiments reported in this manuscript. Our study did not involve endangered or protected species.

Competing interests

The authors declare that they have no competing interests.

Funding

This research does not receive external funding

Consent for publication

Not applicable.

Authors' contributions

MA conceived and designed the study; MA, EAE, FAE and MKA performed experiments, MA wrote the paper. All authors discussed the results and commented on the manuscript and participated in the analysis of the data. All authors participated in reading and approving the final manuscript.

ACKNOWLEDGEMENTS

This work is under the activity of the Egyptian Desert Gene Bank (EDGB), Genetic Resources Department, Desert Research Center (DRC), Egypt. Special thanks are given to Dr. Ahmed Ali at Department of Plant Agricultural, Faculty of Agriculture Science, Al-Azhar University, Assiut, Egypt for valuable support. We also owe thanks to Dr. Wael Moussa at Desert Research Center (DRC) for constructive comment and help.

REFERENCES

Ali M., Hussain R. M., Rehman N. U., She G., Li P., Wan X., Guo L. and Zhao J. (2018). *De novo* transcriptome sequencing and metabolite profiling analyses reveal the complex metabolic genes involved in the terpenoid biosynthesis in blue anise sage (*Salvia guaranitica* L.). DNA Res., 25(6): 597-617. doi.org/10.1093/dnares/dsy028

Ali M., Li P., She G., Chen D., Wan X. and Zhao J. (2017). Transcriptome and metabolite analyses reveal the complex metabolic genes involved in volatile terpenoid biosynthesis in garden sage (*Salvia officinalis*). Sci. Rep., 7(1): 16074. doi.org/10.1038/s41598-017-15478-3

Alziar G. (1988-1993). Catalogue synonymique des *Salvia* L. dumonde (*Lamiaceae*). I.–VI. Biocosme Mesoge´en., 5 (3–4): 87-136; 6 (1–2, 4): 79–115, 163-204; 7 (1–2): 59-109; 9 (2–3): 413-497; 10 (3–4): 33-117.

Aminfar Z., Rabiei B., Tohidfar M. and Mirjalili M. H. (2019). Identification of key genes involved in the biosynthesis of triterpenic acids in the mint family. Sci. Rep., 9 (1): 15826. doi.org/10.1038/s41598-019-52090-z

Aubourg S., Lecharny A., Bohlmann J. (2002) .Genomic analysis of the terpenoid synthase (*AtTPS*) gene family of *Arabidopsis thaliana*. Mol. Genet. Genom., 267:730-745. doi: 10.1007/s00438-002-0709-y.

Bohlmann J., Meyer-Gauen G. and Croteau R. (1998). Plant terpenoid synthases: molecular biology and phylogenetic analysis," Proc. Natl. Acad. Sci., USA., 95, 8: 4126-4133.

Chen F., Tholl D., Bohlmann J. and Pichersky E. (2011). The family of terpene synthases in plants: a mid-size family of genes for specialized metabolism that is highly diversified throughout the kingdom. Plant J., 66 (1): 212-229. doi:10.1111/j.1365-313X .2011 .04520.x.

Christianson D. W. (2006). Structural biology and chemistry of the terpenoid cyclase's, Chem Rev.,

106 (8): 3412-3442.

Danner H., Boeckler G. A., Irmisch S., Yuan J. S., Chen F., Gershenzon J., Unsicker S. B. and Köllner T. G. (2011). Four terpene synthases produce major compounds of the Gypsy moth feeding induced volatile blend of *Populus trichocarpa*. Phytochemistry, 72 (9): 897-908.

Degenhardt J., Köllner T. G. and Gershenzon J. (2009). Monoterpene and sesquiterpene synthases and the origin of terpene skeletal diversity in plants. Phytochemistry, 70: 1621-1637. https://doi.org/10.1016/j. phyto. Chem.2009.07.030.

Dereeper A., Guignon V., Blanc G., Audic S., Buffet S., Chevenet F., Dufayard J. F., Guindon S., Lefort V., Lescot M., Claverie J. M. and Gascuel O. (2008). Phylogeny.fr: robust phylogenetic analysis for the non-specialist. Nucleic Acids Res 36:W465-W469. doi.org/ 10.1093/nar/gkn180

Falara V., Akhtar T. A., Nguyen T. T. H., Spyropoulou E. A., Bleeker P. M., Schauvinhold I., Matsuba Y., Bonini M. E., Schilmiller A. L., Last R. L., Schuurink, R. C., and Pichersky E. (2011).The tomato terpene synthase gene family. Plant Physiol. 157:770–789. doi: 10.1104/pp.111.179648.

Tholl D., Boland W., Hansel A., Loreto F., Röse U. S. and J. P. Schnitzler (2006). Practical approaches to plant volatile analysis. Plant J. 45: 540-560.

Gershenzon J. and W. Kreish (1999). Biochemistry of terpenoids: monoterpenes, sesquiterpenes, diterpenes, sterols, cardiac glycosides and steroid saponins. In: Wink M., editor. Biochemistry of plant secondary metabolism. Florida: CRC Press, 222-299.

Gutensohn M., Orlova I., Nguyen T. T., Davidovich-Rikanati R., Ferruzzi M. G., Sitrit Y., Lewinsohn E., Pichersky E. and N. Dudareva (2013). Cytosolic monoterpene biosynthesis is supported by plastid-generated geranyl diphosphate substrate in transgenic tomato fruits. Plant J., 75 (3): 351-363.

Keilwagen J., Lehnert H., Berner T., Budahn H., Nothnagel T., Ulrich D., Dunemann F. (2017). The terpene synthase gene family of carrot (*Daucus carota* L.): Identification of QTLs and candidate genes associated with terpenoid volatile compounds. Front. Plant Sci. 8:1930. doi: 10.3389/fpls.2017.01930.

Köllner T. G., Held M., Lenk C., Hiltpold I., Turlings T. C., Gershenzon J. and Degenhardt J. (2008). A maize

(E)-beta-caryophyllene synthase implicated in indirect defense responses against herbivores is not expressed in most American maize varieties. Plant Cell, 20(2): 482-94. doi: 10.1105/tpc.107.051672. Epub, Feb 22. PMID: 18296628; PMCID: PMC2276456.

Korankye A. E., Lada R., Asiedu S. and Claude C. (2017). Plant senescence: the role of volatile terpenecompounds (VTCs). Am. J. Plant Sci., 8: 3120-3139.

Külheim C., Padovan A., Hefer C., Krause S. T., Köllner T. G., Myburg A. A., Degenhardt J. and W. J. Foley (2015). The Eucalyptus terpene synthase gene family. BMC genomics, 16 (1): 450. doi.org/10.1186/.

Li G., Köllner T. G., Yin Y., Jiang Y., Chen H., Xu Y., Gershenzon J., Pichersky E., Chen F. (2012). Nonseed plant *Selaginella moellendorffii* has both seed plant and microbial types of terpene synthases. Proc. Natl. Acad. Sci. USA. 2012;109:14711-14715. Doi: 10.1073/pnas.1204300109.

Martin D. M., Aubourg S., Schouwey M. B., Daviet L., Schalk M., Toub O., Lund S. T., Bohlmann J. (2010). Functional annotation, genome organization and phylogeny of the grapevine (*Vitis vinifera*) terpene synthase gene family based on genome assembly, FLcDNA cloning, and enzyme assays. BMC Plant Biol. 2010;10:226. doi: 10.1186/1471-2229-10-226.

Nieuwenhuizen N. J., Green S. A., Chen X., Bailleul E. J. D., Matich A. J., Wang M. Y., Atkinson R. G. (2013). Functional genomics reveals that a compact terpene synthase gene family can account for terpene volatile production in apple. Plant Physiol. 161:787-804. doi: 10.1104/pp.112.208249.

Luck K., Chen X., Norris A. M., Chen F., Gershenzon J. and Köllner T. G. (2020). The reconstruction and biochemical characterization of ancestral genes furnish insights into the evolution of terpene synthase function in the *Poaceae*. Plant. Mol. Biol. 104, 1-2: 203-215. doi:10.1007/s11103-020-01037-4

Pott D. M., Osorio S., and Vallarino J. G. (2019). From central to specialized metabolism: an overview of some secondary compounds derived from the primary metabolism for their role in conferring nutritional and organoleptic characteristics to fruit. Front. Plant Sci. 10:835. doi: 10.3389/fpls.2019.00835

Ro D., Ehlting J., Keeling C., Lin R., Mattheus N. and J. Bohlmann (2006). Microarray expression profiling and functional characterization of *AtTPS* genes: Duplicated *Arabidopsis thaliana* sesquiterpene

synthase genes *At4g13280* and *At4g13300* encode root-specific and wound-inducible (Z)-Y-bisabolene synthases. Arch. Biochem. Biophys., 448, 1-2: 104-116. : doi.org/10.1016/j.abb.2005.09.019.

Ruzicka L. (1953). The isoprene rule and the biogenesis of terpenic compounds. Experientia, 9: 357-367.

Ruzicka L. (1959). Faraday Lecture (History of the isoprene rule), Proc. Chern. Soc. (Lond.): 341-360.

Ruzicka L. (1973). In the borderland between bioorganic chemistry and biochemistry, Annu. Rev. Biochem., 42: 1-20.

Su-Fang E., Zeti-Azura M., Roohaida O., Noor A. S., Ismanizan I. and Zamri Z. (2014). Functional Characterization of Sesquiterpene Synthase from *Polygonum minus*. Scientific World Journal. doi.org/10.1155/2014/840592.

Sunjung P. (2006). *Agrobacterium tumefaciens* –mediated transformation of tobacco (*Nicotiana tabacum* L.) leaf disks: evaluation of the co-cultivation conditions to increase β -Glucuronidase gene activity. (Master's dissertation). Retrieved from http://etd.lsu. edu /docs/available/etd-07052006-173930/unrestricted/Park_thesis.Pdf .

Takano A. and Okada H. (2011). Phylogenetic relationships among subgenera,species, and varieties of *Japanese Salvia* L. (*Lamiaceae*), J. Plant Res., 124: 245–52.

Trapp S. and Croteau R. (2001). Defensive resin biosynthesis in conifers. Ann. Rev. Plant Physiol., Plant Mol. Biol., 52: 689-724.

Volke D. C., Rohwer J., Fischer R. and Jennewein S. (2019). Investigation of the methylerythritol 4-phosphate pathway for microbial terpenoid production through metabolic control analysis. Microb Cell Fact. 18, 1,192. doi: 10.1186/s12934-019-1235-5

Wallach O. (1887). Zur KentniB der Terpene uDd dec atherischen Oele,Liebig's Ann. Chern., 239: 1-54.

Wang Q., Jia, M., Huh J. H., Muchlinski A., Peters R. J. and Tholl D. (2016). Identification of a dolabellane type diterpene synthase and other root-expressed diterpene synthases in *Arabidopsis*. Front Plant Sci., *7*: 1761. doi.org/10.3389/fpls.2016.01761

Wang Q., Quan S. and Xiao H. (2019). Towards efficient terpenoid biosynthesis: manipulating IPP and DMAPP supply. Bioresour. Bioprocess. 6**,** 6. doi.org/10.1186/s40643-019-0242-z

Zhou H. C., Shamala L. F., Yi X. K., Yan Z., Wei S. (2020). Analysis of terpene synthase family genes in Camellia sinensis with an emphasis on abiotic stress conditions. Sci. Rep. 10:933. doi.org/10.1038/s41598-020-57805-1

Table (1): BLASTX analysis *SgTPS4* was compared with the NCBI protein database for gene identification purposes.

NCBI Accession	[a]Descriptiona	Organism	*E* value	Identity (%)	Accession length
XP_041989963.1	Bicyclogermacrene synthase-like	*Salvia splendens*	0	97.07%	555
XP_041993267.1	Bicyclogermacrene synthase-like isoform	*Salvia splendens*	0	86.76%	557
XP_042006403.1	Bicyclogermacrene synthase-like	*Salvia splendens*	0	72.81%	558
XP_042005662.1	Bicyclogermacrene synthase-like	*Salvia splendens*	0	69.27%	559
XP_042008743.1	Bicyclogermacrene synthase-like	*Salvia splendens*	0	71.06%	559
XP_042006468.1	Bicyclogermacrene synthase-like	*Salvia splendens*	0	70.52%	557
XP_041993268.1	Bicyclogermacrene synthase-like isoform	*Salvia splendens*	0	84.89%	485

[a]Description—homology search using blastx.

Table (2): The major terpenoid compositions in transgenic *N. tabacum* leave over-expressing of *SgTPS4*.

N	Compound name	R.T (min.)	Formula	Molecular Mass (g mol-1)	Terpene of Type	% Peak area	
						NtW.T	*SgTPS4*
1	6-Amino-o-toluic acid; Benzoic acid, 2-amino-6-methyl-	6.882	C8H9NO2	151.1626		11.13	
2	Lupetidin	8.217	C7H15N	113.2007		0.61	
3	Piperidine, 2,6-dimethyl-;	14.27	C7H15N	113.2007		1.44	
4	4-Pipecoline	14.845	C6H13N	99.1741		1.38	
5	Dimethylsiloxane cyclic trimer	17.016	C6H18O3Si3	222.4618		4.44	
6	3,5-Dihydroxy-6-methyl-2,3-dihydro-4H-pyran-4-one	19.901	C6H8O4	144.1253		1.34	
7	Dimethylsiloxane cyclic trimer	26.286	C6H18O3Si3	222.4618		0.59	
8	**L-(-)-Nicotine**	27.823	C10H14N2	162.232		**50.96**	
9	α-Nicotine	28.319	C10H14N2	162.232		4.13	
10	Tetradecamethylcycloheptasiloxane	29.69	C14H42O7Si7	519.0776			0.02
11	trans-β-Ionone	30.644	C13H20O	192.2973			0.05
12	Topanol;Stavox	31.345	C15H24O	220.3505	Sesqui		0.07
13	Ethyl isopropylidene(cyano)acetate	32.112	C8H11NO2	153.1784		0.92	
14	Hexadecamethylcyclooctasiloxane	34.574	C16H48O8Si8	593.2315			0.06
15	Bisphenol C	34.748	C17H20O2	256.3395		0.61	
16	6-Aminouracil	35.302	C4H5N3O2	127.1014		0.55	
17	m-Cresyl N-methylcarbamate	36.029	C9H11NO2	165.1891			0.09
18	2(1H)-Pyrimidinone, tetrahydro-1,3-dimethyl-	37.487	C6H12N2O	128.1723		2.72	
19	Myristaldehyde	37.76	C14H28O	212.3715			0.14
20	(+)-Pyrethronyl (+)-trans-chrysanthemate;	38.579	C21H28O3	328.4452		1.28	
21	Octadeamethyl-cyclononasiloxane	38.761	C18H54O9Si9	667.3855			0.14
22	Methyl isohexadecanoate	39.636	C17H34O2	270.4507			0.39
23	2(1H)-Pyrimidinone, tetrahydro-1,3-dimethyl-	40.11	C6H12N2O	128.1723		3.37	
24	Hexadecane, 1,2-epoxy-; Hexadecylene oxide	40.777	C16H32O	240.4247			1.29
25	Cyclohexane, tert-pentyl-	42.053	C11H22	154.2924		0.53	

Table (2): Cont’

26	Alpha.-Linolenic acid, trimethylsilyl ester	42.458	C21H38O2Si	350.6107			0.8
27	1-(3-methylbutyryl)pyrrolidine	42.837	C9H17NO	155.237		0.76	
28	Palmitic acid, methyl ester	43.187	C17H34O2	270.4507			0.1
29	Linolenic acid, methyl ester	44.012	C19H32O2	292.4562			3.48
30	Bromocriptine	44.52	C32H40BrN5O5	654.594		1.84	
31	n-Hexadecanoic acid	44.686	C16H32O2	256.4241			
32	2,5-Piperazinedione, 3,6-bis(2-methylpropyl)-	45.151	C12H22N2O2	226.3153			11.74
33	Palmitic acid	45.848	C16H32O2	256.4241		2.94	
34	Hexadecamethylcyclooctasiloxane	45.865	C16H48O8Si8	593.2315		5.33	
35	4,8,13-Duvatriene-1,3-Diol	45.95	C20H34O2	306.4828			0.3
36	1,3-Distearin	46.238	C39H76O5	625.018			0.2
37	δ-Guaiene;	46.392	C15H24	204.3511	Sesqui		0.11
38	(+)-Ledol	46.691	C15H26O	222.3663	Sesqui		0.65
39	All-trans-Retinol acetate	46.926	C22H32O2	328.4883			0.63
40	Methyl cis,cis-9,12-octadecadienoate; Methyl linoleate	47.192	C19H34O2	294.4721			0.87
41	Linolenic acid, methyl ester	47.341	C19H32O2	292.4562			0.45
42	Phytol	47.603	C20H40O	296.531	Diter		0.74
43	4,8,13-Duvatriene-1,3-Diol	48.064	C20H34O2	306.4828			4.82
44	Cycloartanyl acetate	48.148	C32H54O2	470.77			1.22
45	Phytol, TMS derivative	48.303	C23H48OSi	368.7121	Diter	0.64	
46	Geranylgeraniol	48.418	C22H36O2	332.52			0.28
47	α-Linolenic acid;	48.907	C18H30O2	278.4296			23.73
48	Stearic acid	49.281	C18H36	284.477			2.86
49	cis-Bicyclogermacradiene	49.552	C15H24	204.3511	Sesqui		1.15
50	(Z)-9-Tetradecenal	50.013	C14H26O	210.36		2.49	
51	**Bicyclogermacrene**	50.461	C15H24	204.3511	Sesqui		**33.8**
52	d-Ledol	51.493	C15H26O	222.3663	Sesqui		0.07
53	Octadeamethyl-cyclononasiloxane	52.037	C18H54O9Si9	667.3855			0.65
54	6,9-Octadecadienoic acid, methyl ester	53.436	C19H34O2	294.4721			0.05

Table (2): Cont'

55	Squalene	54.046	C30H50	410.718	Triter		0.43
56	n-Heneicosane	54.964	C21H44	296.5741			0.05
57	Octadeamethyl-cyclononasiloxane	56.355	C18H54O9Si9	667.3855			0.79
58	Linolenic acid, methyl ester	57.393	C19H32O2	292.4562			0.09
59	n-Pentatriacontane	58.992	C35H72	492.9462			0.79
60	Phthalic acid dioctyl ester	60.497	C24H38O4	390.5561			0.15
61	Nopol	61.574	C11H18O	166.26			0.13
62	Octadeamethyl-cyclononasiloxane	62.682	C18H54O9Si9	667.3855			1.06
63	n-Tetracontane	64.117	C40H82	563.0791			0.14
64	Isovaleric acid, allyl ester	68.645	C8H14O2	142.1956			0.23
65	n-Tetracontane	69.7	C40H82	563.0791			1.61
66	Octadeamethyl-cyclononasiloxane	70.054	C18H54O9Si9	667.3855			1.15
67	Tetrapentacontane	71.42	C54H110	759.4512			0.03
68	n-Pentatriacotane	72.462	C35H72	492.9462			0.19
69	O-Benzyllinalool	73.038	C17H24O	244.37			0.15
70	3-Methyloctadecane	73.842	C19H40	268.5209			0.03
71	n-Nonacosane	75.547	C29H60	408.7867			0.38
72	Octadeamethyl-cyclononasiloxane	77.732	C18H54O9Si9	667.3855			1.17
73	n-Nonacosane	79.245	C29H60	408.7867			0.27
	Total % of sesquiterpene						35.85
	Total % of titerpene						0.43
	Total % of diterpene					0.64	0.74

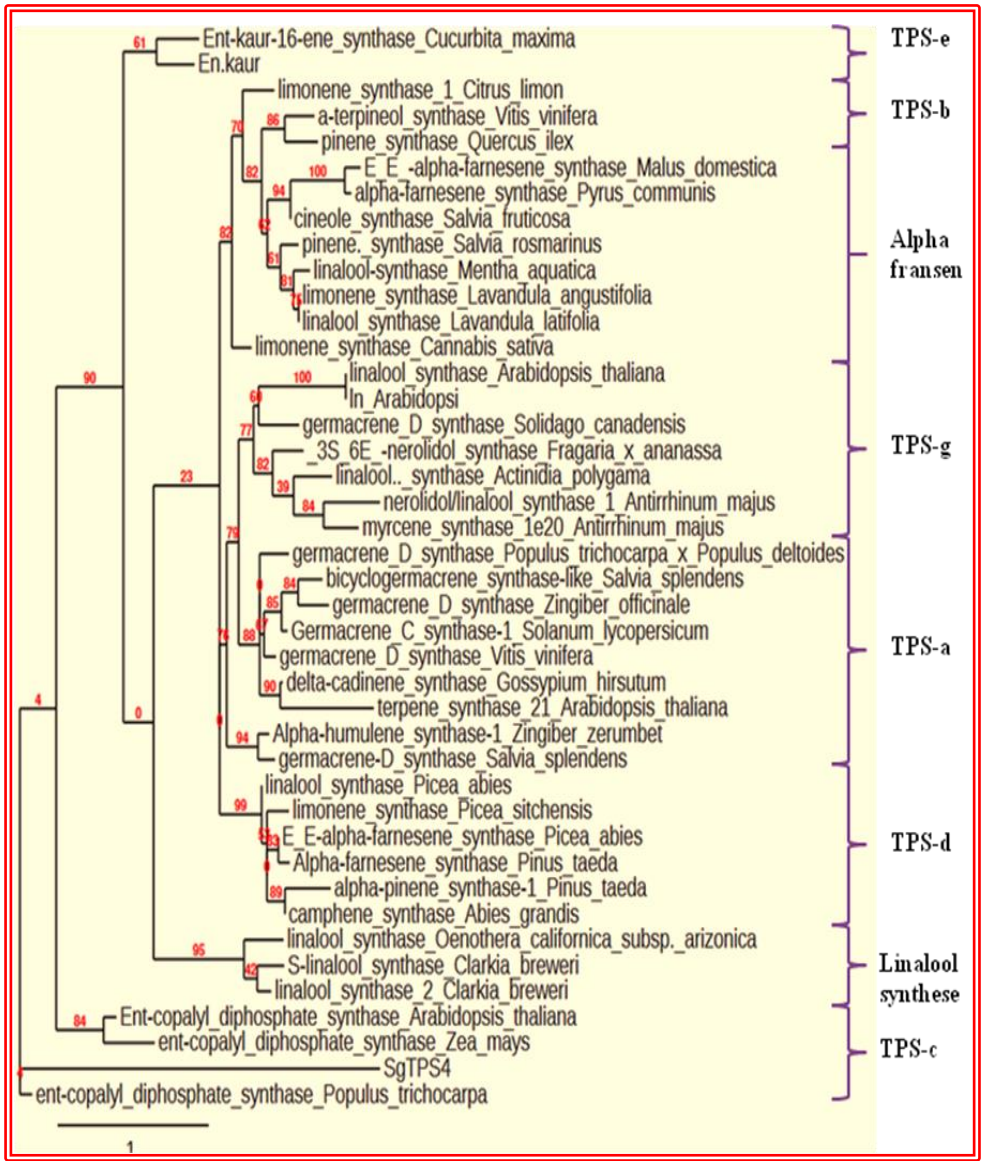

Fig. (1): Phylogenetic tree of *SgTPS4* with selected terpene synthases from other plants. Seven previously identified TPS subfamilies (Tps-a to Tps-g) were chosen based on Bohlmann *et al*., (1998) and Danner *et al*., (2011). The alignment was performed using the PhyML server. The numbers indicated are the actual bootstrap values of the branches.

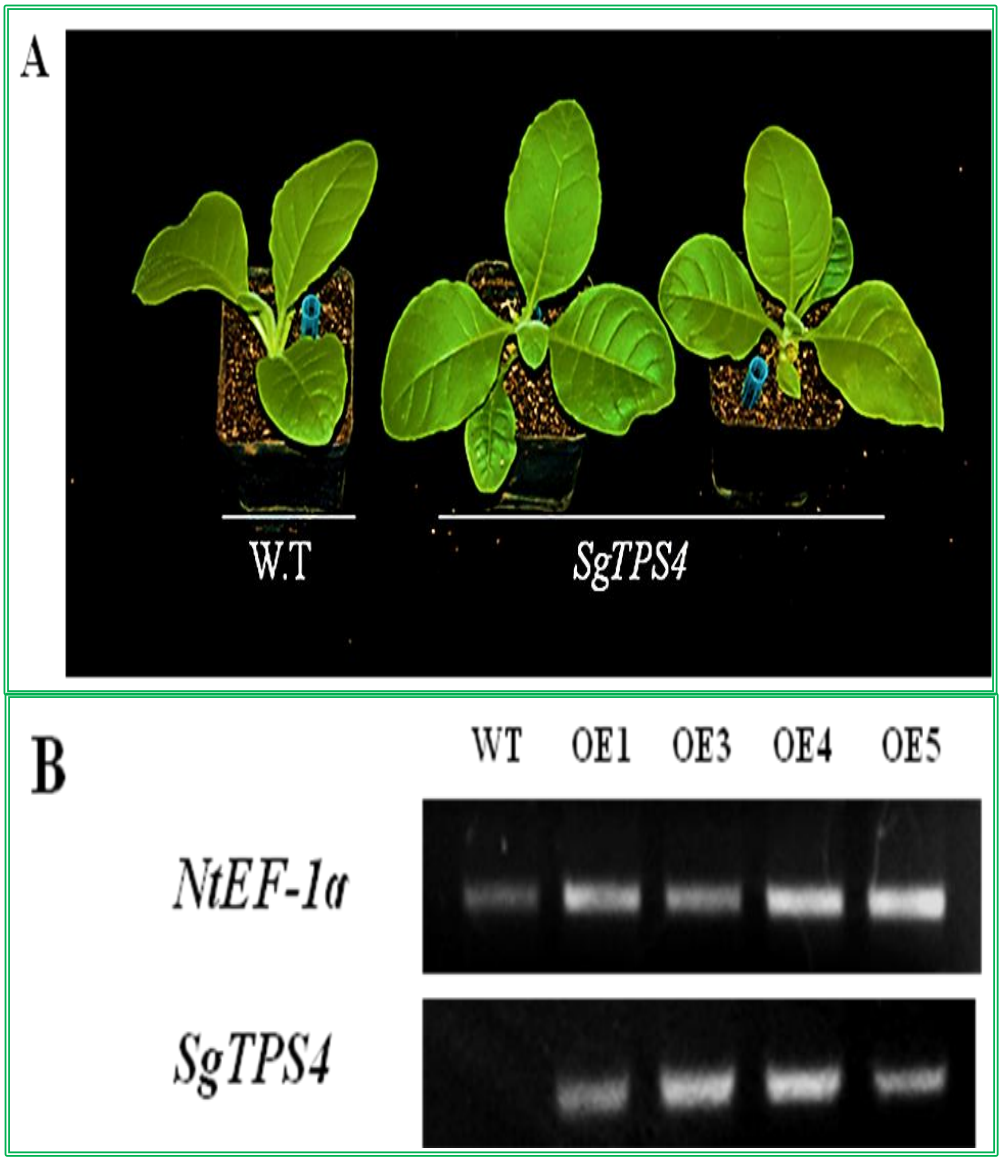

Fig. (2): Overexpression of *S. guaranitica* Terpene synthase 4 gene (*SgTPS4*) in transgenic tobacco. (A) Comparison of the phenotypes of the transgenic *N. tabacum* and wild type (W.T) *N. tabacum*. (B) Semiquantitative RT-PCR to confirm the expression of Terpene synthase 4 gene.

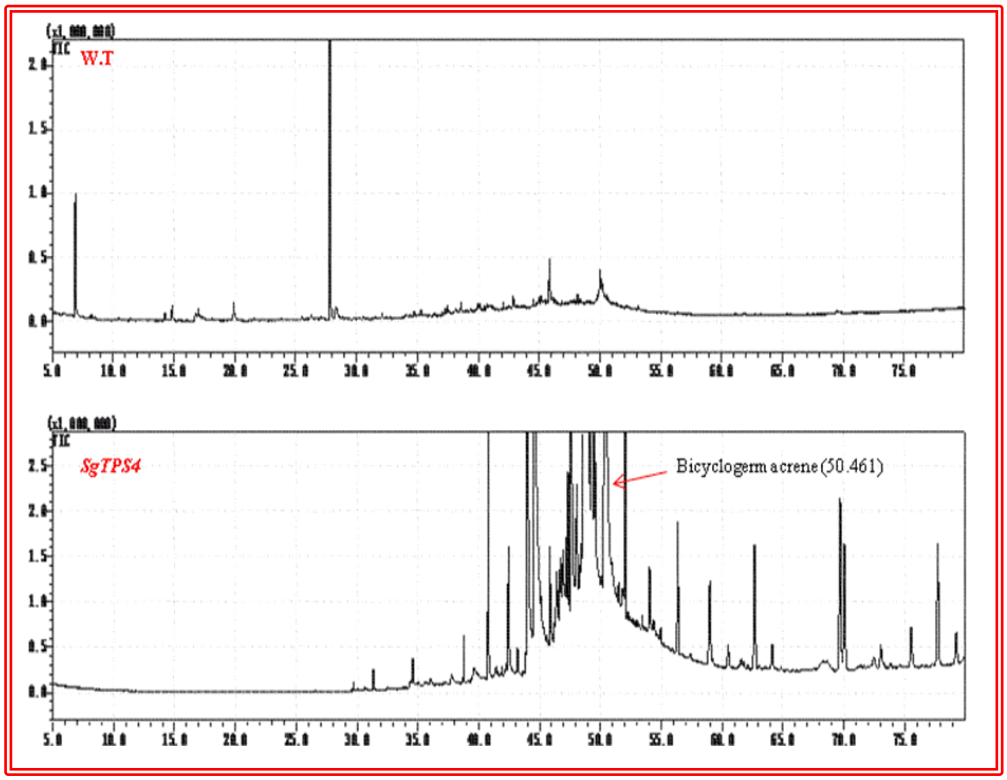

Fig. (3): Typical GC-MS mass spectrographs for terpenoids from leaf of *N. tabacum* plants.

MICRO RNA192 EVALUATION AS EARLY DIABETIC RETINOPATHY DIAGNOSTIC BIOMARKER IN Egyptian PATIENTS WITH TYPE 2 diabetes mellitus

FATH ELBAB AMANY G.[1], M. Y. NASR[1], GHADA M. I. NASR[2] AND M. I. NASR[1]

1. Molecular Biology Department, Genetic Engineering and Biotechnology Research Institute (GEBRI), University of Sadat City, Egypt
2. Molecular Diagnostics Department, Genetic Engineering and Biotechnology Research Institute (GEBRI), University of Sadat City,Egypt

Keywords: Diabetes Mellitus, miRNA 192, Diabetic Retinopathy, Gene regulation.

Diabetes is a major and quickly spreading health issue on a global scale. One of the most prevalent metabolic illnesses in the world is Type 2 Diabetes Mellitus (T2DM), which is primarily brought on by the interaction of two key factors: impaired insulin production by pancreatic beta-cells and impaired insulin sensitivity in tissues (Roden and Shulman, 2019). About 90-95% of all instances of diabetes worldwide are T2DM, and this number is continually rising (Hegazi *et al*., 2015). With approximately 8,850,400 cases and an adult prevalence of 15.2%, Egypt ranks ninth globally (Azzam *et al*., 2021). Microvascular problems including retinopathy, nephropathy, and neuropathy as well as macrovascular consequences are all highly correlated with T2DM (An *et al*., 2021).

The most prevalent microvascular consequence of diabetes and the main factor contributing to blindness globally is diabetic retinopathy DR (Ting *et al.*, 2016). The World Health Organization estimates that between 1980 and 2014, the incidence of diabetes increased by around 29%, and that the frequency of diabetes-related early mortality is increasing (NCD-RisC, 2016). Due to the increased prevalence of diabetes globally, DR become the major cause of blindness in people of working age. DR has an impact on patients personally, but it also places a significant financial and healthcare cost on society (WHO, 2021).

A major class of short (22 nt) non-coding RNAs called microRNAs works to inhibit the translation of messenger RNA targets and/or hinder protein synthesis. The target messenger RNA's 3′-UTR (untranslated) region contains complementary sequences to bind (O'Brien *et al.*, 2018). Numerous critical procedures pertaining to cellular development, apoptosis, differentiation, metabolism, and immune

response are controlled by these short RNAs (Annese *et al*., (2020). MicroRNAs (miRNAs) have a role in the micro-vascularization associated with DR, and miRNAs whose expression changes during the pathogenesis of DR have been reported (Mastropasqua *et al*., 2014). Similar to this, certain miRNAs regulate the pathophysiology of DR by acting on a variety of targets, including the immune system, fibrosis, oxidative stress, inflammation, and cell function, in response to different signaling pathways. The phenotypes of serum miRNAs may develop into novel types of diagnostic indicators (Deshpande *et al*., 2018; Wang *et al*., 2019). MiR-192 is one of the earliest studied miRs that controls pathogenic pathways triggered in DR, however its impact on DR is still debatable

This study's goal was to evaluate miR-192 expression and determine its potential as blood-based biomarkers in patients with T2D who were developing diabetic retinopathy and diabetic nephropathy.

SUBJECTS AND METHODS

Study design and population

Hundred patients who attended the Internal medicine Clinic and the Diabetes Specialized Clinic at El Menoufia University Hospital were the subjects of a case study. Four groups of people were created: a healthy non-diabetic control group of 30 person, 35 diabetic patients without complications, and 35 diabetic patients and diabetic retinopathy. The study excluded participants who had a history of chronic diseases. Patients, who were being treated for diabetes using diet, oral anti-diabetic drugs, and/or insulin to achieve glycemic control, as well as those with fasting plasma glucose levels ≥ 126 mg/dl and haemoglobinA1c levels ≥ 6.5 %, were also included in this study. The participants' age, sex, fasting blood glucose (FBG) levels, glycated haemoglobin (HbA1c), serum creatinine, lipid profile, as well as alanine liver functions, and complete blood count (CBC), were all examined.

Blood collection and microRNA isolation

Participants provided peripheral blood samples (5 ml), which were drawn from them into EDTA-coated tubes for RNA isolation. Observing the guidelines provided by the manufacturer, whole blood was used to isolate total RNA that contained small RNA using the MagNA Pure Compact Nucleic Acid Isolation Kit I (Roche, Germany, Cat. no. 03730964001). RNA concentration and quality were evaluated with a NanoDrop ND-1000 spectrophotometer (Thermo Fisher Scientific, Inc.). By comparing the absorbance ratios of 260/280 nm and 260/230 nm, RNA purity was ascertained. The final concentrations of each RNA sample were identically diluted: 20 ng/µl.

Quantification of miR-192 expression level

Observing the guidelines provided by the manufacturer, 100 ng of miR was reverse transcribed into complementary DNA (cDNA) using the Reverse Tran-

scription Kit (Thermo Scientific) and stem-loop primers unique to miRNA. With the Real-time 7500 Fast PCR System and Applied Biosystems' SensiSMARTTM SYBR Master Mix, the quantitative Real-Time (qRT-PCR) analysis was carried out twice (Thermo Fisher Scientific). Each reaction had a final volume of 20 µl and contained a cDNA template, SensiSMARTTM SYBR Master Mix, and nuclease-free water. The Applied Biosystems Application Note recommended using the non-coding short RNA U6 snRNA (internal control). The relative expression levels of the target miRNAs were demonstrated using the difference in Ct between the target miRNAs and U6 snRNA (ΔCt), which is comparable to the ratio of log2-transformed absolute copy numbers. Predenaturation at 95ºC for 2 minutes, followed by 40 cycles of 95ºC for l0 seconds of denaturation and 60ºC for 1 minute of annealing and extension, were the prescribed reaction conditions set in accordance with the manufacturer's protocol. The difference between the cycle threshold (CT) value of miRNA-192 and the average CT value of reference genes across all samples in a particular sample set serves as the expression for this miRNA.

Statistical Analysis

Utilizing SPSS (Statistical Package for Social Sciences) version 25 for Windows®, the gathered data were coded, processed, and analyzed (IBM SPSS Inc, Chicago, IL, USA). Frequency distributions and relative percentages were used to display qualitative data. To compare between two or more sets of qualitative variables, the chi-square test (χ^2) was used. The mean SD format was used to express quantitative data (Standard deviation). To compare between two independent groups of normally distributed variables, the independent samples t-test was utilized (parametric data). Two-tailed P values were used to determine statistical significance ($p<0.05$). In order to calculate the diagnostic indices (sensitivity, specificity, positive and negative predictive values, and accuracy) for micro-RNA 192, the Receiver Operating Curve (ROC) test was employed to distinguish between the diseased (diabetic retinopathy) and un-diseased (control) groups.

RESULTS

Demographic and clinical data of study participants

Table (1) summarizes the demographic and biochemical data for both patients and healthy controls. The current study involved 70 T2DM patients—38 males and 32 females-as well as 30 healthy people, of whom 16 were men and 14 were women. Patients with T2DM were divided into two groups: those without ocular problems, consisting of 35 individuals (22 male and 13 female), and those with DR, consisting of 35 patients (24 males and 11 females). Regarding age and sex distribution, there were no statistically significant variations between the two groups. Diabetes patients had significantly higher levels of the biochemical

markers FBG, HbA1c, total cholesterol, LDL, HDL, and triglycerides, as well as ALT and AST, than healthy controls ($P<0.05$).

Blood relative expression of miR-192 and diabetic complications

The expression levels of miR-192 in the blood of diabetic patients and healthy non-diabetic controls were assessed using qRT-PCR analysis. The largest value was in patients with DR with a significant difference. The relative expression of miR-192 in diabetic patients' blood indicated a direct link with diabetes complications. The expression level of miR-192 shown in Table (2) is explained by data. In terms of DR severity, the level considerably rises as the disease progresses. Table (3) displayed the correlation between biochemical variables and the levels of mir-192 expression in each group under investigation.

After ROC analysis (Fig. 1), the area under the curve (AUC) for miR-192 was 0.967 (95% confidence interval [CI], CI0.790 - 1.000) with DR. A cutoff value of >0.68 was chosen from a range of ROC analysis cutoff values, as the sensitivity of 83.3% and specificity of 100% at the selected cutoff were optimal for miR-192 with DR (Table 4).

DISCUSSION

It is acknowledged that type 2 diabetes is a serious public health problem that has a significant impact on human life and healthcare costs. In many regions of the world, rapid economic growth and urbanization have led to an increase in the prevalence of diabetes (Onyango and Onyango, 2018). The majority of people with T2DM have at least one complication, such as DR, which are the leading causes of morbidity and mortality (Zheng *et al*., 2017). The ability of traditional diabetes indicators like FBG and HbA1c to predict the likelihood of acquiring diabetic complications in a sensitive group is limited. MiRNAs have the ability to be more effective problem-specific indicators associated with diabetes. Current treatment approaches for diabetes management worldwide need for the discovery of distinctive miRNA profiles to identify diabetes and, ideally, to determine the likelihood of acquiring diabetes-related problems in a vulnerable population (Banerjee *et al*., 2017).

In this study, there was no statistically significant difference in age or gender distribution across the analyzed groups. This is in line with the findings of Saadi *et al*., (2019), who observed no significant changes in gender or age distribution across all study groups. In terms of biochemical analysis, FBG, HbA1c, Cholesterol, Triglyceride, LDL ($P<0.001$), HDL ($P<0.05$), and ALT, AST ($P<0.001$) all increased statistically significantly in the current study. This is in line with Rai and Rai (2018), who found that T2DM without complications and T2DM with nephropathy had significantly higher TC, TG, LDL-c, and HbA1c values when compared to controls. T2DM

without complications and T2DM with nephropathy had significantly lower HDL-c levels when compared to controls.

The focus of this study was to confirm if miRNA-192 expression level variations are implicated in diabetes microvascular complications and know if there is a correlation between miRNA-192 expressions and diabetic retinopathy, with the purpose of diagnosis. Compared to the control group, all diabetic groups had significantly higher mean expression levels of circulating miRNA-192, according to the study's findings (P< 0.0001). These results are in line with those of Khamis *et al*. (2021), who discovered that neutrophil gelatinase-associated lipocalin (NGAL) and miRNA-192 levels were significantly higher in T2DM patients. Hamdia *et al*. (2013) demonstrated that diabetics have blood miR-192 levels that are significantly higher than non-diabetics, with levels even higher in patients with long-term disease without microvascular problems. In contrast to Ma *et al*., (2016) and Lotfy *et al*., (2021), who found a statistically significant decrease in micro RNA-192 levels in macro-albuminuria compared to other groups, as well as in microalbuminuria compared to normal albuminuria and healthy control.

In the present study, there was a significant positive association between the levels of miRNA 192 expression and the diabetic retinopathy group's blood sugar, HbA1c, and cholesterol (P<0.05), but not with triglycerides, HDL cholesterol, ALT, or AST (P> 0.05). Creatinine showed a negative connection (P<0.05). While in keeping with the same study's findings regarding creatinine, Yang *et al*. (2017) discovered that the expressions of serum miR-192 were adversely linked with HbA1c.

In this study with DR, the area under the curve (AUC) of miR192 was 0.967 (95 % confidence interval [CI], CI0.790 - 1.000). A cutoff value of >0.68 was chosen because miR-192 had a sensitivity of 83.3 % and a specificity of 100 % at the chosen cutoff, As a result of these findings, it was shown that detecting miR192 lowered the incidence of false positives in diabetic retinopathy patients.

CONCLUSION

According to the findings, upregulated expression of miRNA-192 in type 2 diabetes is a risk factor for the progression of renal and ocular complications in diabetics. MiRNA-192 may act as early markers of changes in particular biological processes in the retina, as well as molecular signatures in diabetic microvascular complications. In clinical practice, the miR192 cutoff values were crucial. The diagnostic, prognostic, therapeutic, and use of anti-miRNA-192 in different diabetic microvascular problems all need further investigation. We can increase the sample size, follow the cases, and go more deeply into the underlying mechanism in the future

Funding: None

ABSTRACT

Background and Objective: Short non-coding RNAs known as microRNAs have been associated with different disorder types, like diabetes mellitus (DM) and its complications such diabetic retinopathy and nephropathy. In order to ealy diagnose diabetic retinopathy (DR), the study purpose was to assess the expression level of miRNA 192 in type 2 diabetes patients and explore its association with these problems.

Subjects and Method: The participants in the current study were 30 healthy non-diabetic people and 70 type 2 diabetes patients who were categorized into two main groups according to the time from the onset of DM (age and sex-matched). Diabetic retinopathy is one of the most common consequences of diabetes. The complete set of data was collected, including sociodemographic and laboratory data. RT-PCR assay was used to determine the levels of miRNA192 expression in whole blood.

Results: All diabetic groups, particularly diabetic patients with retinopathy, had mean expression levels of miRNA 192 that were considerably greater than those of healthy subjects. The expression levels of miRNA 192, blood glucose and HbA1c, were significantly positively correlated in the group with diabetic retinopathy. Mir-192 had a sensitivity of 83.3% in diabetic retinopathy and specificity of 100 % at the specified cut-off.

Conclusion: According to the findings, up-regulated of miRNA 192 in type 2 diabetes is correlated to the prevalence of diabetic retinopathy. Warning indications of diabetes complications could be miRNA 192.

REFERENCES

An J., Nichols G. A., Qian L., *et al.* (2021). Prevalence and incidence of microvascular and macrovascular complications over 15 years among patients with incident type 2 diabetes. BMJ Open Diabetes Research and Care, 9:e001847.

Annese T., Tamma R., De Giorgis M. and Ribatti D., (2020). microRNAs Biogenesis, Functions and Role in Tumor *Angiogenesis*. Front. Oncol. 10:581007 doi:10.3389/fonc. 2020. 581007.

Azzam M. M., Ibrahim A. A. and Abd El-Ghany M. I., (2021). Factors affecting glycemic control among Egyptian people with diabetes attending primary health care facilities in Mansoura District. Egypt J. Intern Med 33: 33.

Banerjee J., Nema V., Dhas Y. and Mishra N., (2017). Role of MicroRNAs in Type 2 Diabetes and Associated Vascular Complications. Biochimie. 139: 9-19.

Deshpande S., Abdollahi M., Wang M., Lanting L., Kato M., Natarajan R., (2018). Reduced autophagy by a microRNA-mediated signaling cascade in diabetes-induced renal glomerular hypertrophy. Scientific Reports, 8(1):p. 6954.

Hamdia E., Abdelwahab M., Fatma A. *et al.* (2013). Expression of micro RNA192 in type 2 diabetes mellitus relation to glycemic control, metabolic abnormalities, renal and ocular complications. Am J Biochem., 3: 97- 106.

Hegazi R., El-Gamal M., Abdel-Hady N. and Hamdy O., (2015). Epidemiology of and risk factors for type 2 diabetes in Egypt. Ann Glob Health, 81:814-820.

Khamis S. S., Yassin Y. S., Tawfeek A. R., Kasem H. E., Ibrahim S. M., and Ghonamy E., (2021). Role of microRNA as a marker in detection of diabetic nephropathy in type-2 diabetic Egyptian patients. J. Egypt Soc. Nephrol Transplant, 21:167-73.

Lotfy E., Ayoub M., Mohamed L. and Elsayed H., (2021). Study of MicroRNA192 as an Early Marker of Nephropathy in Type 2 Diabetic Patients. The Egyptian Journal of Hospital Medicine, 85: 4046-4051.

Ma X., Lu C., Lv C., *et al.* (2016). The expression of miR192 and its signifcance in diabetic nephropathy patients with different urine albumin creatinine ratio. J. Diabetes Res., 16: 6789402.

Mastropasqua R., Toto L., Cipollone F., D., Santovito, Carpineto P., and Mastropasqua L., (2014). “Role of microRNAs in the modulation of diabetic retinopathy,”Progress in Retinal and eye Research, vol. 43: 92-107.

NCD Risk Factor Collaboration (NCD-RisC, 2016). Worldwide trends in diabetes since 1980: a pooled analysis of 751 population-based studies with 4.4 million participants. Lancet. 2016 Apr 9;387(10027):1513-1530. doi: 10.1016/S0140-6736(16)00618-8.

Onyango E. M. and Onyango B. M., (2018). The rise of noncommunicable diseases in Kenya: an examination of the time trends and contribution of the changes in diet and physical inactivity. J Epidemiol Glob Health; 8:1-7.

O'Brien J., Hayder H., Zayed Y. and Peng C., (2018). Overview of MicroRNA Biogenesis, Mechanisms of Actions, and Circulation. Front. Endocrinol. 9:402. doi: 10.3389/fendo. 2018.00402

Rai Srinidhi and Rai Tirthal., (2018). Lipid profile in Type 2 diabetes mellitus and in diabetic nephropathy. 4.

Roden M., and Shulman G. I. (2019). The integrative biology of type 2 diabetes. Nature, 576:51-60.

Saadi G., El Meligi A. and El-Ansary M. *et al.* (2019). Evaluation of microRNA-192 in patients with diabetic nephropathy. The Egyptian Journal of Internal Medicine, 31: 122-128.

Ting D. S. W., Cheung G. C. M., and Wong T. Y., (2016). Diabetic retinopathy: global prevalence, major risk factors, screening practices and public health challenges: a review. Clinical & Experimental Ophthalmology, 44: 260-277. doi: 10.1111/ceo.12696.

Wang T., Zhu H., Yang S., and Fei X., (2019). Let-7a-5p may participate in the pathogenesis of diabetic nephropathy through targeting HMGA2. Molecular Medicine Reports, 19: 4229-4237.

WHO (2021). *Diabetes.* Available online at: https://www.who.int/news-room/fact-sheets/detail/diabetes (accessed March 2, 2022).

Yang X., Liu S., Zhang R., Sun B., Zhou S., Chen R., and Yu P., (2017). Microribonucleic acid-192 as a specific biomarker for the early diagnosis of diabetic kidney disease. Journal of diabetes investigation, 9: 602-609. Advance online publication.

Zheng Y., Ley S. H., and Hu F. B., (2017). Global aetiology and epidemiology of type 2 diabetes mellitus and its complications. Nature Reviews Endocrinology, 14: 88-98.

Table (1): Data on the demographics and biochemistry of the all study population.

Variables		Control (n=30)	Diabetic (n =35)	DR (n=35)	P-value
Gender: M/F		16/14	22/13	24/11	P>0.05
Age		45.67 ± 5.99	48.03 ± 4.71	46.71 ± 5.17	P>0.05
Duration of T2DM		--	5.3±1.21	5.9± 3.56	P>0.05
FBG(mg/dl)		79.4±4.7	142.5±15.1	157.3±19.8	P<0.001
HbA1C (%)		4.9±0.5	7.6±0.4	8.2±0.6	P<0.001
Cholesterol(mg/dl)		167.2±21.4	189.6±22.8	229.5±24.6	P<0.001
Triglyceride(mg/dl)		132.5±18.8	191.1±28.3	249.3±37.6	P<0.001
HDL cholesterol(mg/dl)		51.4±2.3	48.6±3.5	46.9±3.4	P>0.05
LDL cholesterol(mg/dl)		103±19.1	107±18.5	128±28.5	P<0.001
ALT(IU/L)		18.39±7.42	28.8± 7.2	30.4± 6.9	P<0.0001
AST(IU/L)		20.29±8.24	29.3 ± 7.9	32.6± 7.7	P<0.0001
Creatinine (mg/dl)		0.77±0.17	0.79±0.18	0.74±0.13	P>0.05
CBC	Hb	11.6±2.3	11.2±2.6	10.8±3.1	P>0.05
	TLC	6.6±3.9	6.9±3.8	7.1±4.1	P>0.05
	PLT	223±52.9	214±54	205±49	P>0.05

P value< 0.05 is significant

Table (2): Comparison of the expression levels of miRNA 192 in all studied groups.

Groups	miRNA192 mean± SD	*P* value
Non-diabetic healthy Control	0.40± 0.23459	P < 0.0001
T2DM	2.568± 0.539	
Diabetic retinopathy (DR)	4.624± 1.33	

Table (3): Correlations between mir-192 expression levels with biochemical Parameters in patient groups.

mir-192 expression level	T2DM (n = 30)		DR (n = 35)	
	r	P	r	P
FBG(mg/dl)	-0.66	<0.05	0.70	<0.05
HbA1c (%)	-0.54	<0.05	0.74	<0.05
Cholesterol (mg/dl)	1	<0.05	0.99	<0.05
Triglyceride (mg/dl)	-0.38	>0.05	0.98	>0.05
HDL cholesterol (mg/dl)	-0.46	>0.05	0.95	>0.05
ALT(IU/L)	-0.5	>0.05	0.48	>0.05
AST(IU/L)	-0.5	>0.05	0.44	>0.05
Creatinine	- 0.26	<0.05	-0.38	<0.05

r: Pearson correlation significance at P<0.05

Table (4): Validity of micro RNA-192 in the diagnosis of DR.

Parameters	Cutoff value	AUC	95% CI	Sensitivity	Specificity	PPV	NPV	P-value
DR	>0.68	0.967	0.790 -1.000	83.3%	100%	100%	85.7%	<0.001

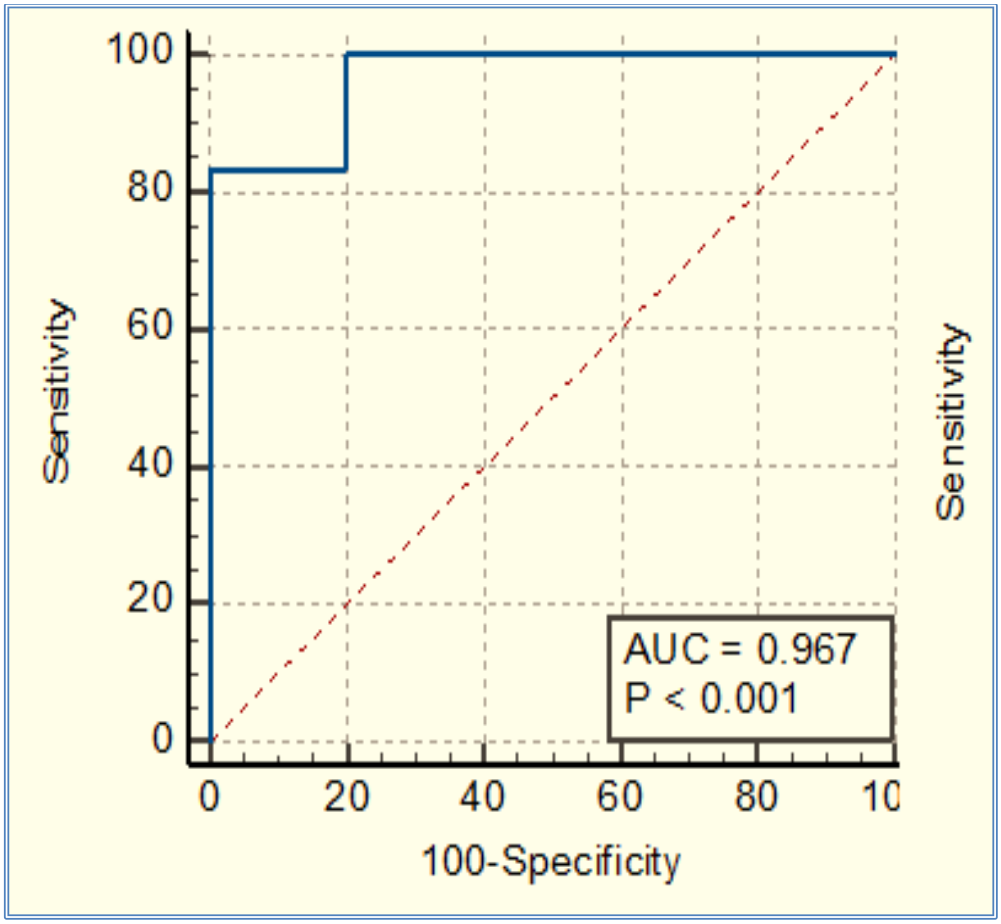

Fig. (1): The ROC curve of miR-192 in DR group.

MOLECULAR EVALUATION OF CELL CYCLE INHIBITORS AFTER *Hepatocellular carcinoma* (HCC) TREATMENT *In Vitro*

NASR M. Y. [1], MONA M. DARWISH [2], A. F. ELSABRUTI[3], WA. H. ROSHDY [4], AND H. A. EL-RABEAY[5]

[1] (Molecular Cell Biology & Molecular Biology Department, Genetic Engineering and Biotechnology Research Institute, (GEBRI)University of Sadat City, Egypt.).

[2] (Chemistry Department, Faculty of Sciences, Zagazig University, Egypt.

[3] Postgraduate Researcher, Alexandria University, Egypt.

[4] (Central Public Health Laboratories, Ministry of Health and Population, Cairo, Egypt.

[5] (Bioinformatics Department Genetic Engineering and Biotechnology Research Institute, (GEBRI)University of Sadat City, Egypt.

Key words: Hepatocellular carcinoma (HCC), HUH-7, Liver Cancer, P21, c-MYC, Cell cycle, Graphene quantum dots (GQDs), nano medicine

Cancer arises from the transformation of normal cells into tumor cells in a multi-steps process that normally progresses from a pre-cancerous lesion to a malignant tumor. Richard Doll and Richard Peto produced a groundbreaking study on the aetiology of cancer in 1981 that was partially based on an analysis of cancer incidence in numerous nations. A World Health Organization expert committee came to the conclusion that frequent deadly cancers are potentially preventable because of lifestyle choices and other environmental factors, such as hormone imbalances, dietary inadequacies, and environmental carcinogens, in 1964 (Colditz *et al*., 2005).

Cancer is neither a single type nor a new disease. According to a recent study by Faguet (2015), more than 200 distinct forms of cancer have been found in humans, depending on the type of tissue. Cancer was described in several ancient texts, including Egyptian "Edwin Smith" and "George Ebers" papyri written between 3000 BC and 1500 BC (Faguet, 2015).

According to estimates from the year 2000, liver cancer is still the eighth most prevalent disease in women and the fifth most common cancer in men worldwide. An estimated 564,000 new cases, including 166,000 women and 398,000 men, are reported per year. Liver cancer can develop before the age of 20 in high-risk nations, although it rarely occurs before the age of 50 in low-risk nations. Male liver cancer rates are typically 2 to 4 times greater than female rates (Bosch *et al*., 2004).

HCC is the most frequent primary liver cancer and the leading cause of cancer-related mortality globally (O'Connor *et al*., 2018). Despite breakthroughs in preventative strategies, screening, and new diagnostic and treatment technologies, incidence and fatality rates continue to climb (Balogh *et al*., 2016). ACS Cancer Facts & Figures, (2022) Conducted a research shows that many variables are known to increase the chance of acquiring cancer, some of which are controlled (such as cigarette smoking and excess body weight), while others are not, even if the mechanics of cancer formation are not completely understood (e.g., inherited genetic mutations). These risk factors may initiate or accelerate the progression of cancer, either simultaneously or sequentially (Cancer Facts & Figures 2022, ACS).

More than 90% of primary liver tumors are hepatocellular carcinomas (HCC), which are primary tumors of the liver. Of patients with cirrhosis, HCC affects about 85% of them (Ioannou *et al*., 2007).

Tumorigenesis is caused by an imbalance between cell growth and cell death (apoptosis). p21, a wellknown cyclindependent kinase (cdk) inhibitor, was shown to be critical in regulating cell cycle progression (Harper *et al*., 1993).

The p21 gene is changed in a number of malignancies and works as a cell cycle inhibitor and anti-proliferative effector in normal cells (Wan *et al*.,1996). Some evidences indicated the link between tumor development and p21 protein alteration (Mousses, S. *et al*., 1995) The role of p21 in phenotypic plasticity and its oncogenic/anti-apoptotic activity, dependent on p21 subcellular localization and p53 status, have lately been thoroughly investigated, despite the fact that the tumor-suppressor function of p21 has gotten the greatest attention in cancer research (Shamloo & Usluer, 2019).

According to a review made by Prochownik (2004), c-MYC is involved in the control of a number of normal cellular functions, which includes differentiation, proliferation, and maintenance of cell size, regulation of the intercellular redox state, angiogenesis and apoptosis. In cancer cells this is frequently dysregulated as many of the c-MYC transcription factor's target genes encode proteins that initiate and sustain the transformed state (Prochownik, 2004).

Given the role of c-Myc in HCC carcinogenesis, it's no surprise that it's an appealing target for creating new therapeutics. The first evidence that c-Myc downregulation can be utilized to treat HCC comes from an inducible c-Myc animal model, in which c-Myc inactivation triggered the regression and differentiation of liver tumors (Lin *et al*., 2010).

Despite significant improvements, the present strategy for treating cancer is fundamentally reductionist. Single molecular aberrations or cancer pathways have been the focus of successful treatment interventions that have marginally improved survival in several cancers. The

"magic bullet" approach of using a single medicine to target a specific characteristic or route, however, is unlikely to result in the cure of cancer (Zugazagoitia *et al*., 2016).

The discovery and implementation of various nanotechnologies for more efficient and safe cancer treatment—hereafter referred to as cancer nanomedicine—was spurred by the inherent limitations of conventional cancer therapies (Shi *et al*., 2016). Engineered nanoscale materials have been created as new prototypes for biomedical applications and improved therapy as a result of recent advancements in nanotechnology and biotechnology. Numerous nanomaterials have been created as a result of their distinctive characteristics, which include a large surface area, structural characteristics, and a longer blood circulation time than small molecules. These materials have the potential to completely change how diseases are detected and treated (Sanna *et al*., 2014).

Nanomaterials from the graphene family, such as graphene oxide and reduced graphene, have been the subject of numerous investigations. These investigations ultimately led to the creation of GQDs by Ponomarenko and Geim in 2008, which signaled the start of a wealth of medicinal applications. Then, researchers concentrated their attention on GQDs and discovered that they are the best quantum dots for biological applications (Xu *et al*., 2013).

GQDs the most recent member of the graphene family, have sparked a lot of attention in recent years due to their excellent physical, chemical, electrical, optical, and biological properties (Iannazzo *et al*., 2020). Being a one-dimensional (0D) object (GQDs) Promising biomedical applications have been discovered due to their ultra-small size, non-toxicity, biocompatibility, high photo stability, tunable fluorescence, water solubility, and so on, garnering substantial interest in the biomedical area (Younis *et al*., 2020).

This work investigates the effect of GQDs on HCC therapy *in vitro*, through observing its effect on two key cell cycle inhibitors, the P21 and c-MYC genes.

MATERIALS AND METHODS

Chemicals

All chemicals were obtained from Egypt's Central Public Health Laboratories (CPHL). Primers were purchased from (Applied Biosystems), the RNA extraction kit from (Qiagen, Hilden, Germany), and the PCR kit HERA SYBER GREEN/ROX RT-qPCR from (Applied Biosystems) (Applied Biosystems, Foster City, California, USA). All work was done in Egypt's Central Public Health Laboratories (CPHL).

Graphene quantum dots

The graphene Quantum Dots were purchased from Sigma-Aldrich, Egypt.

Cell line and Cell culture

Human hepatocarcinoma cell line (Huh-7), the cell line was obtained from central public health laboratories in Egypt (CPHL). The cells were cultivated in T75 tissue culture flasks in low glucose Dulbecco's modified Eagle's medium (DMEM) supplemented with 10% fetal bovine serum, 100 µg/mL penicillin, 100 µg/mL streptomycin, 2 mM/L-glutamine and incubated in a 95% humidified incubator containing 5% CO2 at 37ºC. Now cells ready for treatment with Graphene quantum dots.

Cytotoxicity

To evaluate the cell viability and the cytotoxicity was assessed using the 3-(4, 5-dimethylthiazol -2-yl)-2, 5-diphenyltetrazolium bromide (MTT) assay. Briefly, cells were seeded in 96-well plates in DMEM supplemented with 10% fetal bovine serum, and 1% antibiotic antimycotic mixture. After 24 h of cell preparation, the growth medium was aspirated from each well and the cells washed with 1X phosphate buffered saline (PBS). Different concentrations of Graphene Quantum dots were two fold serially diluted in DMEM then added to cultured cells in 96-well plate in triplicate and incubated for 24 h post treatment to determine the cytotoxic concentration 50 (CC50). The medium was then removed and the monolayer of cells washed with 1X PBS three times before adding MTT solution (20 µL/well of 5 mg/ml stock solution) and incubated at 37ºC for 4 h till formulation of formazan crystals. Crystals were dissolved using a volume of 200 µL of of acidified isopropanol and the absorbance measured at λmax 540 nm using an ELISA microplate reader. Finally, the percentage of cytotoxicity compared to the untreated cells was determined. The CC50 of Graphene Quantum dots were determined from a linear exponential equation.

Cytotoxicity (%)=

(Absorbance of cell without treatment – Absorbance of cell with treatment) / Absorbance of cell without treatment X100

Real-Time RT PCR Analysis

Total RNA was extracted from cells using RNeasy Mini Kit (Qiagen) extraction kit according to the manufacturer's protocol (Qiagen, Hilden, Germany). Five hundred nanograms of purified mRNA was used to generate cDNA with random hexamer primers (Thermo Scientific) and with Reverse Transcriptase according to the manufacturer's protocol (HERA SYBR® green RT-qPCR kit). The quantitative real-time PCR (qRT-PCR) reaction mixture (25 μL) consisted of the following: 12.5 μL of Maxima SYBR green PCR master mix (Thermo Scientific), 0.5 μL of cDNA template, and 1 μL of each primer (100 μM forward and reverse primers). Reactions were run in duplicate on Applied Biosystems 7500 real-time PCR system. The cycling conditions were as follows: 2min at 50ºC, 2min at 95ºC, and 50 cycles, with 1 cycle consisting of 15 s at 95ºC and 30s at 60ºC. Threshold cycle (Ct) values were normalized to the values for β-actin house-

keeping transcripts and log fold change was calculated according to the equation of 2^-ΔΔCT (Rao *et al.*, 2013).

Gene	Primers
c-Myc	5'-CCTGGTGCTCCATGAG GAGAC-3' (forward)
	5'-CAGACTCTGACCTTTT-GCCAGG-3' (reverse)
P21	5'-GTGGCTCTGATTGGCTT TCTG-3' (forward)
	5'-CTGAAAACAGGCAGCC CAAG-3'(reverse)
β actin	5'- CACCATTGG-CAATGAGCGGTTC - 3'(forward)
	5'-AGGTCTTTGCG-GATGTCCACGT - 3'(reverse)

The primers of p21, C-MYC and β actin

RESULTS AND DISCUSSION

- **Results**

The effect of (graphene quantum dots) on HUH7 cell lines as models of human liver cancer cell lines was examined in this work. P21, c-MYC, and B.Actin as housekeeping gene (positive control).

1-Cytotoxicity of graphene quantum dots against HUH-7 Cell Lines Using MTT assay.

Cytotoxicity assays are normally based on assessing damage to cellular membranes or cell viability or cell apoptosis or cell proliferation. Creative Biolabs has explored a variety of assays for your flexible choice to best fit current results. To evaluate the cytotoxic activity of two different concentrations of the GQDs against human Liver cancer cells (HUH-7), were incubated with different concentrations (0.5% to 1%) of GQDs. After 24 hours of incubation, cell viability was determined by the MTT assay. The results of cytotoxicity assay are presented in (Fig .1).

Cytotoxicity assays are typically designed to evaluate damage to cellular membranes, cell viability, cell apoptosis, or cell proliferation. Creative Biolabs has investigated a number of assays for your flexible selection to best match my results. To assess the cytotoxic efficacy of two distinct doses of Graphene quantum dots against human liver cancer cells (HUH-7), the cells were treated with Graphene quantum dots at varying concentrations (0.5 percent to 1 percent). The MTT test was used to measure cell viability after 24 hours of incubation. The cytotoxicity assay results are shown in (Fig.1)

The cytotoxicity of the graphene quantum dots extract was evaluated in HUH7 cells using MTT assay. Graphene quantum dots were almost not toxic for studied cells up to a dose of 4.2 0r 4.3 µg/ml for graphene quantum dots. The toxic effect of tested graphene quantum dots was dose dependent. The result showed that the cytotoxic concentration 50 (CC50) value of graphene quantum dots was 4.2 OR 4.3 µg. Therefore, for further studies we selected the safe concentrations of 1 -0.5 µg/ml for subsequent cellular signal studies.

Evaluation of P21 and c-MYC gene expression after treatment with different concertation of Graphene quantum dots.

To investigate the effects of Graphene quantum dots on c-MYC and P21 expression in Hepatocellular carcinoma, reverse-transcription PCR was done after treatment with 1 -0.5 µg /ml Graphene quantum dots for various time periods (0 h, 8h, 16h, 24h, 32h, 40h, 48h, 56h, 64h and 72h). In comparison to untreated controls, gene expression of c-MYC was considerably down regulated (decreased) with 1 -0.5 µg /ml Graphene quantum dots treatment. Furthermore, when 1 -0.5 µg/ml Graphene quantum dots were used, gene expression of P21 was considerably upregulated (raised) compared to untreated controls.

Table (1) shows that, there was significant statistical increase in Graphene quantum dots 1% compared to Graphene quantum dots 0.5% at 8, 16, 32, 48, and 64 hours, (p=0.007, 0.034, 0.003, 0.038, and 0.000, respectively.

Table (2) shows that there was significant statistical increase in P21 in Graphene quantum dots 1% compared to Graphene quantum dots 0.5% at 16, 24, 32, 40, 48, 56, 64, and 72 hours, (p=0.014, 0.001, 0.000, 0.047, 0.000, 0.000, 0.000 and 0.000, respectively.

• DISCUSSION

Hepatocellular carcinoma is one of the most common causes of cancer-related death globally. The recent study discovered that Graphene dots made from spies had the ability to prevent several cancer cell types from proliferating and migrating. More cancer cells were suppressed by a combination of Graphene dots and a traditional chemotherapy medication than by either therapy by itself. Together, these results imply that Graphene dots may be a potent complementary and alternative medicine for the treatment of cancer (Xia *et al*., 2019). c-Myc is among the most frequently overexpressed genes in human cancers. Overexpression of c-Myc in hepatic cells leads to Progression of liver cancer. c-Myc can currently regulate up to 15%–20% of human genes either directly or indirectly. These genes are involved in the regulation of the cell cycle, protein synthesis, the cytoskeleton and cell motility, cell metabolism, and microRNA, which are tiny regulatory molecules that influence the stability and translation of target mRNA (Lin *et al*., 2010). Studies have found that c-Myc interacts with Miz-1 and recruit DNA methyltransferase DNMT3 to p21 promoter to silence p21 transcription, a critical step during tumorigenesis (Brenner *et al*., 2004). Results means, when we used different concentrations of curcumine(0.5-1 µg/ml) for different duration time (0 h, 8h, 16h, 24h, 32h, 40h, 48h, 56h, 64h and 72h) on different genes related to liver cancer (c-Myc and p21), this is lead to down regulation c-Myc and up regulation of P21.Given the importance of c-Myc in HCC carcinogenesis, it is not surprising that c-Myc is an attractive target for developing novel therapies. The

first evidence that down-regulation of c-Myc can be used as a strategy to treat HCC comes from an inducible c-Myc animal model, in which inactivation of c-Myc induced the regression and differentiation of liver tumors (Shachaf *et al*., 2004).

SUMMARY

Hepatocellular carcinoma (HCC) is one of the most prevalent types of cancer. HCC is the sixth most popular cancer in the world and the fourth most common cancer in Egypt, respectively. Egypt is the third and fifteenth most populated countries in Africa and the globe, respectively. The goal of this study is to examine the effect of graphene quantum dots (GQDs) on the expression of P21 & c-MYC genes on a cell line in liver cancer namely "HuH-7 cell line." The area of studying the anticancer effect of GQDs is attracting growing attention because of its valuable properties. Especially due to its nano-sized sheets, it tends to infiltrate the cell nucleus and interfere with DNA function due to its ultra-small size. The results emphasize the validity of using GQDs as anticancer agent, with varied concentrations of GQDs inhibiting the development of cancer cells (HuH-7) *via* gene up regulation.

REFERENCES

Balogh J., Victor D., Asham E. H., Burroughs S. G., Boktour M., Saharia A., Li X., Ghobrial R. M. and Monsour H. P., (2016). Hepatocellular carcinoma: A Review. Journal of hepatocellular carcinoma. 5:41-53. Retrieved September 23, 2022, from https://www.ncbi.nlm.nih.gov /pmc/ articles/PMC5063561.

Bosch F. X., Ribes J., Díaz M. and Cléries R., (2004). Primary liver cancer: Worldwide incidence and Trends. Gastroenterology, 127(5):s5-s16 https://doi.org/ 10.1053/j.gastro.2004.09.011.

Brenner C., Deplus R., Didelot C., Loriot A., Vir E., De Smet C., Gutierrez A., Danovi D., Bernard D., Boon T., Giuseppe Pelicci P., Amati B., Kouzarides T., de Launoit Y., Di Croce L. and Fuks F., (2004). Myc represses transcription through recruitment of DNA methyltransferase corepressor. The EMBO Journal, 24(2): 336-346. https://doi.org/10.1038/sj.emboj.7600509.

Cancer facts and; figures (2022). American Cancer Society. (n.d.). from https://www.cancer.org/research/cancer-facts-statistics/all-cancer-facts-figures/cancer-facts-figures-2022.html#:~:text=The Facts & Figures annual report,deaths in the United States.

Colditz G. A., Sellers T. A. and Trapido E., (2005). Epidemiology-identifying the causes and preventability of cancer? Nature Reviews Cancer, 6:75-83. https://doi.org/10.1038/nrc1784.

Faguet G. B. (2015). A brief history of cancer: age-old milestones underlying our current knowledge database. International journal of cancer, 136: 2022-2036.

Harper J. W., Adami G. R., Wei N., Keyomarsi K. and Elledge S. J. (1993). The p21 Cdk-interacting protein Cip1 is a potent inhibitor of G1 cyclin-dependent kinases. Cell, 75: 805-816.

Iannazzo D., Celesti C. and Espro C., (2020). Recent advances on graphene quantum dots as multifunctional Nanoplatforms for cancer treatment. Biotechnology Journal, 16(2):1-13. 1900422. https://doi.org/10.1002/biot. 201900422.

Ioannou G. N., Splan M. F., Weiss N. S., McDonald G. B., Beretta L. and Lee S. P., (2007). Incidence and predictors of hepatocellular carcinoma in patients with cirrhosis. Clinical Gastroenterology and Hepatology, 5(8):938-945. https://doi.org/10.1016/j.cgh.2007.02.039.

Lin C. P., Liu C. R., Lee C. N., Chan T. S. and Liu H. E., (2010). Targeting C-myc as a novel approach for hepatocellular carcinoma. World Journal of Hepatology, 2(1): 16-20. https://doi.org/10.4254/wjh.v2.i1.16

Mosmann T. (1983). Rapid colorimetric assay for cellular growth and survival: application to proliferation and cytotoxicity assays. J. Immunol Methods. Dec 16, 65 (1-2):55-63. doi:10.1016/0022-1759(83)90303-4. PMID: 6606682.

Mousses S., Ozçelik H., Lee P. D., Malkin D., Bull S. B. and Andrulis I. L., (1995). Two variants of the CIP1/WAF1gene occur together and are associated with human cancer. Hum. Mol. Genet., 4: 1089-1092.

O'Connor S., Ward J. W., Watson M., Momin B. and Richardson L. C., (2010). Hepatocellular carcinoma-United States, 2001-2006. Morbidity and Mortality Weekly Report, 59(17): 517-520.

Prochownik E. V. (2004). C-myc as a therapeutic target in cancer. Expert Review of Anticancer Therapy, 4(2): 289-302. https://doi.org/10.1586/14737140.4.2.289

Shachaf C. M., Kopelman A. M., Arvanitis C., Karlsson Å., Beer S., Mandl S., Bachmann M. H., Borowsky A. D., Ruebner B., Cardiff R. D., Yang Q., Bishop J. M., Contag C. H. and Felsher D. W., (2004). Myc inactivation uncovers pluripotent differentiation and tumour dormancy in hepatocellular cancer. Nature, 431(7012): 1112-1117.

https://doi.org/10.1038/nature03043.

Sanna V., Pala N. and Sechi M., (2014). January 15). Targeted therapy using nanotechnology: Focus on cancer: IJN. International Journal of Nanomedicine. 9:467-483. Retrieved from https://doi.org/10.2147%2FIJN.S36654.

Shamloo and Usluer. (2019). P21 in cancer research. Cancers, 11(8): 1178. https://doi.org/10.3390/cancers11081178.

Shi J., Kantoff P. W., Wooster R. and Farokhzad O. C., (2016). Cancer nanomedicine: Progress, challenges and opportunities. Nature Reviews Cancer, 17(1): 20-37. https://doi.org/10.1038/nrc.2016.108.

Wan M., Cofer K. and Dubeau L., (1996). WAF1/CIP1 structural abnormalities do not contribute to cell cyclederegulation in ovarian cancer. Br. J. Cancer, 73: 1398-1400. doi:10.1038/bjc.1996.265.

Xia Haoran, Ma Zhu, Xiao Zheng, Zhou Weiya, Zhang Hua, Du Caichen, Zhuang Jia, Cheng Xiaowei, Xingchong Liu and Yuelong Huang, (2019). Interfacial modification using ultrasonic atomized graphene quantum dots for efficient perovskite solar cells, Organic Electronics, Vol. 75, 105-415, ISSN 1566-1199, https: //doi.org /10.1016/j. orgel.2019.105415.

Xu C., Yan Z., Zhou L. and Wang Y., (2013). A comparison of glypican-3 with alpha-fetoprotein as a serum marker for hepatocellular carcinoma: A meta-analysis. Journal of Cancer Research and Clinical Oncology, 139(8): 1417-1424. https: //doi.org/10.1007/s00432-013-1458-5.

Younis M. R., He G., Lin J. and Huang P., (2020). Recent advances on graphene quantum dots for bioimaging applications. Frontiers in Chemistry, 8:424. https://doi.org/10.3389/fchem.2020.00424.

Zugazagoitia J., Guedes C., Ponce S., Ferrer I., Molina-Pinelo S. and Paz-Ares L., (2016). Current challenges in cancer treatment. Clinical Therapeutics, 38(7): 1551-1566. https://doi.org/10.1016/j.clinthera.2016.03.026.

Table (1): Effect of concentration of Graphene quantum dots 0.5% and 1% on c.MYC expression on Cell line: HUH7.

concentration of Graphene quantum dots 0.5% and 1% on Cell line: HUH7 on C-MYC expression				
Hours	Graphene quantum dots 1% on Cell line: HUH7	Graphene quantum dots 0.5% on Cell line: HUH7	T test	P value
0	22.41±0.025	22.43±0.230	0.125	0.907
8	26.87±0.321	25.24±0.122	8.210	0.007*
16	30.23±0.306	29.31±0.020	5.224	0.034*
24	31.267±0.586	31.23±0.045	0.098	0.926
32	33.00±0.173	32.103±0.108	7.612	0.003*
40	35.43±0.611	34.62±0.153	2.246	0.140
48	37.08±0.473	36.23±0.047	3.039	0.038*
56	38.37±0.666	37.94±0.049	1.098	0.334
64	39.99±0.100	39.02±0.072	12.363	0.000*
72	39.97±0.058	39.07±0.025	0.183	0.867

Table (2): Effect of concentration of Graphene quantum dots 0.5% and 1% on P21 gene expression.

concentration of Graphene quantum dots 0.5% and 1% on Cell line: HUH7 on P21 Expression				
Hours	Graphene quantum dots 1% on Cell line: HUH7	Graphene quantum dots 0.5% on Cell line: HUH7	T test	P value
0	30.00±0.092	29.94±0.046	1.014	0.387
8	28.20±0.269	28.56±0.081	2.237	0.135
16	26.40±0.252	26.99±0.101	3.757	0.041*
24	24.32±0.095	25.557±0.031	21.384	0.001*
32	23.71±0.035	27.03±0.104	52.152	0.000*
40	23.08±0.101	26.063±1.178	4.369	0.047*
48	21.20±0.095	23.973±0.021	49.311	0.000*
56	19.62±0.046	21.97±0.015	84.144	0.000*
64	19.04±0.061	21.697±0.100	39.169	0.000*
72	18.64±0.076	20.92±0.03	48.610	0.000*

Table (3): Effect of graphene quantum dots concentration 1% on gene expression of C.Myc in cell line HuH7.

Hours	c.MYC	B. Actin	ΔCt	ΔΔCt	2^-ΔΔCt	log (2^-ΔΔCt)
0 hr	22.4	22	0.4	0	1	0
8 hr	26.9	22.2	4.7	4.3	0.051	-1.294
16 hr	30.2	22.4	7.8	7.4	0.006	-2.228
24 hr	31.3	22.1	9.2	8.8	0.002	-2.649
32 hr	33	22.6	10.4	10	1E-03	-3.01
40 hr	35.4	23	12.4	12	2E-04	-3.612
48 hr	37	22.8	14.2	13.8	7E-05	-4.154
56 hr	38.4	22.9	15.5	15.1	3E-05	-4.546
64 hr	40	23.1	16.9	16.5	1E-05	-4.967
72hr	40	23.6	16.4	16	2E-05	-4.816

Table (4): Effect of graphene quantum dots concentration 1% on gene expression of P21 in cell line HuH7 for 72 hours.

	P21	B. Actin	ΔCt	ΔΔCt	2^-ΔΔCt	log (2^ΔΔCt)
0 hr	30	22	8	0	1	0
8 hr	28.2	22.2	6	-2	4	0.602
16 hr	26.4	22.4	4	-4	16	1.204
24 hr	24.3	22.1	2.2	-5.8	55.72	1.746
32 hr	23.7	22.6	1.1	-6.9	119.4	2.077
40 hr	23	23	0	-8	256	2.408
48 hr	21.2	22.8	-1.6	-9.6	776	2.89
56 hr	19.6	22.9	-3.3	-11.3	2521	3.402
64 hr	19	23.1	-4.1	-12.1	4390	3.642
72hr	18.6	23.6	-5	-13	8192	3.913

Table (5): Effect of graphene quantum dots concentration 0.5% on gene expression of C.Myc in cell line HuH7.

	c.MYC	B.Actin	ΔCt	ΔΔCt	2^-ΔΔCt	log (2^-ΔΔCt)
0 hr	22.4	23	-0.6	0	1	0
8 hr	25.2	23.6	1.6	2.2	0.218	-0.662
16 hr	29.3	23.4	5.9	6.5	0.011	-1.957
24 hr	31.2	24.1	7.1	7.7	0.005	-2.318
32 hr	32.1	23.9	8.2	8.8	0.002	-2.649
40 hr	34.6	23.7	10.9	11.5	3E-04	-3.462
48 hr	36.2	24.2	12	12.6	2E-04	-3.793
56 hr	37.9	24.6	13.3	13.9	7E-05	-4.184
64 hr	39	24.6	14.4	15	3E-05	-4.515
72hr	40	24.8	15.2	15.8	2E-05	-4.756

Table (6): Effect of graphene quantum dots concentration 0.5% on gene expression of P21 in cell line HuH7.

	P21	B.Actin	ΔCt	ΔΔCt	2^-ΔΔCt	log (2^-ΔΔCt)
0 hr	30	23	7	0	1	0
8 hr	28.6	23.6	5	-2	4	0.602
16 hr	27	23.4	3.6	-3.4	10.56	1.024
24 hr	25.6	24.1	1.5	-5.5	45.25	1.656
32 hr	27	23.9	3.1	-3.9	14.93	1.174
40 hr	26.1	23.7	2.4	-4.6	24.25	1.385
48 hr	24	24.2	-0.2	-7.2	147	2.167
56 hr	22	24.6	-2.6	-9.6	776	2.89
64 hr	21.7	24.6	-2.9	-9.9	955.4	2.98
72hr	21	24.8	-3.8	-10.8	1783	3.251

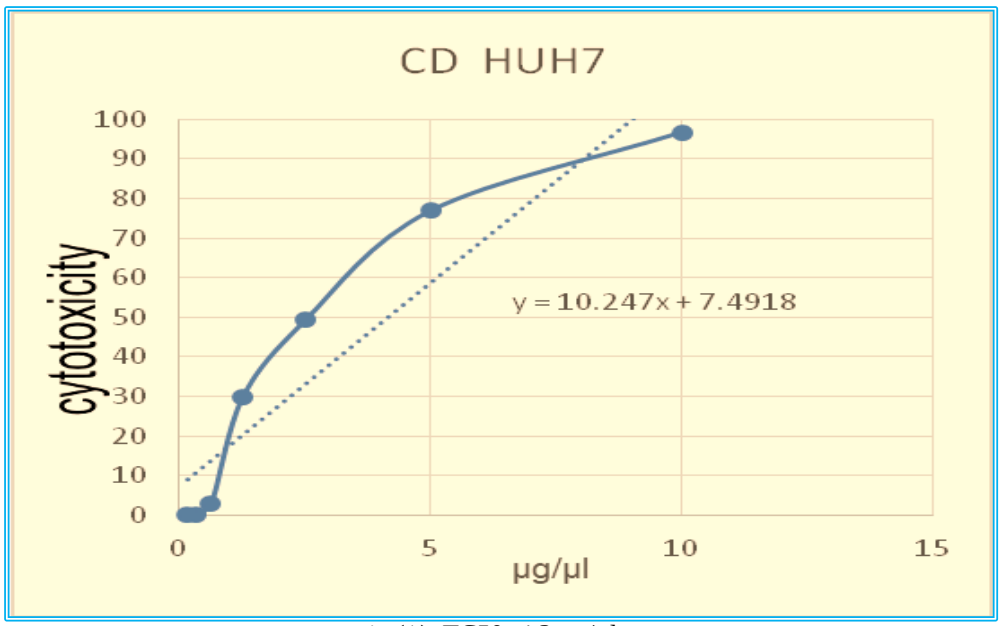

ig.(1)*:* TC50=4.3 µg/µl

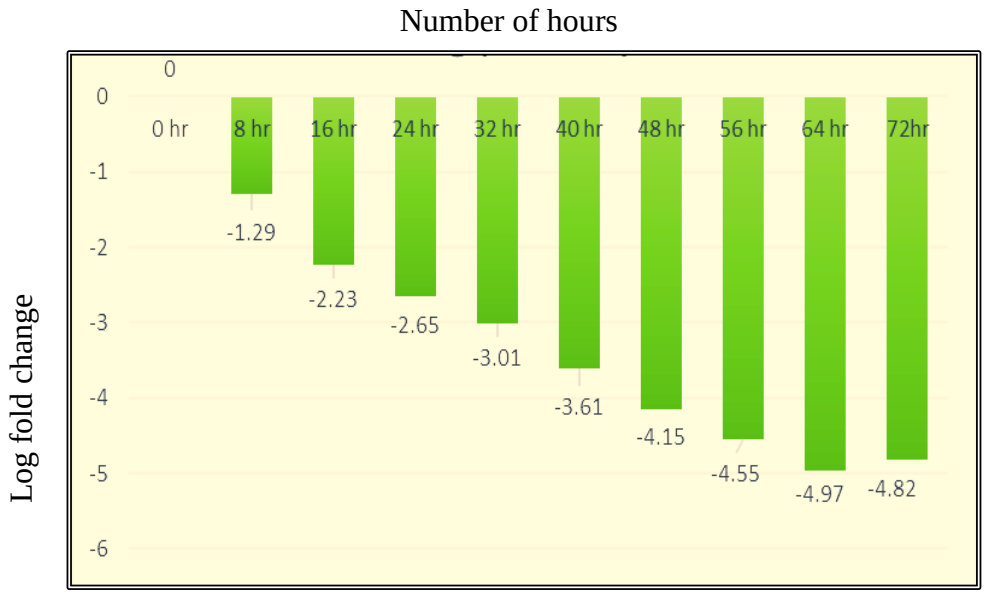

Fig. (2): the impact of concentration of Graphene quantum dots 1% on the gene expression of the C-Myc Gene in HUH7 cell line. The data represent a significant difference from control group across different exposure hours to Graphene quantum dots as when the time increase the down regulation of the gene C-MYC was increase.

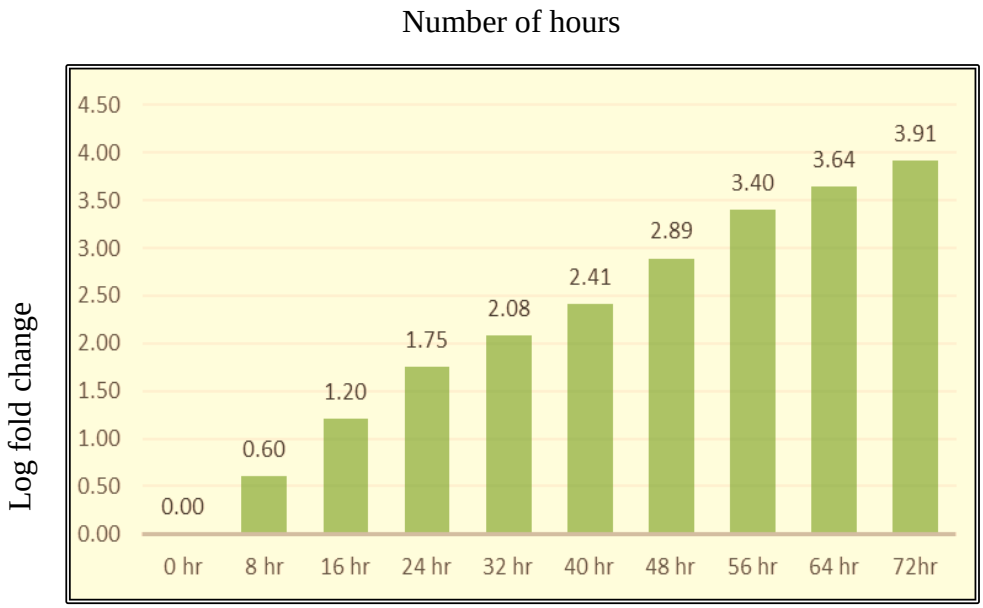

Fig. (3): the impact of concentration of Graphene quantum dots (1%) on the gene expression of the P21 Gene in HUH7 Cell Line. The data represent a significant difference from control group across different exposure hours to Graphene quantum dots as the time increase the Up regulation of the P21 gene was increase.

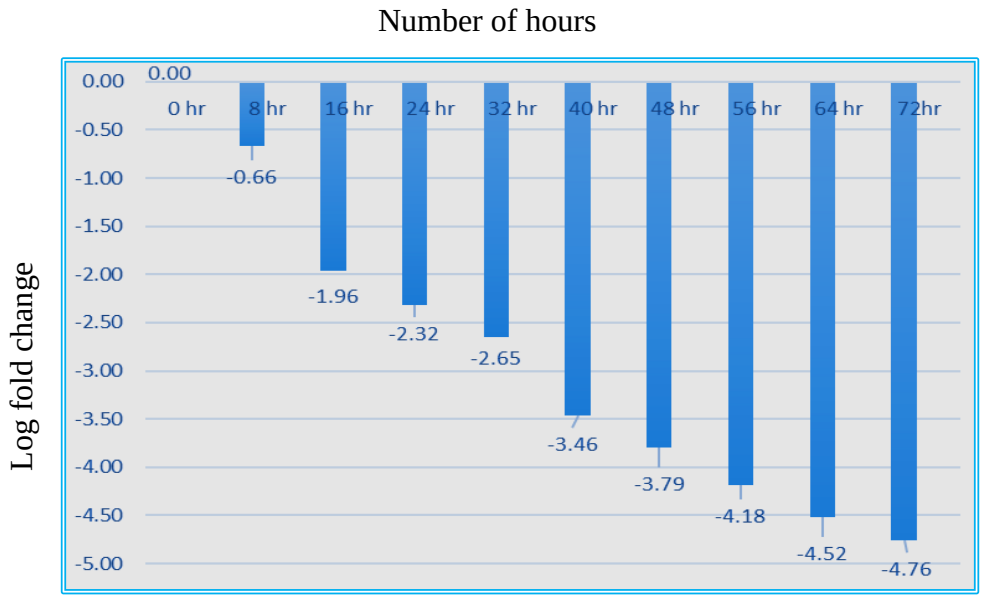

Fig. (4): the impact of concentration of Graphene quantum dots 0.5% on the gene expression of the c.MYC Gene in HUH7 cell line. The data represent a significant difference from control group across different exposure hours to Graphene quantum dots as when the time increase the down regulation of the gene C-MYC was increase.

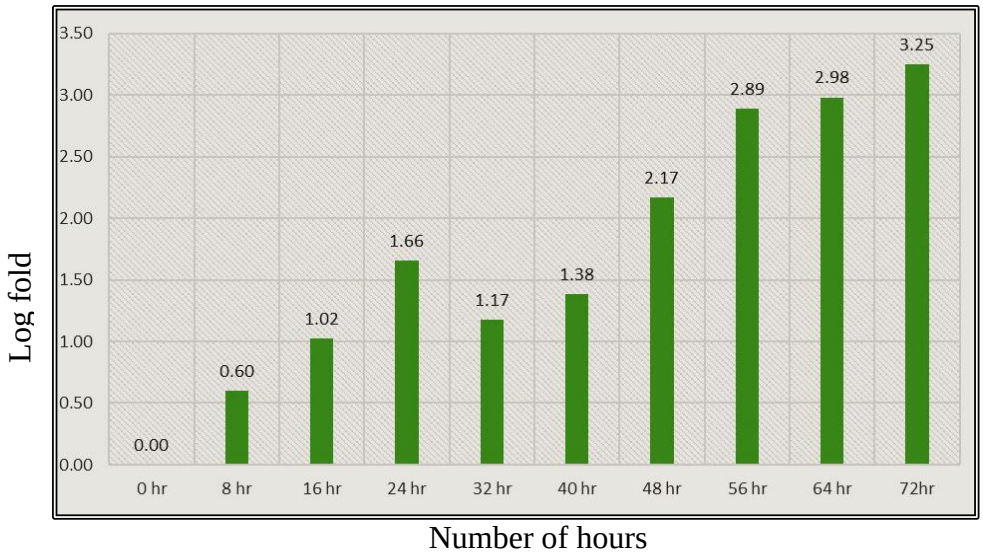

Fig. (5): the impact of concentration of Graphene quantum dots 0.5% on the gene expression of the P21 Gene in HUH7 cell line. The data represent a significant difference from control group across different exposure hours to Graphene quantum dots as the time increase the Up regulation of the P21 gene was increase.

GENOTOXICITY AND BEHAVIOURAL EFFECTS OF SODIUM BENZOATE AND SOME FUNGAL STRAINS ON *Drosophila melanogaster*

MANAR ELDESOKY[1], AZZA ABDELRAHMAN[2], A. ABDEL KHALKHAL[3] AND AMIRA ELKEREDY[1]

1 Genetics Department, faculty of Agriculture, Tanta University, Egypt.

2 Environmental and Biological Sciences Department, Faculty of Home Economics, El-Azhar University, Tanta, Egypt.

3 Plant protection and Biomolecular Diagnostic Dep., The Scientific Research City, Borg El-Arab, Alexandria, Egypt.

Sodium benzoate (E211) is a preservative in food industry. Benzoic acid is found in some plants. It is also used as an anti-fungal (Hong *et al.*, 2009). Sodium benzoate (SB) as the European nomenclature E211 is a salt of benzoic acid and is easy soluble in water, tasteless, odourless, as well as it has antifungal and antibacterial properties. It inhibits the growth of bacteria, yeast, and mold (Davidson *et al.*, 2021). Using *Drosophila* as ideal model for geneticists, toxicology and behavioural studies (Rand *et al.*, 2015). Genotoxicity assays include mortality and chromosomal aberrations, DNA damage, disorder behaviour, and mutations (El-Keredy 2014 and 2017; Nohmi *et al*. 2012).

Drosophila melanogaster is a standered genetic model (lifespan, SMART, behaviour, ect.) in diseases of human, mammalian especially fly proteins (Tasset *et al*.,2010; Bourg. 2011; Aysal *et al.*, 2012 and Aysal *et al.*,2013).

The immune system of *Drosophila* distinguishes between different types of infections and activates signal transduction pathways to combat invading microorganisms (Gottar *et al.*, 2006). *Drosophila* social attraction larvae to fungal-infected sites leading to suppression of mould growth may reflect an adaptive behavioural response that increases insect larval fitness and can thus be discussed as an anti-competitor behaviour. The relationship between spatial oviposition patterns, allee effects and the suppression of mould, spatial aggregation in *Drosophila* can be interpreted as an adaptive behaviour against competing fungi on larval feeding sites in order to enhance offspring survival, (Marko 2005). Characterization of the genetic variation underlying gene expression can easily be compromised by lack of environmental control (Hodgins-Davis. and Townsend, 2009). More DNA damage in comet assay resulting treated by benzoic acid, boric acid and sodium sulphite concentrations indicating muta-

Egypt. J. Genet. Cytol., 51:51-72, January, 2022

Web Site (*www.esg.net.eg*)

genicity and genotoxic materials (El-Hefny *et al*., 2020).

MATERIALS AND METHODS

The experiments of this study were carried out at the faculty of Agriculture, Tanta University and Technological Application (SRTA) City (Department of plant protection and biomolecular diagnostic) 2017-2021. To examined the effect of food additives sodium benzoate (SB) on larva and adult of *Drosophila melanogaste*. Also measuring behaviour of larvae under the influence of different concentrations of sodium benzoate (SB), the effect of some fungal species on *D. melanogaster* was studied.

Drosophila Medium

The best media was corn flour media for breeding *Drosophila* in the local environment (El-keredy, 2017). After cooling one drop of yeast suspension was spread on the surface of the media.

SB effective line point determination of Petri dishes

Whereas the other half added equal number were used to it 0.007 or 0.075g SB. For half of the control and SB treates cases. These larvae in each plat were growing for a time points (1, 2,4, 8min) as mentioned in the results, data was recorded as the number of larvae located at the control and SB treated using the following equation

$$\text{PREF}_{\text{Gustatory}} = \frac{\#SB - \#PURE}{\#TOTAL}$$

Thus, PREF values were confined between 1 and -1, positive values indicating preference for SB and negative values indicating hatred of the SB according to (König *et al.*, 2014).

The used fungal species

Three *Aspergillus* species *A.pergillus flaves, Aspergillus niger* and *Aspergillus terreus* were isolated from different soil samples in addition to three *Trichoderma* species (*Trichoderma cremeum, Trichoderma viride* and *Trichoderma citririnoviride*) as well as *Penicillium spp* were used to infect the different *Drosophila* flies strains.

Infected flies with fungi

Females and equal number of males were infected with each fungus in the flask. The flies inside the flask loaded with spores for 3-4 minutes and then were transferred back to the culture bottles. The rate of death, flight rate, egg laid and activity were recorded daily. The infected flies were kept in liquid nitrogen and then saves it in -80ºC until the required analyses for immunity gene expression.

RNA extraction

RNA was extracted according to (Mangalathu *et al.*, 2001) from *Drosophila* flies.

cDNA extracted and PCR reaction

cDNA was synthesized using Moloney Murine Leukemia Virus Reverse

Transcriptase Enzyme (Fermentas, USA). Reverse transcription reactions were performed using primer oligo dT primer (Table 1). Each 25 µl reaction master mix containing 2 µl of 5X buffer with 6 µl of H2O, 2 µl of mM dNTPs mix, 5 µg of primer, 1 µg RNA and 2 µl Reverse Transcriptase Enzyme. RT-PCR amplification was performed in a thermal cycler (Eppendorf, Germany) programmed at 37ºC for 20 min and 95ºC for 10 min. Amplification products were visualized using gel documentation system (Syngene, USA) in 1.5% agarose gel that was electrophoresed in 0.5X TBE buffer. cDNA was then stored at -20ºC until used. Protocol for cDNA synthesis (Mangalathu *et al.*, 2001).

Statistical analysis

Analysed by using one-way ANOVA followed by LSD test through SPSS 16 (version 4). The trait means were compared using least significant difference (LSD) tested at significant levels of 5% as described by **(**Gomez and Gomez, 1984). Real-time Q-PCR data analysis: The relative expression ratio was accurately quantified and calculated according to Livak and Schmittgen, (2001).

RESULTS AND DISCUSSION

This experiment was conducted to know how sodium benzoate with different concentrations and fungi strains had affected on different strains of *Drosophila melanogaster* in different generations from flies or larvae.

In the ninth generation (F9) the mortality was 97.14%. While the sexual ratio was zero, as the flies died and did not complete the tenth generation in Tanta flies (Fig. 1).

Figure (2) showed that the effect of sodium benzoate with different concentrations on *Drosophila* which collected from *Kafr el-Sheikh* strain. It is also clear that *Kafr El-Sheikh* flies dynasty was more affected, while the mortality in the highest concentration was 67.69% compared to the lowest concentration (0.007 g) while reached 41%,53% and (sexual ratio was 0.91). The effect of SB was significant in strain *Kafr El-Sheikh*, reached 84.37%, as well as in the case of the sexual ratio, which reached up to 0.87.

The same results were obtained in Fig. (3) to Fig. (6) where the sodium benzoate affected both flies' mortality and sexual ratio was zero in most strains. In the highest concentration of (SB), also, the 0.157mM, 0.35mM, 0.5mM, and 0.7mM concentrations from (SB) resulted in increase DNA tail and decrease DNA head with Comet assay (Sahin *et al.*, 2015) which was led to the genetic mutation, and genotoxic, cytotoxic and proapoptotic effects (Tasset *et al.*, 2010).

Determination of the itemize point (choice behavior)

Larvae third- instar feeding – stages *Drosophila melanogaster* were used. Choice-behaviour differs in their dose-effect characteristics. Those results rev-

elled that different sets of gustatory receptors *Gr*-gene family (El-Keredy., 2017).

The results of behaviour experiments in the Figures (5 to (7A-12A)) which explained the relationship between sodium benzoate concentrations and its preference in the different Egyptian *Drosophila* strains in the fifth generation after 8 minutes treatment for each strain. The sodium benzoate was affected on larval behaviour similarly in different strains (*Tanta, Kafr El-Sheikh, Canton-S*) in the highest SB concentration 0.075g although *Canton-S* (wild type strain) was highly diverged compared to the Egyptian local strains in Africa (Khatab *et al.,* 2015), which indicates the extent to behaviour effects of genotoxicity and mutation with SB treatment. In some studies, like (Walczak-Nowicka and Mariola, 2022) were discussed sodium benzoate and their relationship to neurodegenerative diseases (autism spectrum disorder ASD, Schizophrenia, major depressive disorder MDD, and pain relief. Electrical system in *Drosophila* nervous system was played essential roles in neuronal function (Ammer, *et al.,* 2022).

The effect of treatment with sodium benzoate concentrations on gene expression

The mRNA expression of *Im1* and *Im2* genes in the different *Drosophila* strains which used (*Tanta, Kafr El-Sheikh, Mansoura, Alex, Canton-S*, and *OR*) with 0.007 and 0.075g concentrations in middle and last generation of each *Drosophila* strain. In Tables (2 and 3) which recorded gene expression for each gene in *Drosophila* strain for 0.007g and 0.075g SB concentrations at middle and last generation of each strain, where we find a significant difference between the decrease within one generation (*Tanta, Kafr El-Sheikh, Mansoura, Alex*, and *OR* flies) as well as between generations. The results were recorder will be Aledwany *et al.,* (2018) where be reported sodium benzoate was affected on lymphocytes, inhibited DNA synthesis also increased micronuclei and anaphase bridges formation. More differences were recorded between *Drosophila* strains in two generations for *Im2* gene.

With more than 60% of human disease were similarity to morphology of eucaryotic organism, so, *Drosophila* was used as a model organism of genetic experiments (Sahin. *et al.,* 2015), also in the modern studies like (Ganglberger, *et al.,* 2022) included the *Drosophila* larvae, human, and mouse for brain network visualization.

Gene expression studies in these experiments from Figs. (11 to 16) recorded the differences of gene expression between *Im1* and *Im2* in different *Drosophila* strains in the lowest (0.007g) and highest (0.075g) SB concentrations compared to control at two generation for each strain. Sodium benzoate was affected on P^{21}, homocysteine levels, tryptophan metabolism, inhibited of microglia activation and inhibited of neopterin production (Łucja and Mariola 2022 and Klapoetke *et al.,* 2022).

Influence of gene expression in *Drosophila* strains by infection with different species of fungi

In *Drosophila melanogaster*, fungal infections depends on invariant microbial patterns and the virulence on the host, because *Drosophila* immune system detected kinds of infections and activated signal pathways (like *Toll* pathway) to combat microorganisms which were invading (Gottar *et al.,* 2006). Data in Table (4) monitored RT-PCR for *Im1* gene in different *Drosophila* flies (*Tanta, Kafr El-Sheikh, Mansoura, Canton-S* and *OR*) infected with different fungal *ssp*. (*Penicillium, Trichoderma, Aspergillus*).

The gene expression of *Im1* gene was significantly affected in *Tanta* and *Kafr El-Sheikh* flies when infected with *T. citrinoviride*, while *Penicillium ssp, and T. viride* affected in gene expression on *Mansoura strain*, but gene expression on *Alx*. and *OR* strains effected of infection with *A. terreus.*

Table (5) recorded significant *Im2* gene expression effect to *T. viride* for both *Kafr El-Sheikh and Mansoura* flies. *Alex*. strain was affected with *T. viride*, *A. flavus*, and *A. terreus*. *Canton -S* flies was more affected with *Penicillium ssp* and *A. flavus* infection. The *OR Drosophila* strain was the most affected in the lower gene expression of *Im2* gene for infection with different species of fungi except *A. niger*. Antifungal response in *Drosophila* was studied using human pathogenic yeast, entomopathogenic fungi, and resulted that gene expression levels of *Toll*-dependent *Drosophila* gene (Gottar *et al.,* 2006). In *Drosophila* Toll receptors activation in larval fat body by infection, which caused reduction of insulin-like growth factor1 (IGF1).

Toll pathway activation led to growth reduced and there was a relationship between innate immune signalling and endocrine regulation of growth (Suzawa *et al.,* 2019). Also, antifungal immunomodulator downstream of Toll improving our knowledge of *Drosophila* antimicrobial response (Hanson *et al*., 2021).

Infection of *Drosophila* strains with different species of fungi led to the death of a large proportion of flies. This affected the gene expression of both *Im1* and *Im2* genes, it turned out to be clear from Table (2) to Table (5).

PCR products were electrophoretic ally analysed confirm these results for *Im1* gene 187bp which determined in *Drosophila* flies by Leader (L) for *Drosophila* stains (*OR, Canton-S*, and *Alexandria*) which infected with Fungal *ssp*: *Penicillium* (P), *Trichoderma* (T), *Aspergillus* (A) in Fig. (17).

About PCR product gel electrophoresis for Im2 gene 90bp which located in Drosophila (Tanta, Kafr El-Sheikh, and Mansoura) strain with different sodium benzoate concentrations in Fig. (18). Based on experiments which Drosophila were infected with fungal ssp. and the Im1, Im2 genes were expressed to combat attacking fungi. Marko Rohlfs (2005) re-

ported that fungi competed Drosophila flies on resources and led to suppression of mould growth may adaptive behavioural response. In Drosophila investigating the relationship between the inter-kingdom competition and the behaviour in insects.

Pathological condition of Alzheimer diseases AD controlling bacteria in the oral cavity and the body (Matsushita *et al.*, 2020).

SUMMARY

Sodium benzoate (E211) used as a food additive was researched on *Drosophila melanogaster* (*Tanta, Kafr El-Sheikh, Mansoura, Alexandria, Canton-S,* and *OR* strains) and fungi strains from (*Aspergillus* species, *Trichoderma* species, *Penicillium spp*). Adult and larvae in third larvae stages were treated with medium of *Drosophila* which was mixed with different concentrations of sodium benzoate (SB) 0.007, 0.012, 0.037. 0.050. 0.075g. Mortality and sex ratio were affected with this treated so in fifth generation F5 in the number of flies and the sexual ratio that reached zero (0%) in the highest concentration of benzoate (0.075 g) in *Kafr El-Sheikh* flies and the mortality reached its highest rate in the highest concentration of sodium benzoate which was 98.03%. In the ninth and final generation (F9) of the *Tanta* flies. Behaviour experiments choice were curry out on third larvae after treated with different fungal species concentrations. Sodium benzoate (SB) concentrations from 0.007 g to 0.075 g recorded avoidance in different generations about more than -7 in *Tanta, Mansoura,* and *Alexandria* strains at 8 minutes. Rail time PCR (Rt. PCR) was used to determine gene expression of *Im1* and *Im2* genes, gene expression was zero for highest BS concentration for *Im1* gene in *Alexandria* flies in the sixth generation, while was 4.52 compared the control (1.0) for *Im2* gene. *Im1* and *Im2* genes (PCR product) were run in gel electrophoresis. Results led to genetics, behaviour and toxicity effects to SB on *Drosophila melanogaster* and the over load to fungi strains on the *Drosophila* behaviour through the effect of their genes. Thus, it affected flies mortality, sex ratio and behaviour, as well as the gene expression of its immune response *Im1*and *Im2* genes.

ACKNOWLEDGEMENTS

Thanks to the professor Bertram Gerber, Head of the Department, Department of Learning and Memory. Magdeburg, Germany, for the support and advice he provided. We particularly grateful and would like to thank (Biotechnology laboratory, Animal Production Department, Agriculture Faculty, Tanta University) for the facilities required for the performance of the research study.

REFERENCES

Aledwany A. Z., Basha W. T., Al-Senosy N. K. and Issa A., (2018). Assessment of genotoxicity of potassium nitrate and sodium benzoate in *Drosophila melanogaster* using

Smart and Comet Assays. Egypt. Acad. J. Biolog. Sci., 10(2): 83- 97.

Anter J., Tasset I., Demyda-Peyrás S., Ranchal I., Moreno Millan M., Romero-Jimenez Muntané J., Luque de Castro M. D., Muñoz-Serrano A. and Alonso-Moraga A., (2010).

Ammer G., Vieira F. S. and Borst A., (2022). Anatomical distribution and functional roles of electrical synapses in *Drosophila*. Current Biology, 32: 1-15.

Aysal H. Kızılet H., Ayar A. and Taheri A., (2012). The use of endemic Iranian plant, *Echium amoenum*, against the ethyl methane sulfonate and the recovery of mutagenic effects. Toxicol and Health.

Aysal H. Semerdoken S., Colak D. A. and Ayar A. (2013). The hazardous effects of the three natural food dyes on developmental stages and longevity of *Drosophila melanogaster*.Toxicol Ind. Health.

Bourg E. I. (2011). Using *Drosophila melanogaster* to study the positive effects of mild stress on aging. Experimental Gerontology, 46: 345-348.

Davidson P. M., Taylor T. M. and David J. R. D., (2021). Antimicrobials in Food, 4th ed.; CRC Press: Boca Raton, FL, USA, ISBN 978-0-367-17878-9.

El-Hefny I., Hozayen W., AlSenosy N., Basal W., Ahmed A. and Diab A., (2020). Evalution of genotoxicity of three food preservatives melanogaster using smart and comet assays. J. Microbiol. Biotech, Food Sci., 10 (1): 38-41.

El-Keredy A. (2017). Experiment on the genetic toxicity of atrazine yellow and behavioral effects on *Drosophila melanogaster*. Egypt. J. Genet. Cytol., 46:33-42. Web Site (www.esg.net.eg).

Ganglberger F., Wibmann M., Wu H- Y., Swoboda N., Thum A., Haubensak W. and Buhler K., (2022). Spatial-Data-Driven layouting for brain network visualization. Computers and Graphics, doi: https//doi.org/1016/j.cag.2022.04.014.

Gottar M., Gobert V., Matskevich A., Reichhart J. M., Wang C., Butt T. M., Hoffmann J. A. and Ferrandon D., (2006). Dual Detection of Fungal Infections in *Drosophila via* Recognition of Glucans and Sensing of Virulence Factors. Cell 127: 1425-1437.

Hanson M., Cohen L., Marra A., Wasserman I. S. and Lemaitre B., (2021). *Drosophila* Baramicin polypeptide gene protects against fungal infection. https://doi.org/ 10.1101/2020.11.23.394148.

Hodgins-Davis. A. and Townsend P. J., (2009). Evolving gene expression: from G to E to G × E. Trends in Ecology & Evolution, 24 (12): 649-658.

Hong H., Liang X. and Liu D., (2009). Assessment of benzoic acid levels in milk in China. Food Control. 20: 414-8.

Klapoetke N. C., Nern A., Rogers E. M., G. Rubin M., Reiser M. B. and Card G. M., (2022). A functionally ordered visual feature map in the *Drosophila* brain. Neuron, 110: 1-12.

Łucja Walczak-Nowicka J. and Mariola H., (2022). Sodium Benzoate—Harmfulness and Potential Use in Therapies for Disorders Related to the Nervous System: A Review. Nutrients, 14: 1497. https://doi.org/10.3390/nu14071497.

Mangalathu S., Rajeevan Ranamukhaarachchi G., Suzanne D. and R. U. Elizabeth., (2001). Use of Real-Time Quantitative PCR to Validate the Results of cDNA Array and Differential Display PCR Technologies. doi:10. 1006/meth. 2001.1266, available online at http://www.idealibrary. com.

Marko Rohlfs (2005). Clash of kingdoms or why *Drosophila* larvae positively respond to fungal competitors. Frontiers in Zoology, 2:2.

Matsushita K., Furukawa Y., Kurosawa M. and Shikama M. Y., (2020). Periodontal Disease and Periodontal Disease- Related Bacteria Involved in the Pathogenesis of Alzheimer's Disease. Journal of Inflammation Research,13:275-283.

Mangalathu S. R., Ranamukhaarachchi G., Suzanne D. V. and Elizabeth R. U., (2001). Use of Real-Time Quantitative PCR to Validate the Results of cDNA Array and Differential Display PCR Technologies. doi:10.1006/meth.2001. 1266, available online at http:// www.idealibrary.com

Nohmi T., Yamada M. and Masumura K., (2012). *In vivo* approaches to identify mutations and *in vitro* research to reveal underlying mechanisms of genotoxic thresholds. Gen.Environ., 34(4): 146-152.

Pal S. (2006). Role of NF-κB/REL proteins in mediating innate immune responses in *Drosophila melanogaster*. https://www.researchgate.net/publication/36119224.

Rand M. D., Sara L., Montgomery L. P. and Vorojeikina D., (2015). Developmental Toxicity Assays Using the Drosophila Model. Curr Protoc Toxicol, 59: 1.12.1-1.12.20.

Suzawa M., Muhammad N., Bradley S. and Michelle Bland L., (2019). The Toll signaling pathway targets the Insulin-like peptide Dilp6 to inhibit growth in *Drosophila* cell reports, 28 (6): 1439-1446. e5.

Suzawa M. M., Bradley N. S. and Michelle L. B., (2019). The Toll Signaling Pathway Targets the Insulin-like Peptide Dilp6 to Inhibit Growth in Drosophila Cell Reports 28 (6): 1439-1446. e5.

.

Table (1): The primer was used to determined genes.

Gene name	Primer sequence 5 - ⟶3 -	Reference
Im1	F-TGTGGCCAATGGTGAGTAAA R –TTTTTCGAATCCTTGGGTTG	Pal, (2006)
Im2	F-TGGCCAACGCTGTTCCC R –CCTACTTTCCACCGTGCACAT	Suzawa *et al.*, (2019)

Table (2): RT-PCR for IM1 gene affected with sodium benzoate of middle and last generation on *Drosophila* strains.

D. strains	Generation	*Tanta*	*Kafr EL-Sheikh*	*Mansoura*	*Alex*	*canton s*	*OR*
0.007 g	middle	2.323576628	0.017398302	1.89181317	3.006417392	2.094824112	0.155374189
0.075 g		0.956336728	0.524673919	4.19896760	15.69313031	2.243684691	1.281744628
0.007 g	Last	0.649376282	0.250121189	1.2198549	0.065537208	9.782524247	2.715778697
0.075 g		2.609789863	0.341669569	2.46767067	0.055615733	1.202189604	0.351897834

Table (3): RT-PCR for IM2 gene affected with sodium benzoate of middle and last generation on *Drosophila* strains.

D. strains	Generation	Tanta	Kafr El-Sheikh	Manoura	Alex	Canton- S	OR
0.007 g	middle	1.4421854	1.014803	2.2808611	1.026922	3.2843106	0.035498
0.075 g		2.0157366	0.308685	1.765406	0.773355	7.0141152	0.1738421
0.007 g	Last	1.549387	0.488369	1.5107136	3.194129	2.0228763	0.7581166
0.075 g		1.7003876	0.130516	1.6908913	4.520974	6.7602381	0.3725139

Table (4): RT-PCR for *Im1* gene affected with fungal species on *Drosophila* strains.

Fungi Strains / ***D*. strains**	***Penicillium spp***	***Trichoderma cremeum***	***T.viride***	***T.citrinoviride***	***Aspergillus flavus***	***A.niger***	***A.terreus***
Tanta	2.5224760	2.6551941	2.0641988	0.4469937	1.8381355	0.9428623	2.4923231
Kafr EL-Sheikh	0.1321307	0.1218611	0.2495725	0.1196591	0.5289880	179.61769	0.2900998
Mansoura	0.7868657	2.9785481	0.8017627	2.7251718	2.6126504	1.0604094	3.0948537
Alex.	1.8435548	0.0825481	1.5550947	0.5679740	1.2301358	754.81543	0.0018094
Canton S	2.412298	2.0668264	0.7465376	1.2481404	0.5298889	300.7808	3.5126718
OR.	0.358164	0.2266982	0.2513814	0.2154741	0.7634411	146.97095	0.1804719

Table (5): RT-PCR for *Im2* gene affected with fungal species on *Drosophila* strains.

Fungi Strains / *D*. strains	*Penicillium spp*	*Trichoderma cremeum*	*T.viride*	*T.citrinoviride*	*Aspergillus flavus*	*A.niger*	*A.terreus*
Tanta	1.5555444	1.6349001	2.021730	0.444933	1.9651255	1.047759	2.598037
Kafr EL-Sheikh	0.266161	0.151730	1.111547	0.354497	0.528988	179.6176	0.290100
Mansoura	0.290100	1.5823242	1.113428	1.9181273	1.8072784	1.060409	3.094853
Alex.	22.769389	1.829020	0.773093	1.053535	0.722500	694.3785	0.818635
Canton S	0.0248605	7.0128458	4.963395	0.7115672	0.2404112	151.1706	0.624165
OR.	0.2226971	0.399363	0.223904	0.1582196	0.1220537	76.81911	0.559855

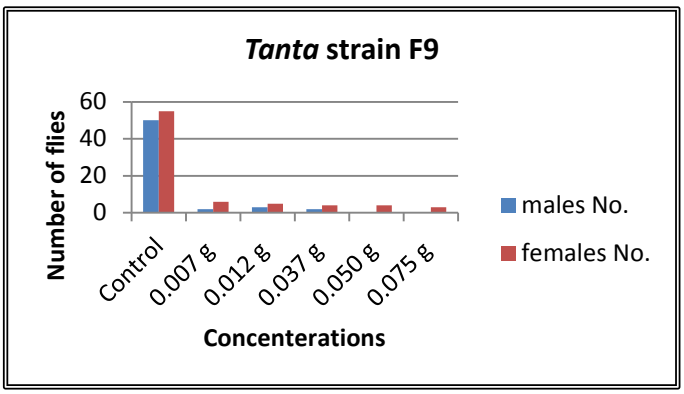

Fig. (1) The progeny number of *Drosophila melanogaster* in the last generation (F9) with sodium benzoate concentrations males, females were counted in *Tanta* strain.

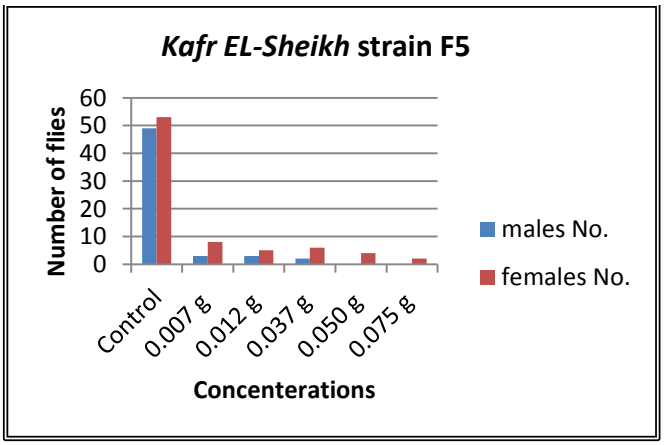

Fig. (2) The progeny number of *Drosophila melanogaster* in the last generation (F5) with sodium benzoate concentrations males, females were counted in Kafr El-Sheikh strain.

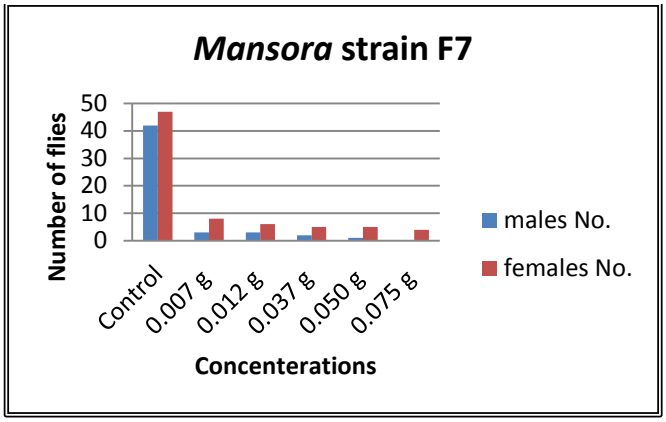

Fig. (3) The progeny number of *Drosophila melanogaster* in the last generation (F7) with sodium benzoate concentrations males, females were counted in Mansoura strain

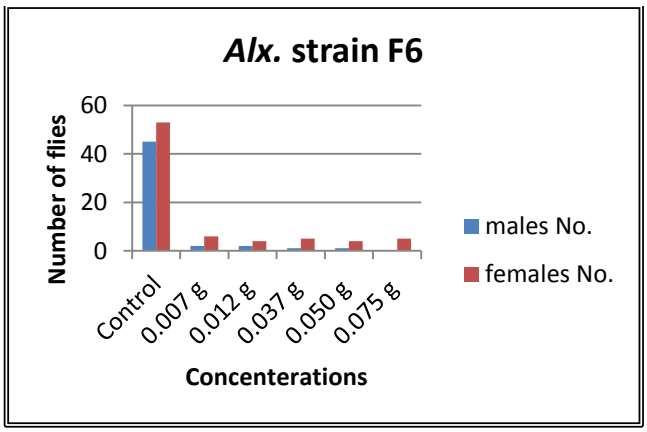

Fig. (4) The progeny number of *Drosophila melanogaster* in the last generation (F6) with sodium benzoate concentrations males, females were counted in Alexandria strain.

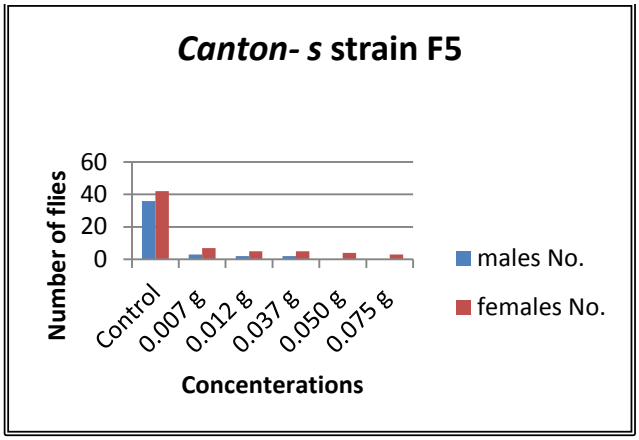

Fig. (5) The progeny number of *Drosophila melanogaster* in the last generation (F5) with sodium benzoate concentrations males, females were counted in Canton-S strain

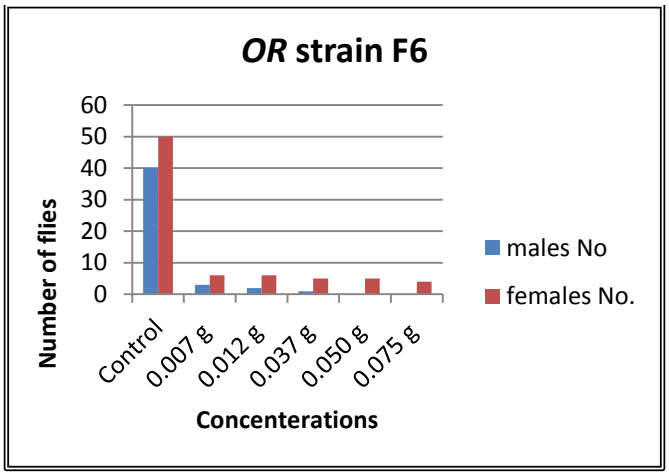

Fig. (6) The progeny number of *Drosophila melanogaster* in the last generation (F6) with sodium benzoate concentrations males, females were counted in OR strain

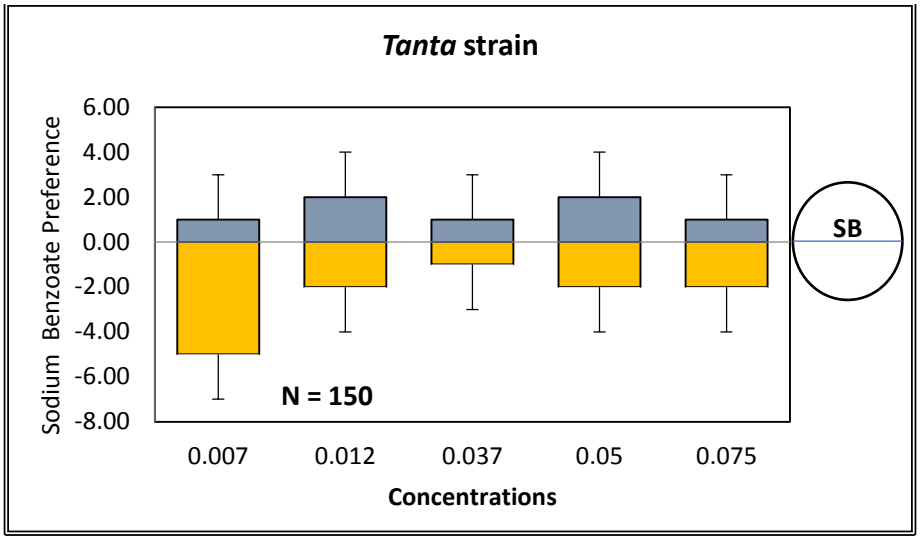

Fig. (7A) Histogram of the average of preference for sodium benzoate concentration on *Tanta* strain larvae in the F5 after 8 minutes.

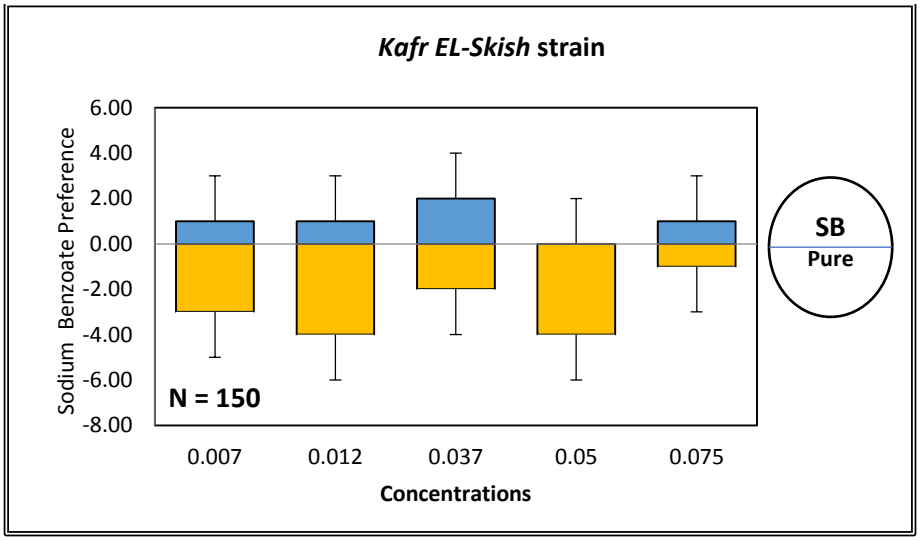

Fig. (8A) Histogram of the average of preference for sodium benzoate concentration on *Kafr El-Sheisk* strain larvae in the F5 after 8 minutes.

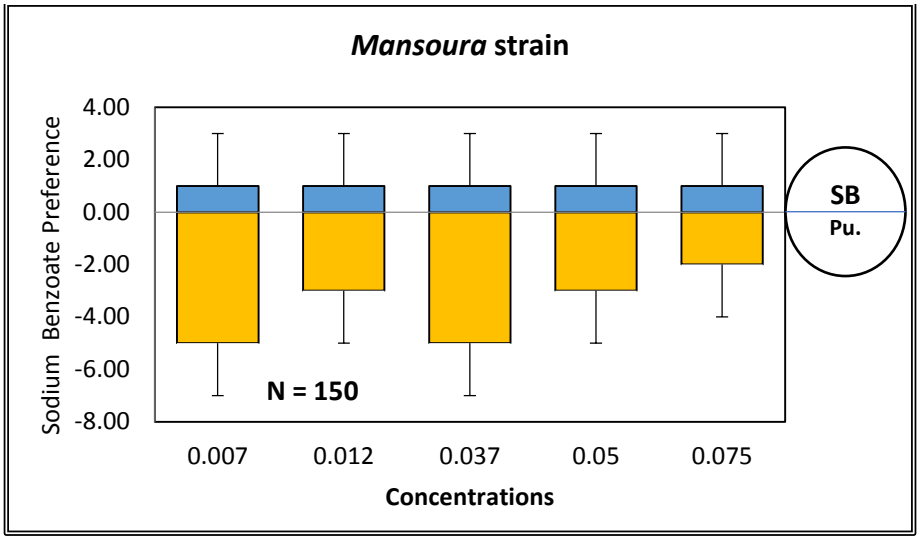

Fig. (9A) Histogram of the average of preference for sodium benzoate concentration on *Mansoura* strain larvae in the F5 after 8 minutes.

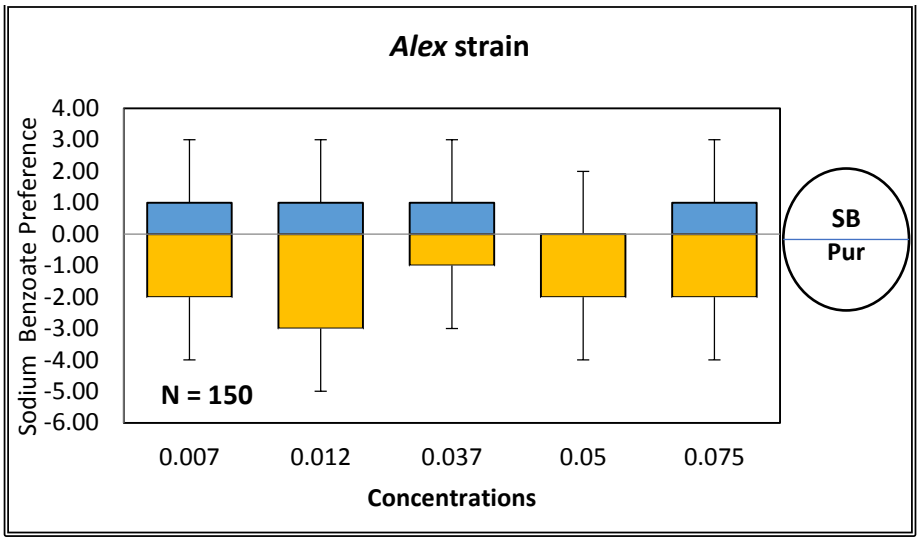

Fig. (10A) Histogram of the average of preference for sodium benzoate concentration on *Alexandria* strain larvae in the F5 after 8 minutes.

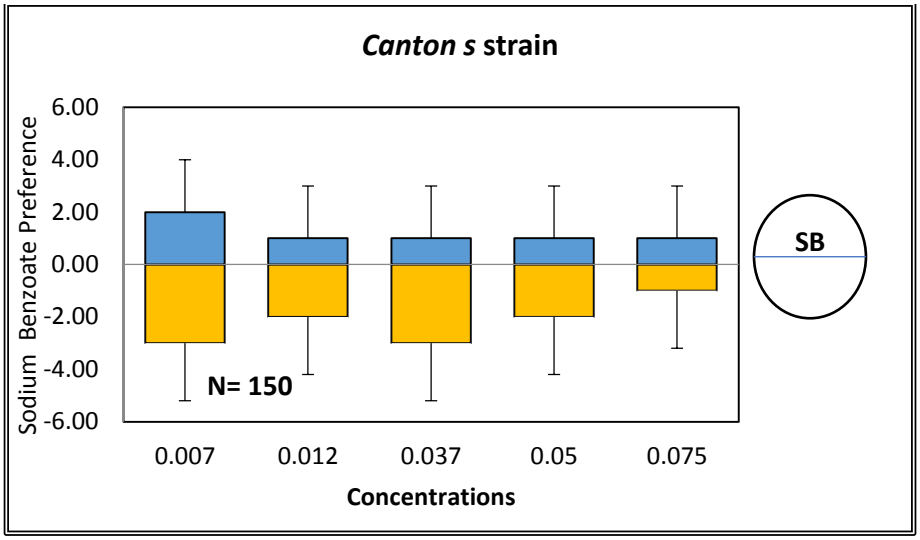

Fig. (11A) Histogram of the average of preference for sodium benzoate concentration on *Canton-S* strain larvae in the F5 after 8 minutes.

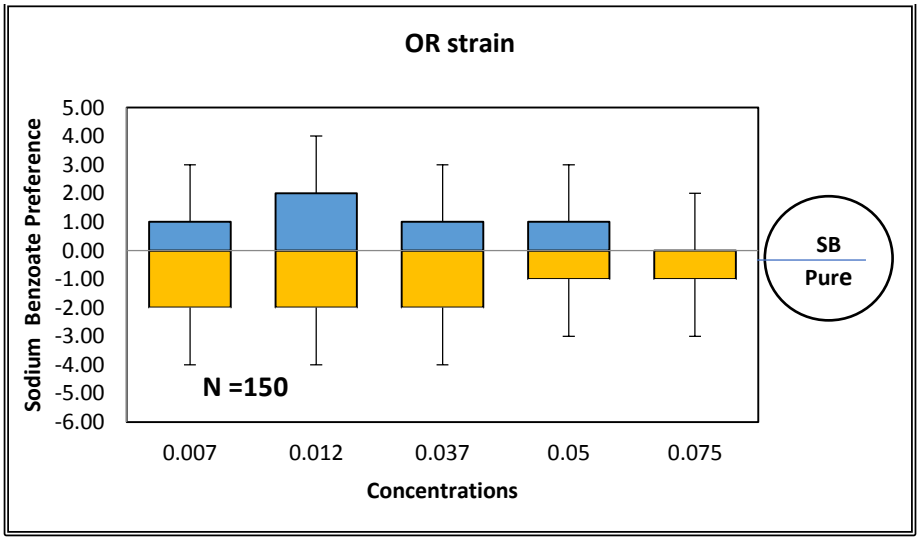

Fig. (12A) Histogram of the average of preference for sodium benzoate concentration on *OR* strain larvae in the F5 after 8 minutes.

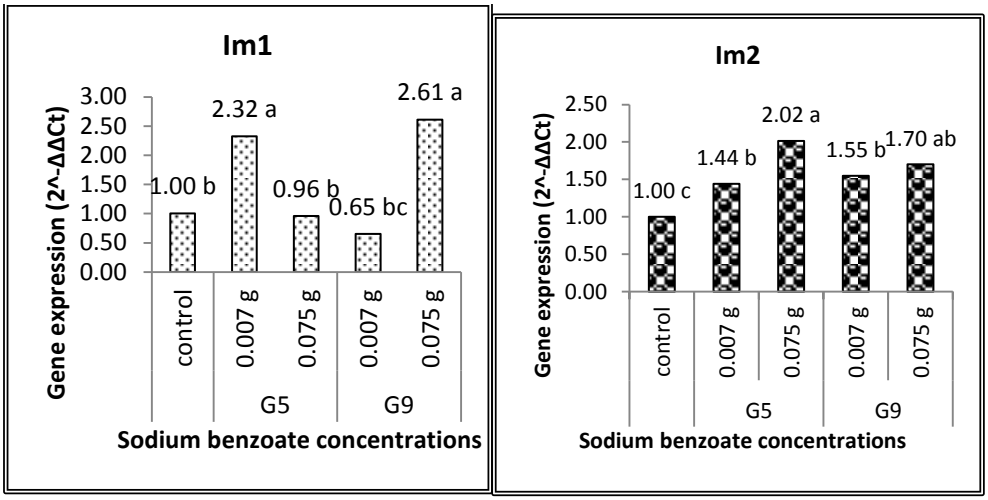

Fig. (11) Gene expression for both gene I*m1* and *Im2* result of the effect of sodium benzoate concentrations in *Tanta* strain.

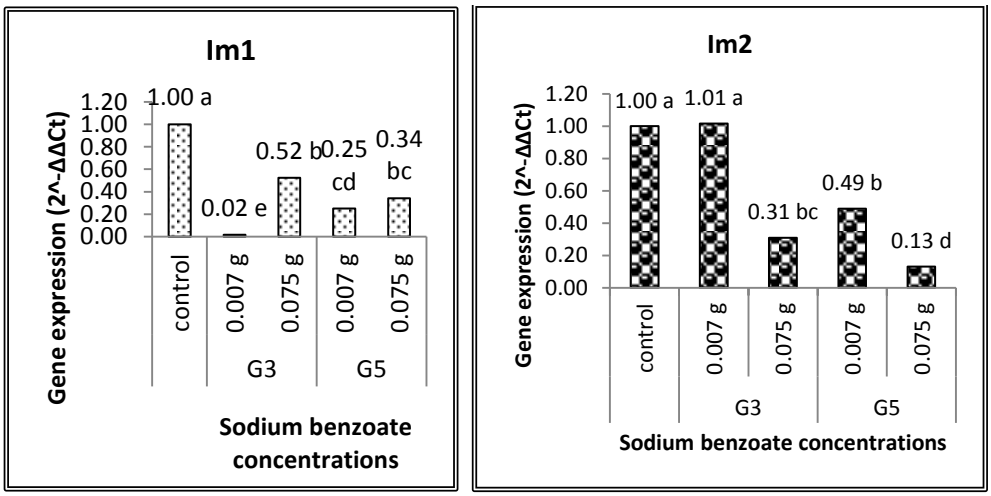

Fig. (12) Gene expression for both gene *Im1* and *Im2* result of the effect of sodium benzoate concentrations in *Kafr El-Sheikh* strain.

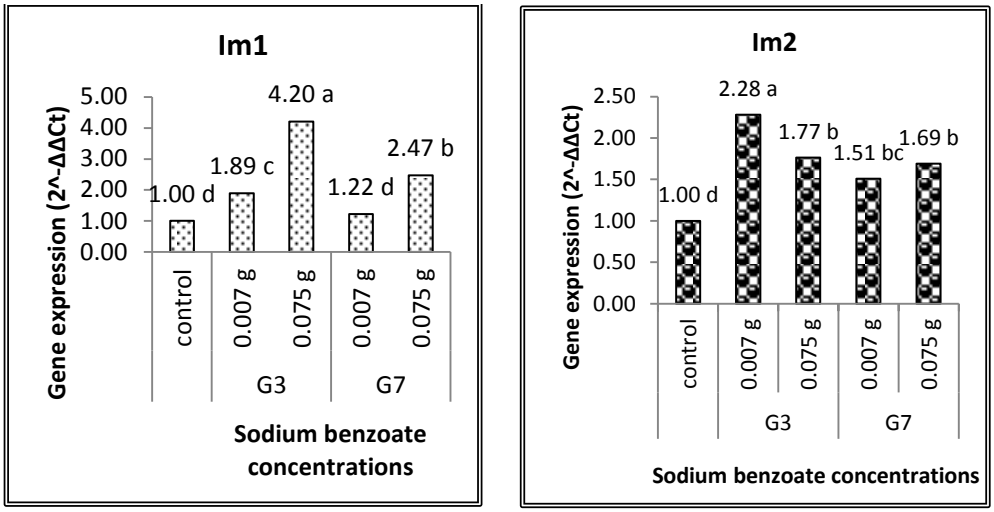

Fig. (13) Gene expression for both gene *Im1* and *Im2* result of the effect of sodium benzoate concentrations in *Mansoura* strain.

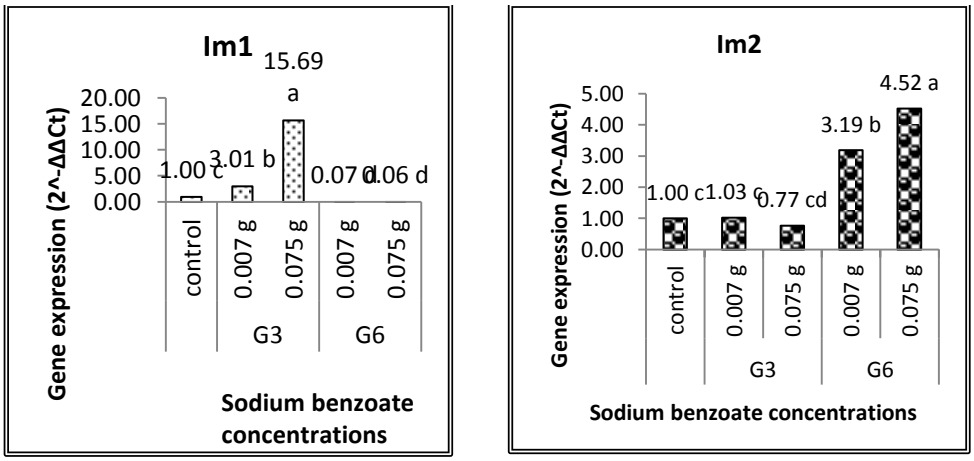

Fig. (14) Gene expression for both gene *Im1* and *Im2* result of the effect of sodium benzoate concentrations in *Alexandria* strain.

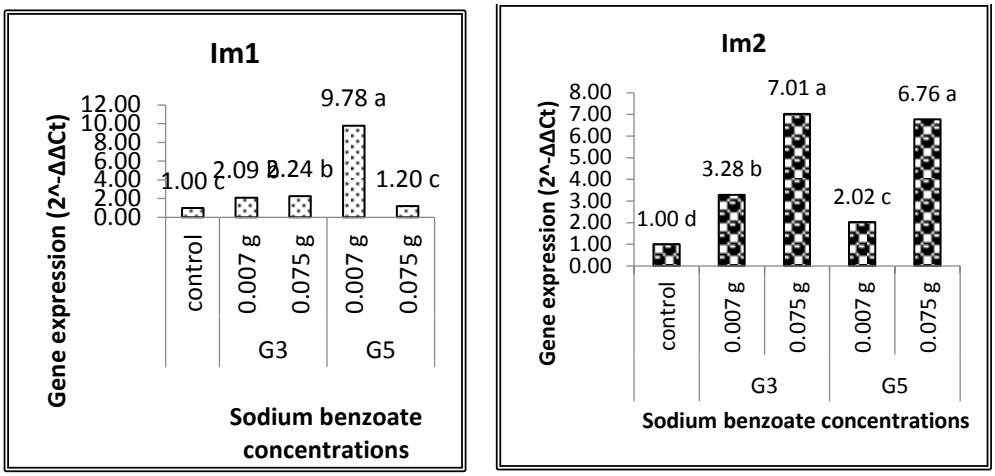

Fig. (15) Gene expression for both gene *Im1* and *Im2* result of the effect of sodium benzoate concentrations in *Canton-s* strain

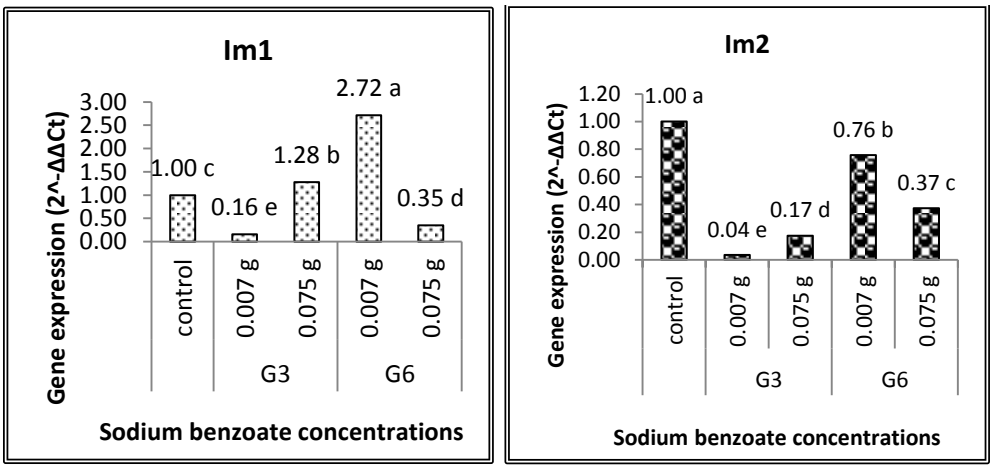

Fig. (16) Gene expression for both gene *Im1* and *Im2* result of the effect of sodium benzoate concentrations in *OR* strain.

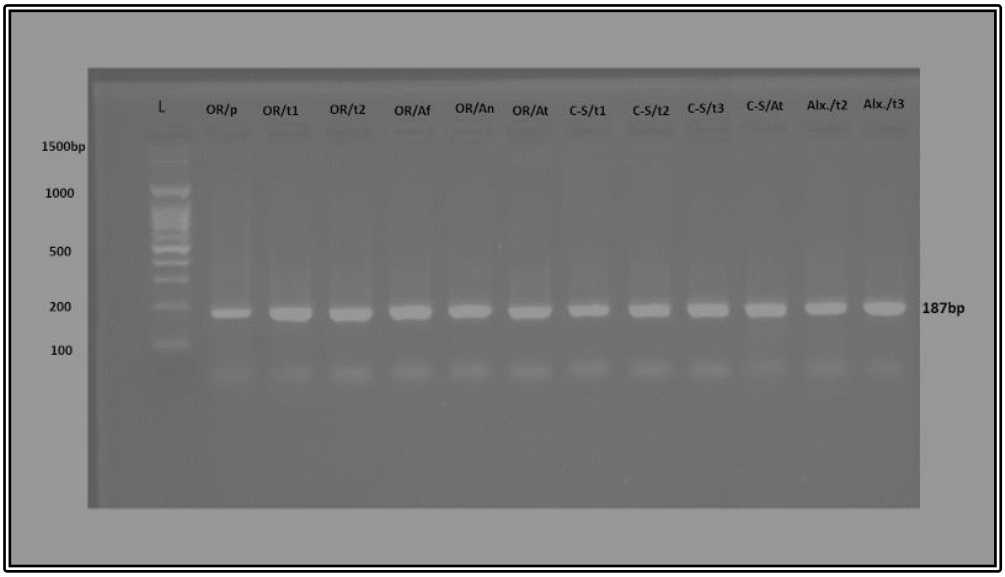

Fig. (17) PCR product gel electrophoresis for *Im1* gene at the last generation of each strain for the effect of sodium benzoate and fungal strains on different *Drosophila* strains

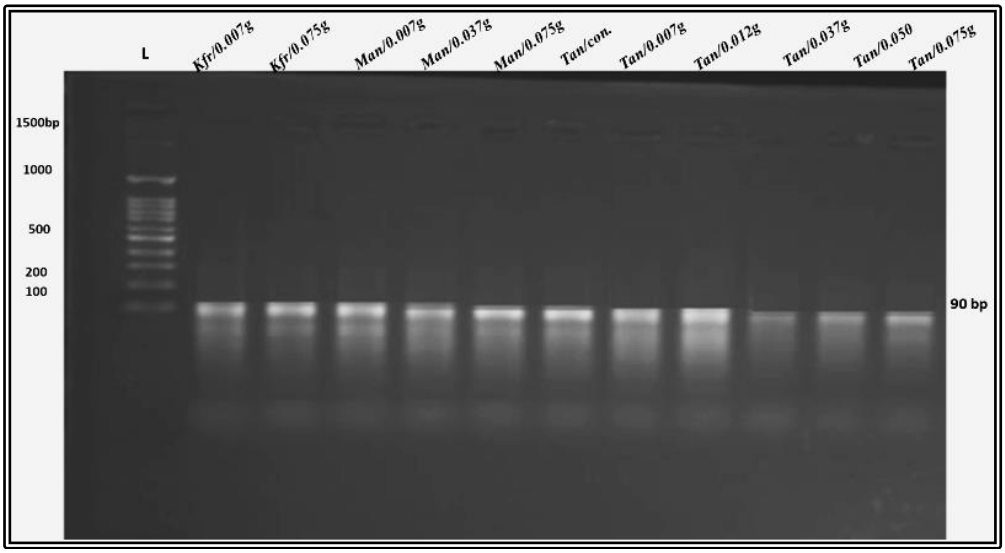

Fig. (18) PCR product gel electrophoresis for *Im2* gene at the last generation of each strain for the effect of sodium benzoate concentrations on different *Drosophila* strains

Effect of Heat Shock on Some Genes Involved in Heat Tolerance System in Barely

Shimaa M. Elshora[1], A. M. Elzoheiry[2], El-Sayed E. El-Shawy[3] and M. E. Eldenary[1]

1- Department of genetics, Faculty of Agriculture, Tanta University, Egypt

2- Department of genetics, Faculty of Agriculture, Zagazig University, Egypt

3- Barley Res. Dept., Field Crops Res. institute, Agricultural Res. Center, Egypt.

***Key words**: Barley. Abiotic stress. Heat shock Proteins . Gene Expression.*

Corresponding Author: Shimaa M. Elshora, shimaaelshora@gmail.com

Barley (*Hordeum vulgare*) is the most important cereal crop in the world after wheat, maize and rice (FAO-STAT, 2015). It is used mainly for animal and poultry feeding, as well as in the pharmaceutical industry and malt (Biel and Jacyno, 2013). Climate changes are one of the most challenging agricultural problems globally cultivation. Barley grain yield and quality are significantly affected by elevated temperature, Lobell *et al., (*2011). Heat stress is the most adverse abiotic constraint that significantly affects plant growth, physiology, yield, and productivity for most crops (Bilal *et al*., 2015 and Lobell *et al*., 2015). Heat stress causes many physiological effects i.e. membrane protein denaturation, enzyme inactivation, and changes in membrane permeability. These changes reduced ion flux, cause leakage of electrolytes and water content as well as cause the production of toxic compounds (*Mafakheri et al*., 2010). Heat shock proteins (HSPs) play a critical role in sensing and initiating heat shock response in plants during high temperature stress. Heat shock response is triggered by HSPs which are swiftly accumulated under temperature increments to reduce expected damage (Serrano *et al*., 2019). Plants induce different stress-responsive biomolecules as a part of their tolerance mechanisms. Molecular chaperones are of the most important biomolecules, which act to reduce the adverse effects of cells by stress. The heat shock response and the HSP are predicted to be evolutionary conserved. There is an intimate association between expressions of HSPs with that of resistance to high temperature stress (HTS) but in-depth mechanism through which HSPs work to increase thermo tolerance is yet to be fully understood (Singh *et al*., 2016).

Heat shock proteins bind to their substrate reversibly and an ATP-dependent in function manner to promote protein folding in a native state, and induce proteolysis and disaggregation of substrate proteins without forming part of

the final product. Among the five major Hsp families, a class of Hsp70 family proteins consists of a conserved N-terminal ATP-binding domain and C-terminal substrate-binding domain along with a C-terminal lid with a variable number of amino acids (Flaherty *et al*., 1990). Another class of molecular chaperone family Hsp90 proteins function in the form of a dimer; each promoter consists of an ATP-binding domain at the N-terminal, and linker M-domain and dimerization domain at the C-terminal (Pearl and Prodromal, 2006).

The Heat Shock Regulators (HSR) has a modular structure and is conserved among eukaryotes. Despite the variability in sequence and size, the mode of promoter recognition and their basic structure show high similarities (Bjork and Sistonen, (2010); Fujimoto and Nakai, (2010). Heat shock factors are in classes and groups, i.e., *Arabidopsis thaliana* has 21 HSFs in three classes (A, B and C), which include 14 different groups (A1 to A9, B1 to B4 and C1), Scharf *et al*., (2012). The roles of heat shock factor A1 (HSFA1) in response to the stress factors other than heat have not been determined. In response to high temperature, HSFA1 triggers the expression of different transcription regulators; Liu and Charng, (2012). HSFA2 is a heat-inducible transcription factor (Busch *et al*., 2005) and it is a secondary regulator under the control of at least one master regulato. Early and late heat shock gene expression can be mediated through this HSFA2 (Nishizawa, 2006).

In this investigation, the differential response to heat shock is studied by comparing heat tolerance with heat sensitive barley genotypes; in an attempt to clarify the correlation between some HSP regulatory and some biochemical indicators for heat tolerance.

MATERIALS AND METHODS

Barley Genotypes and Planting conditions

Four barley (*Hordeum vulgare*) genotypes as shown in Table (1) were obtained from Crop Research Institute, Sakha, Kafr-Elsheikh. Forty barley seeds of each genotype with three replicates were cultivated in plastic plates (20 x 9.5 x 7 cm) containing coco beet, perlite and clay soil. Germinated seeds were grown in a growth chamber at 18ºC and 5000 Lux light for 14/10 Light/Dark. Plants were irrigated with Hoagland solution (0.5) up to 23 days. Samples for heat stress (shock) treatment were collected as follow; control at 18ºC as well as 2h, 4h and 8h at 35°C. One and 48 h recovering treatments at 18ºC were carried out to compare the recovering response of plants.

Electrolyte leakages

Electrolyte leakage (EL) was measured as an indicator for quantification of plant cell membrane damage and cell death. Individual seedlings (0.5 gm. of each) in three replicates were used to measure the electric conductivity (EC meter Adwa-AD32). Seedling parts were placed in a test tube containing 10 ml of

sterile distilled water. The conductivity of the solution was measured three times i.e., immediately after rinsing, after one hour and after one hour of boiling (then cooled to room temperature). Leakage rate of electrolytes (expressed in µS·cm−1.FW·h−1) was calculated as the net conductivity of the solution with seeds immersed for 1 hr., divided by the total conductivity after boiling according to Lutts *et al*., (1996) with some modification.

Electrolyte leakages (EL) = (LEC1) – (LEC0) / (LEC2) – (LEC0).

Where: LEC0 = Measure immediately after soaking the samples in distilled- water, LEC1= Measure after soaking the samples in distilled-water for one hour and LEC2= Measure after boiling the samples for an hour.

Lipid Peroxidation Evaluation

Lipid peroxidation was evaluated as the concentration of 2-thiobarbituricacid (TBA) reactive products, equated with malondialdehyde (MDA), as described by Anjum *et al*., (2012) with slight modifications according to (Hendry and Grime,1993). Plant tissue (0.5 gm.) was homogenized in 5 ml (5% W/V) trichloroacetic acid (TCA), and centrifuged at 4000 rpm at 5ºC for 10 min. The chromogenicity was formed by mixing 2 ml of supernatant with 3 ml of reaction mixture (20% TCA and 0.5% TBA). The mixture was heated at 100ºC for 15 min., and then stopped by rapid cooling in an ice-water bath. The reaction was centrifuged at 4000 rpm at 5ºC for 10 min. The absorbance was then read at 532 nm and correction for unspecific turbidity was done by subtracting the absorbance of the same at 450 and 600 nm. The TBA-reactive products (MDA) were expressed as (nmol. g-1) DW and calculated as flow:

[(Abs 532 – Abs 600) - 0.0571 * (Abs 450 – Abs 600)] / 0.155.

Samples were collected and immediately frozen using liquid nitrogen and kept at –80ºC until use for further biochemical and molecular analysis.

Total soluble protein extraction

One half gram of plant tissue was ground to a fine powder then added to liquid nitrogen. Ground powder was homogenized in ice cold mortar and pestle in 1.0 ml of extraction buffer containing 20% of sucrose, 50mM of Tris, 50mM of NaCl and Protease inhibitors(Sigma-Aldrich) according to (Eldenary and Elshawy, 2014)with some modifications. Concentration of extracted proteins was determined according to Bradford, (1976).

Antioxidant enzymes assays

Changes in isozyme activities for antioxidant enzymes were studied using native PAGE (under non-reduced, non-denatured conditions) at 5ºC according to the suggested method by weydert and Cullen (2010). Native- PAGE was carried out for SuperOxide Dismutase (SOD) and Catalase (CAT).

Native PAGE Analysis of Antioxidant Enzymes

Native PAGE was performed according to (Laemmlie, 1970) without SDS. An equal amount of protein was separated on the native gel which was then rinsed in the detection reaction buffer according to the type of enzyme.

For SODs activity was detected by nitroblue tetrazolium (NBT) reduction by superoxide radicals that were photochemically generated; according to Beauchamp and Fridovich, (1971). After electrophoresis, the gels were covered with a solution containing 0.25 mg/mL−1 of NBT and 0.1 $mg \cdot mL^{-1}$ of riboflavin, and then exposed to a light. The two types of SOD (Mn-SOD and Cu/Zn-SOD) were identified using inhibitors. Mn-SOD was diagnosed by its sensitivity to a 5 mM of H_2O_2 and 1 mM of KCN, while Cu/Zn-SOD was identified by its sensitivity to 1 mM of KCN (Navari-Izzo *et al*., 1998).

CAT activity in native PAGE gels was determined using the methodology According to Woodbury *et al*., (1971).

Total RNA Extraction

Total RNA was extracted from barley seedlings of control and heat treated plants for the different genotypes using EZ-10 Spin column Plant RNA Mini-Preps Kit (BIO BASIC CANADAINC) according to the attached protocol. RNA quantity and purity was determined using Nano drop spectrophotometer (Bio Drop µLITE.UK). RNA samples with 260/280 nm ratio more than 1.9 were considered as acceptable for RT-qPCR reactions. RNA quality and integrity were confirmed via electrophoresis on a 1.5% agarose gel. A two µg of total RNA were used for c-DNA synthesis in a 20-µl of reaction mix using oligo (dT) primer and the HiSenScript™ RH cDNA synthesis kit (iNtRON Biotechnology).

Determination of Gene expression

Five primer pairs (Table 2) were designed using the NCBI Primer-BLAST program (http://www.ncbi.nlm.nih.gov/tools/primer-blast). Real-time quantitation of gene expression (RT-qPCR) analysis was carried out to confirm the induced changes in the gene expression. RT-qPCR reactions were conducted using 5X HOT FIREPol R EvaGreen R q-PCR Mix Plus (ROX) (enzynomics- Korea) in a 20 µL of reaction volume. The reactions were run (Applied Biosystem™ Step One Plus™ Real Time PCR system) using alpha tubulin *Hordeum vulgare* gene as an internal control (Accession number U40042.1). All tested samples were conducted in two biological replicates.

RESULTS AND DISCUSSION

Physiological and biochemical analysis

Electrolyte leakage (EL) is one of the physiological parameters used for estimation of cell membrane stability due to its sensitivity to heat stress (Rehman *et al*., 2016). The electrolyte leakage was measured as an indicator for the injury of the membranes their stability. Figure (1)

showed the measured EL as Electric Conductivity (EC) of seedling leaves of the tested four barley genotypes; according to Faralli *et al*., (2015).

The estimated oxidation rates (SOD) under HS stress comparing with the control is shown in Fig. (2). The reaction on the gel indicated that in the studied genotypes did not show significant increase in the Cu/Zn-SOD isozyme activity. However, Mn-SOD isozyme activity (high molecular weight band) was obtained only in the moderate (adaptive) genotype G2000 which showed the presence of two types of isozyme. In spite of catalase (CAT) all studied genotypes showed only one similar isoform of CAT enzyme under heat shock stress as well as the control plants, Fig. (8). Comparing there results (on shoots) with Kuralay *et al*., (2021) who exposed barley seedlings to combined of drought as well as high temperature stresses and showed considerably lower CAT and SOD activities in the shoots and this may confirm these results. While in the same barley seedlings; SOD and CAT activities in the roots were drastically increased under high temperature stresses and they detected two new SOD isoforms in the roots.

Lipid peroxidation is an indicator for the oxidative effect of the abiotic stress especially in the sensitive genotypes that might have not enough antioxidant content (enzymatic/non-enzymatic). The concentration of 2-thiobarbituricacid (TBA) reactive products, equated with Malondialdehyde (MDA) were evaluated. Although, there were no significant differences in SOD and CAT activities with HS treatment, the MDA showed clear differences between sensitive and tolerant genotypes. Figure 3 showed that G129 genotype (sensitive) appeared high lipid peroxidation compared with the G134 (tolerant) genotype. G134 (tolerant) genotype appeared negative values even with increased HS exposure times. The other sensitive genotype (G135) showed low lipid peroxidation (negative value) in the control and 2h at 35ºC, while the lipid peroxidation was increased with HS times increasing. Interestingly, the G2000 genotype showed high lipid peroxidation but it was reduced when the plants were transferred to 18ºC after 48 h. Yingyan *et al*., (2013) reported that MDA was significantly increased in barley seedlings with the rising of temperature, and the clearest values were at the range of 35°C- 40°C. They also concluded that the tolerant genotypes for HS stress appeared lower in MDA than the sensitive genotypes.

The interpretation for this behavior is that the tolerant genotype G134 may have non enzymatic antioxidant which reduced the harmful oxidative effect.

Differential HSPs gene expression

The four tested genotypes (exposed to HS at 35°C for three different times) were evaluated for gene expression. The selected 4 genes related to heat shock tolerance i.e. HSP70, HSP90, HSFA1 and HSFA2 genes were analyzed using qRT-PCR technique. Two of them (HSFA1&2)

are transcription factors. Expression level was standardized on the α-tubulin gene as the internal control gene. Relative expression (RQ) of the studied genes is shown in Figs. (4, 5, 6 and 7).

Figure (4) illustrated that HSP 70 gene was significantly increased about 15 fold in the sensitive genotype G-135 (2 h at 35°C) compared with the control, while the increased value was only about 4 fold in the tolerant genotype G134 with the same treatment compared with the control. On the other hand, the moderate genotype G2000 and the sensitive one (G129) did not show a significant increase in the expression of HSP70 gene under HS treatments.

The other studied gene of HSP90 (Fig. 5) showed up regulation (70 fold) in the sensitive genotype (G129) under HS (2h at 35ºC condition, but the tolerant genotype (G134) showed a quite increase (3 fold) with the same treatment in comparison with the control plants. This result was agreed with, Faralli *et al*., (2015) who exposed barley seedlings to heat shock stress and found that the expressions for HSP18 and HSP90 genes on qRT-PCR were significantly increased. Moreover, they mentioned that HSP70 gene was transcribed in the control and shocked seedlings, but its expression was not significantly like HSP90 gene .Other investigation by Sadura *et al*., (2020) who concluded that it may rely on the ability of the membranes to continuously accumulation for HSP70 gene proteins; as a result they did not need to perform over expression, but the opposite in HSP90 and HSP18 genes were occurred.

The regulator HSFA1 transcription factor for HSP70 gene showed higher expression levels under HS 8h at35ºC (more than 3 fold) in the tolerant genotype G134 (Fig. 6) compared with the control plants under normal condition (at 18ºC),while the sensitive genotype G129 under all conditions were remain around the control value. Heerklotz *et al*., (2001), and Mishra *et al*., (2002); reported that, in plants, HSFA1 is constitutively expressed and has a unique function as “a master regulator” of heat shock response.

Figure (7) Showed the expression level of HSFA2 transcription factor that was higher (10 fold) for 2h at 35ºC in the sensitive genotype (G135), while moderate high expression (6 fold) in the tolerant genotype (G134) under HS condition was occurred at the same treatment. The adaptive genotype G2000 showed only 2 fold expression at HS for the exposure time 4 h at 35ºC. Scharf *et al*., (1998) pointed out that HSFA1 factor during normal condition is distributed in the cytoplasm and upon activation by heat stress, nuclear localization of HsfA1 starts which then leads to the expression of HSFA2 and HSFB1 and the formation of hetero oligomer (termed super activator complexes) between HSFA1 and HSFA2 transcription factors.

SUMMARY

Sever climatic changes, especially high temperature, is one of the most

important abiotic factors defining the yield potential of temperate cereal crops such as barley. In this work, 4 barley genotypes were used to study the differential response to heat shock. Physiological data pointed that the sensitive genotype showed high leakage and lower electric conductivity. The sensitive genotype (G129) showed high lipid peroxidation compared with G134, the tolerant one. The quantitative PCR analysis for the studied heat shock proteins and transcription factors showed that the level of gene expression of HSP70 was significantly increased after a short time under HS in the sensitive genotype, while a slight increase was observed in the tolerant genotype. The HSP90 showed up regulation in the sensitive genotype G129 under HS condition, but the tolerant genotype G134 showed quite an increase in comparison with control plants. The regulator HSFA1 showed higher expression level in the tolerant genotype G134 comparing with G129. The expression level of HSFA2 was higher in the sensitive genotype (G135), while moderate high expression in the tolerant genotype G134.

REFERENCES

Anjum S. A., Saleem M. F., Wang L., Bilal M. F., Saeed A., (2012). Protective role of glycinebetaine in maize against drought-induced lipid peroxidation by enhancing capacity of antioxidative system. AJCS, 6(4):576-583.

Beauchamp C. and Fridovich, I., (1971). Superoxide dismutase: Improved assays and an assay applicable to acrylamide gels. Analytical Biochemistry, 44:276-287.

Biel W. and Jacyno E., (2013). Chemical composition and nutritive value of spring hulled barley varieties. Bulg. J. Agric. Sci., 19: 721-727.

Bilal M., Rashid R.M., Rehman S. U., Iqbal,F., Ahmed J., Abid M. A., Ahmed Z. and Hayat A., (2015). Evaluation of wheat genotypes for drought tolerance J. Green Physiol. Genet. Genom. 1:11-21.

Bjork J. K. and Sistonen L., (2010). Regulation of the members of the mammalian heat shock factor family. FEBS J.; 277:4126-4139.

Bradford M. M., (1976). A rapid and sensitive method for the quantitation of microgram quantities of protein utilizing the principle of protein-dye binding. Analytical biochemistry, 72: 248-254.

Busch W., Wunderlich M. and Schoffl F., (2005). Identification of novel heat shock factor-dependent genes and biochemical pathways in *Arabidopsis thaliana*. Plant J. 41:1-14.

El Denary M. E. and El-Shawy E. E., (2014). Molecular and Field Analysis of Some Barley Genotypes for Water Stress Tolerance. Egypt. J. Genet. And Cytol., 43: 187-198.

FAOSTAT, (2015). Food and Agriculture Organization of the United Nations. Statistical Database.

Faralli M., Lektemur C., Rosellini D. and Gürel, F., (2015), Effects of heat shock and salinity on barley growth and stress-related gene transcription. Biologia Plantarum, 59: 537-546.

Flaherty K. M., DeLuca F. C. and Mckay D.B., (1990). Three-dimensional structure of the ATPase fragment of a 70k heat-shock cognate protein. Nature, 346:623-628.

Fujimoto M. and Nakai A., (2010). The heat shock factor family and adaptation to phototoxic stress. FEBS J., 277:4112-4125.

Heerklotz D., Döring P., Bonzelius F., Winkelhaus S. and Nover L., (2001). The balance of nuclear import and export determines the intracellular distribution and function of tomato heat stress transcription factor HsfA2. Mol. Cell Biol. 21: 1759-1768.

Hendry G. A. and Grime J. P., (1993). Methods in Comparative Plant Ecology: A laboratory manual. Published in 1993 by Chapman & Hall, London ISBN 0 412 46230 3.

Kuralay Z., Assylay K., Bakhytgul G., Roza Y., Nurgul I., Ulbike A., Assemgul B., Zhanerke T., Rustem O. and Zhaksylyk M., (2021). ROS status and antioxidant enzyme activities in response to combined temperature and drought stresses in barley. Acta Physiologiae Plantarum .43:114.

Laemmli U.K., (1970). Cleavage of structural proteins during the assembly of the head of bacteriophage T4. Nature, 227(5259):680-685.

Liu H. C. and Charng Y. Y., (2012). Common and distinct functions of *Arabidopsis* class A1 and A2 heat shock factors in diverse abiotic stress responses and development. Plant Physiol., 163:276-290.

Lobell D. B., Schlenker W. and Costa-Roberts J., (2011). Climate trends and global crop production since 1980. Science, 333: 616-620.

Lobell D. B., Hammer G. L., Chenu K., Zheng B., McLean G. and Chapman S. C., (2015). The shifting influence of drought and heat stress for crops in northeast Australia Glob. Biol., 21: 4115-4127.

Lutts S., Kinet, J. M. and Bouharmont J. (1996). NaCl-induced senescence in leaves of rice (*Oryza sativa* L.) cultivars differing in salinity resistance. Ann. Bot. 78: 389-398.

Mafakheri A., Siosemardeh A., Baharamnejad B.,Struik P. C. and Sohrabi Y., (2010). Effect of drought stress on yield, proline and chlorophyll contents in three chickpea cultivars. Australian Journal, 4(8):580-585.

Mishra S. K., Tripp J., Winkelhaus S., Tschiersch B., Theres K., Nover L.

and Scharf K. D., (2002). In the complex family of heat stress transcription factors, HsfA1 has a unique role as master regulator of thermo tolerance in tomato. Genes & Development, 16: 1555-1567.

Navari-Izzo N. F., Quartacci, M. F., Pinzino C., and Vecchia, F. D., (1998).Thylakoid-bound and stromal antioxidative enzymes in wheat treated with excess copper. Physiologia Plantarum, 104(4):630-638.

Nishizawa, (2006). The role of class A1 heat shock factors (HSFA1s) in response to heat and other stresses in *Arabidopsis*. Plant J.,l48 (4):535-47.

Pearl L. H. and Prodromou C., (2006). Structure and mechanism of the Hsp90 molecular chaperone machinery. Annu. Rev. Biochem., 75:271-294.

Rehman S. U., Bilal M., Rana R. M., Tahir M. N., Shah M. K. N., Ayalew H. and Yan G., (2016). Cell membrane stability and chlorophyll content variation in wheat (*Triticum aestivum*) genotypes under conditions of heat and drought Crop Pasture Sci., 67:712-718.

Sadura I., Libik-Konieczny M., Jurczyk B., Gruszka D., Janeczko A., (2020). HSP Transcript and Protein Accumulation in Brassinosteroid Barley Mutants Acclimated to Low and High Temperatures. International Journal of Molecular Science, 10 21(5):1889.

Scharf K. D., Berberich T., Ebersberger I. and Nover L., (2012) .The plant heat stress transcription factor (Hsf) family: structure, function and evolution. Biochim. Biophys. Acta, 1819: 104-119.

Serrano N., Ling Y., Bahieldin A. and Mahfouz M. M., (2019). Thermo priming reprograms metabolic homeostasis to confer heat tolerance. Scientific Reports, vol. 9, no. 1, pp. 181.

Singh R. K., Jaishankar J., Muthamilarasan M., Shweta S., Dangi A. and Prasad, M., (2016). Genome-wide analysis of heat shock proteins in C4 model, foxtail millet identifies potential candidates for crop improvement under abiotic stress. Scientific Reports, 32641. DOI:10.1038/srep 32641

Weydert, C. and Cullen J., (2010). Measurement of superoxide dismutase, catalase and glutathione peroxidase in cultured cells and tissue. Nat. Protoc., (1):51-66.

Woodbury W., Spencer A. K., Stahman M. A., (1971). An improved procedure using ferricyanide for detecting catalase isozymes. Analytical Biochemical Nov, 44(1):301-5.

Yingyan H., Shuangxi F., Qiao Z. and Yanan W., (2013). Effect of heat stress on the MDA, proline and soluble sugar content in leaf lettuce seedlings. Agricultural Sciences, 4:112-115.

Table (1): Tested barley genotypes; pedigree and heat stress tolerancy.

Genotype	Pedigree	Heat stress tolerancy
G-129	Deir Alla106/Cel//As 46/Aths *2	Sensitive
G-135	ZARZA/BERMEJO/4/DS4931//GLORIA	Sensitive
G-134	Alanda-01/4/WI2291/3/Api/CM67//L2966-69	Tolerant
G-2000	Giza117/Bahteem52//Giza118/FAO86/3/Baladi16/Gem	Moderate

Sensitivity, Tolerance or Moderation for the Genotypes identification was obtained according to Barley Res. Dept., Field Crops Res. institute, Agricultural Res. Center, Egypt.

Table (2): Gene name, primer sequence and accession number.

Gene	Forward Primer 5'→3'	Reverse Primer 5' →3 '	Accession number
α-Tubulin	AATGCTGTTGGAGGTGGAAC	GAGTGGGTGGACAGGACACT	U40042.1
Hsp70	AAGGACAAGCTTGCGGACAA	ACTAGCTCAGCATACAGGCAC	L32165.1
HSP90	CGTCGTTGGATGGTTTTGGC	GCAGATGAAAGCAATAAGCAGGG	AY325266.1
HSFA1	ATGATGGCCTGAACCCTGAA	TTCCGGGTTGATGAAGAGCT	HM446022.1
HSFA2	AGATGATGGGGTTCTTGGCA	GCTCACTCTGGCTTGTTGTC	HM446025.1

α-Tubulin: Alpha tubulin, Hsp70: Heat shock protein70, HSP90: Heat shock protein 90. HSFA1: Heat shock factor A1, HSFA2: Heat shock factor A2.

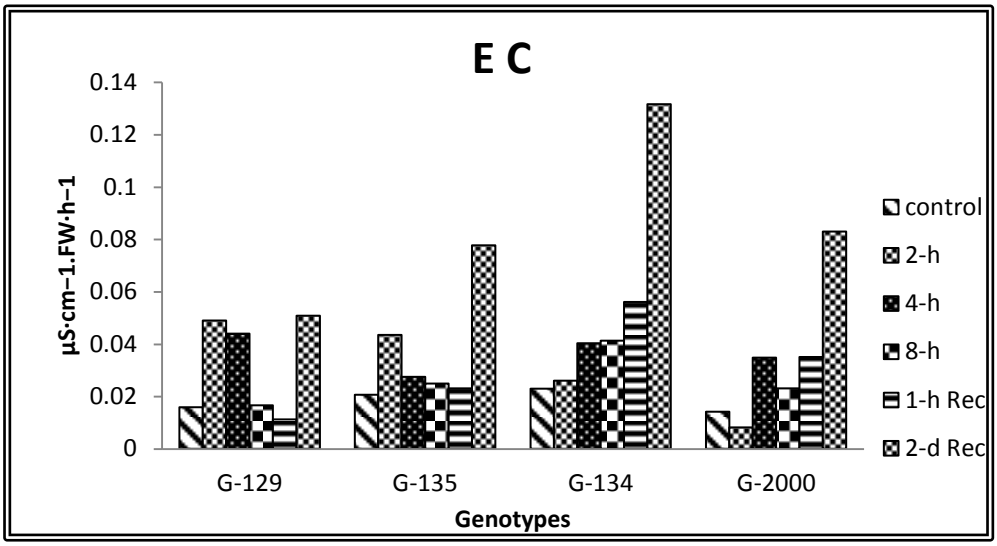

Fig. (1): EC for the tested barley genotypes under heat shock treatment.

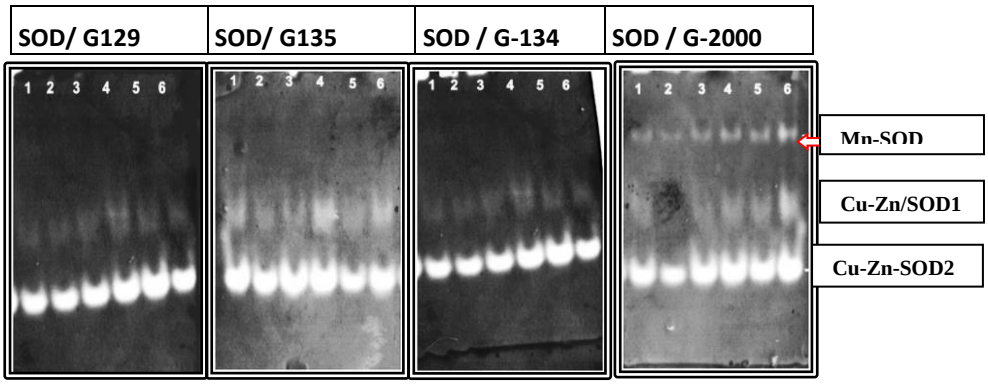

Fig. (2): ative gel showed SOD activities in control and heat shock treated seedlings. Lane 1 was control and lanes 2, 3 and 4 were exposed to 35ºC for 2 h, 4h and 8h, respectively. While lanes 5 and 6 were recovering at 18°C for 1h and 48 h, respectively.

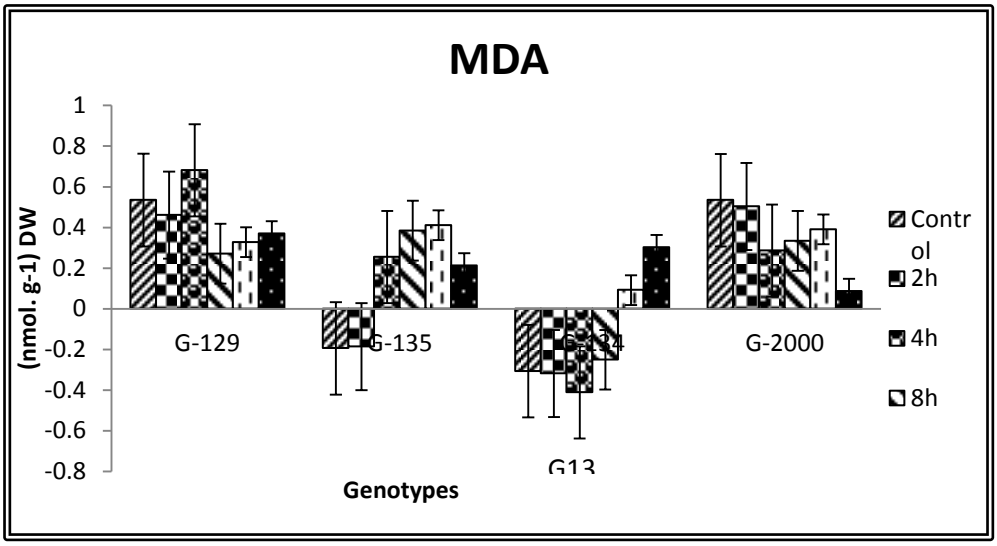

Fig. (3): Showed MDA for the tested barley genotypes under heat shock treatment.

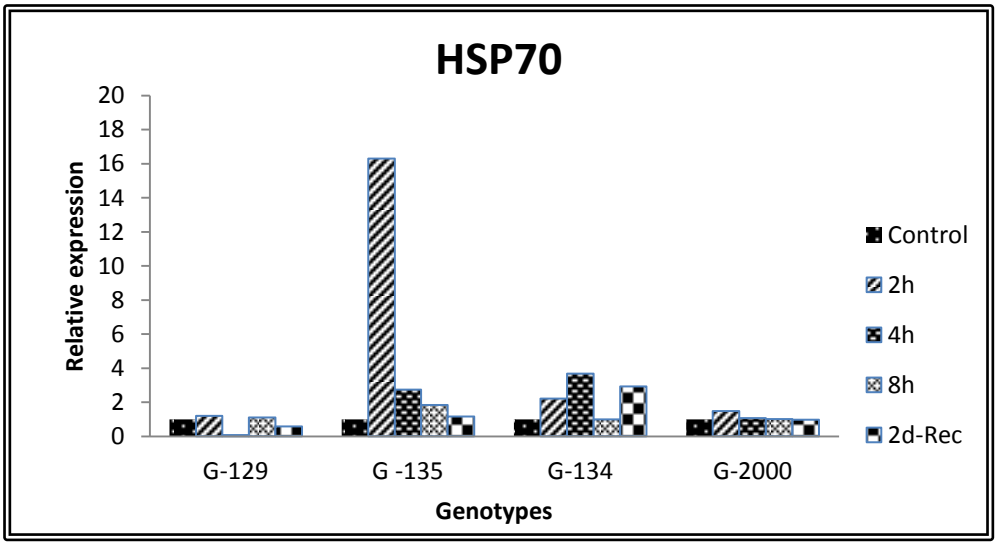

Fig. (4): levels of HSP70 gene expression for the tested barley genotypes under heat shock treatments.

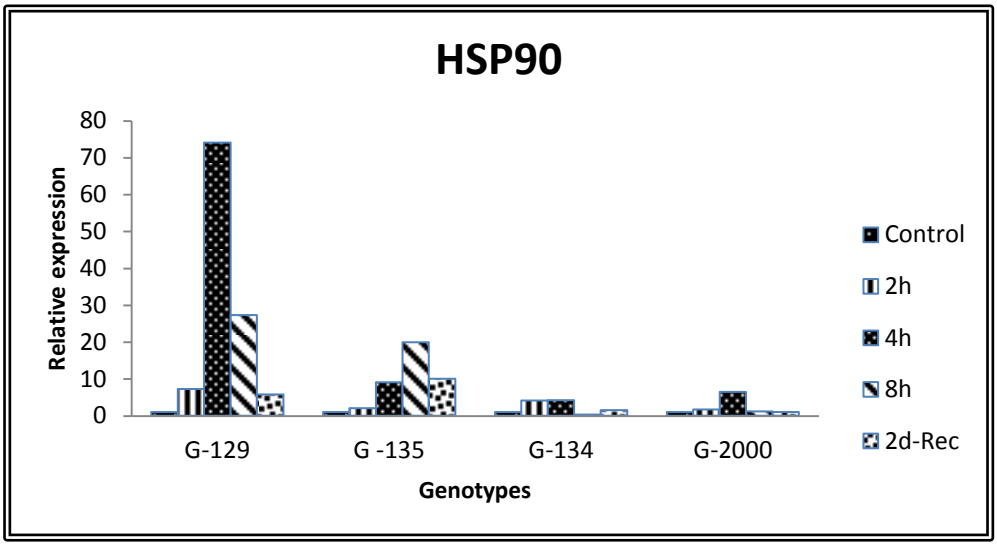

Fig. (5): levels of HSP90 gene expression for the tested barley genotypes under heat shock treatments.

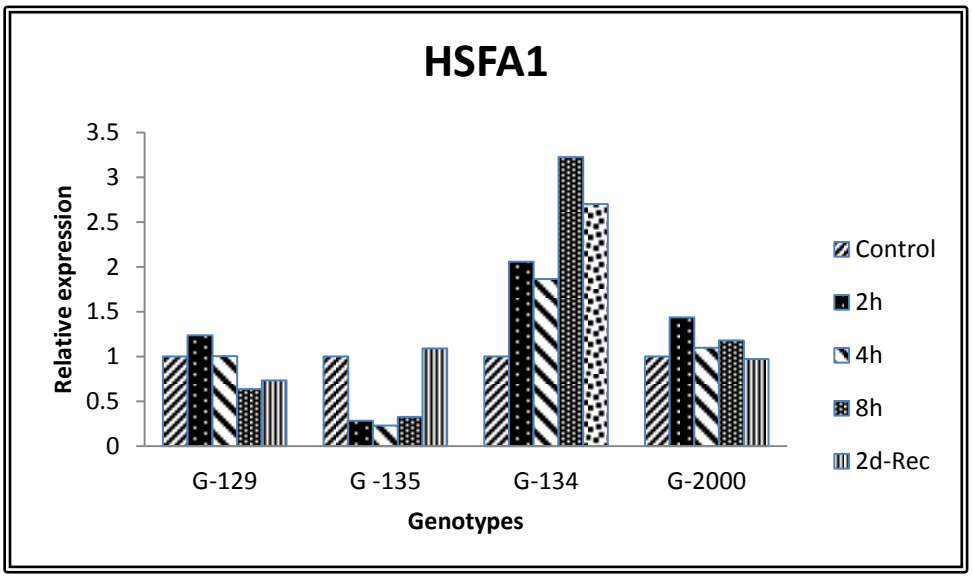

Fig. (6): Levels of HSFA1 gene expression for the tested barley genotypes under heat shock treatments.

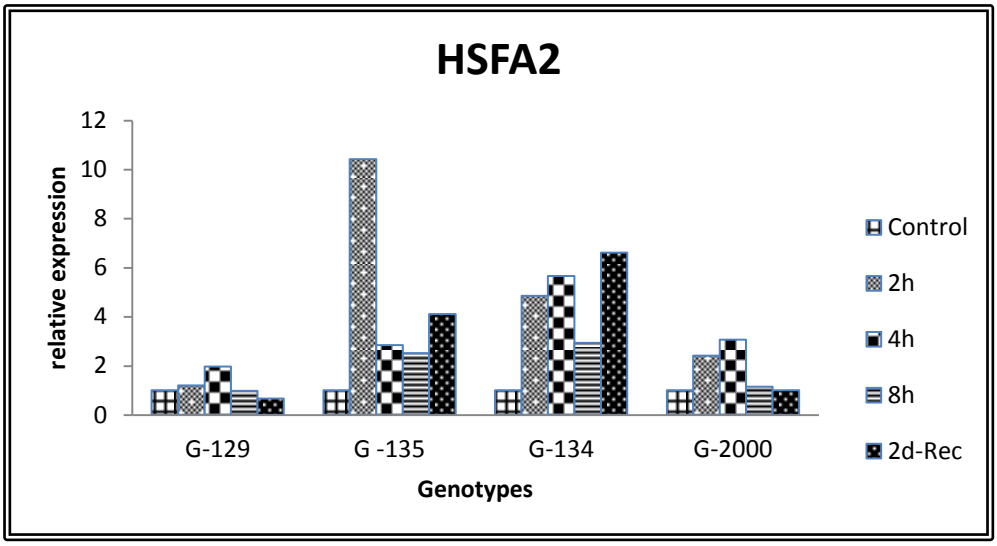

Fig. (7): Levels of HSFA2 gene expression for the tested barley genotypes under heat shock treatments.

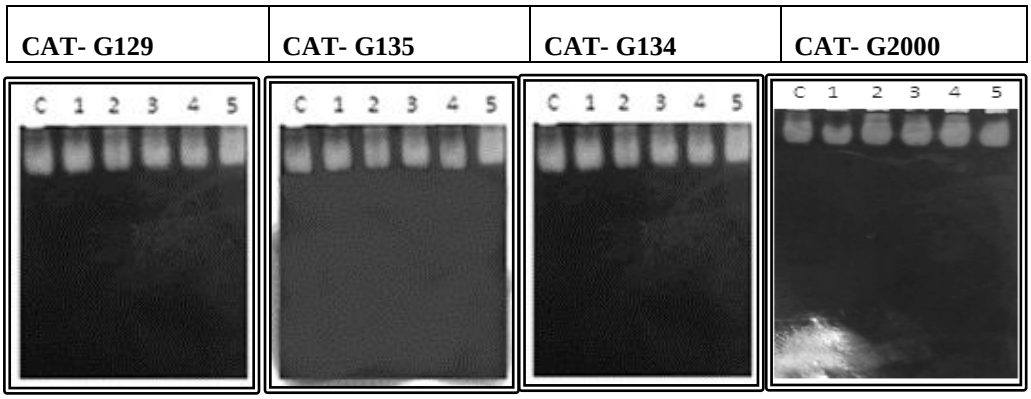

Fig. (8): Native gel showed Catalase activities in control and heat shock treated seedlings. Lane C was control and lanes 1, 2 and 3 were exposed to 35ºC for 2 h, 4h and 8h, respectively. While lanes 4 and 5 were recovering at 18ºC for 1h and 48 h, respectively.

رقـــم الإيـــــداع

ISSN : 0046 – 161 X